CHALMERS
UNIVERSITY OF TECHNOLOGY

Development and validation of a qPCR based high-throughput assay to quantitatively assess the productive uptake of peptide conjugated antisense oligonucleotides (ASO) in a GLP1 receptor over-expressing HEK293 cell line

Master's thesis in Biotechnology

DZENITA BAZDAREVIC

Department of Biology and Biological Engineering
CHALMERS UNIVERSITY OF TECHNOLOGY
Gothenburg, Sweden 2018

Master's thesis 2018, BBTX03

Development and validation of a qPCR based high-throughput assay to quantitatively assess the productive uptake of peptide conjugated antisense oligonucleotides (ASO) in a GLP1 receptor overexpressing HEK293 cell line

Dzenita Bazdarevic

CHALMERS
UNIVERSITY OF TECHNOLOGY

Department of Biology and Biological Engineering
Chalmers University of Technology
Gothenburg, Sweden 2018

Development and validation of a qPCR based high-throughput assay to quantitatively assess the productive uptake of peptide conjugated antisense oligonucleotides (ASO) in a GLP1 receptor overexpressing HEK293 cell line
DZENITA BAZDAREVIC

Supervisor: Carina Ämmälä, Diabetes Bioscience department, IMED CVRM, AstraZeneca
Co-supervisor: Charlotte Wennberg Huldt, Diabetes Bioscience department, IMED CVRM, AstraZeneca
Examiner: Joakim Norbeck, Department of Biology and Biological Engineering, Chalmers University of Technology

Master's Thesis 2018, BBTX03
Department of Biology and Biological Engineering
Chalmers University of Technology
SE-412 96 Gothenburg
Telephone +46 31 772 1000

Cover: The Biomek FX^p laboratory automation workstation was used to pipette qPCR master mix and transfer diluted cDNA in the 384-well plate.

Gothenburg, Sweden 2018

Development and validation of a qPCR based high-throughput assay to quantitatively assess the productive uptake of peptide conjugated antisense oligonucleotides (ASO) in a GLP1 receptor overexpressing HEK293 cell line

DZENITA BAZDAREVIC

Department of Biology and Biological Engineering
Chalmers University of Technology

Abstract

Diabetes mellitus is the name of a collection of different disorders characterized by raised blood sugar levels due to either absolute or relative insulin insufficiency to properly control the blood glucose levels in the body. The β-cells in pancreas don't have the ability to secrete insulin as much as required to meet the demand caused by obesity-driven insulin resistance. Diabetes is a growing public health issue, where type 2 diabetes is the most common form among the population. With the global increase of obesity and the emerging epidemic of type 2 diabetes there is a need for new medicines that cures type 2 diabetes.

Researchers at AstraZeneca are working on developing new drugs that are specifically targeting β-cells using antisense oligonucleotides (ASOs). ASOs have a great potential to become a treatment because of the ability to bind and knockdown genes. There are still challenges that needs to be overcome regarding the delivery to specific cell types. One strategy to enhance the cellular uptake of ASOs is to use ASOs conjugated to a peptide hormone called Glucagon-like peptide 1, that can bind to a receptor found on the β-cells surface. Currently successful uptake of ASOs is quantified by measuring the relative expression of gene inhibited with a manual and low throughput qPCR assay. To speed up the process and to be able to screen several ASOs, the aims of this study were to set up a two-step qPCR-based semi-automated assay on GLP1 receptor overexpressing HEK293 cell line and primary mouse pancreatic islet cells to assess the delivery of a tool compound (ASO targeting *MALAT1*). The assay used in this study was based on another in-house assay, that involves cell lysis, cDNA synthesis of the accessible mRNA and qPCR amplification reaction. However, the assay needed modifications to generate robust and reproducible concentration-response curves showing the relative gene expression.

This study have shown that setting up a high-throughput qPCR based assay is not straightforward and takes time to find the conditions for working assay in GLP1 receptor overexpressing HEK293 cells. Finding the right lysis buffer for the cell type, using a Poly-D-Lysine coated plate, 10% lysate in the cDNA synthesis and using hydrolysis (TaqMan) probes in the qPCR, solved the problem regarding the performance of amplification reaction and relative gene expression (concentration-response curves). The assay developed in this project can now be used for comparing and ranking of ASOs with different conjugated GLP1 peptides based on the efficacy and potency.

Keywords: Quantitiative real-time PCR, Semi-automated, High-throughput, Assay, Type 2 diabetes, Antisense oligonucleotides

Acknowledgements

The master's thesis project was performed at AstraZeneca in the Diabetes Bioscience department, were I have been part of the In vitro Islet biology team. The seven-month full time placement at AstraZeneca, has given me an outstanding and exciting introduction to, and experience of how it is to work in preclinical research and early drug discovery. Doing research at AstraZenca have shown me the excitement and value of working with people with different knowledge and diverse backgrounds.

This project was a collaboration between AstraZeneca and Ionis pharmaceuticals and all the reagents and equipment needed for the work was provided by the companies.

I would like to thank my supervisor Carina Ämmälä for giving me this opportunity because it has given me insight how research is driven outside of academia and how fun it is to work in a global, science-driven and innovative biopharmaceutical company. Thank you for all your help and guidance of this project and making me feel a part of the team.

I would like to thank my co-supervisor, Charlotte Wennberg Huldt for teaching me about qPCR and answering my endless questions. Thank you for patient guidance, help and support troughout the project.

Thank you Eva-Marie Andersson for your enthusiasm and for teaching me how to isolate primary mouse islets.

Thanks to all the members of the In vitro Islet biology team for pleasant conversations and help in the lab.

Without you all it wouldn't been possible to complete this project!

Dzenita Bazdarevic, Gothenburg, April 2018

Contents

List of Figures

List of Tables

1

Introduction

Diabetes mellitus is the name of an assembly of different syndromes characterized of elevated blood glucose as a consequence of defective secretion or action of a peptide-hormone called insulin [1]. If untreated, elevated glucose levels will with time lead to serious negative effects on blood vessels, nerves, kidneys, eyes and heart [2].

Diabetes is a large and growing public health issue. According to the World Health Organization, in 2014 an estimated 422 million people was affected by diabetes worldwide, compared to 108 million, 34 years before [3]. Type 2 diabetes (T2D) is a form of the disease that develops when pancreatic β-cells are unable to secrete enough insulin to meet the demand caused by obesity-driven increased insulin resistance [1, 2]. Today about 300 million people is diagnosed as suffering from T2D, and the incidence is increasing in an alarming rate among the general population [4]. Currently, modern medicines only treat the symptoms and there is no curative treatment for T2D, restoring the underlying β-cell defects [5]. Therefore, discovery of a therapeutic strategy that can improve β-cell function and increase insulin secretion would be of great significance for the patients suffering from the disease.

Researchers at AstraZeneca in the In vitro Islet biology team in the Cardiovascular, Renal and Metabolism IMED biotech unit (CVRM IMED) are currently working on developing drugs that specifically targets β-cells using antisense oligonucleotides (ASOs). ASOs bind to and induce cleavage of mRNA, thereby silencing gene expression [6]. ASOs hold great potential as regenerative treatment, but one key difficulty is to target delivery to specific cell types. Therefore, the ability to quantify the productive uptake of the ASOs is of critical importance to the drug discovery process. The researchers are exploring an approach to enhance cellular uptake of ASOs by using Glucagon-like peptide 1 (GLP1) as a carrier. GLP1 binds to and activates a G-protein-coupled receptor (GLP1R) leading to receptor internalization. The hypothesis is that conjugation to GLP1 will enhance the uptake of ASOs in cells that are expressing GLP1R [7]. Cell and tissue specific delivery of drugs not only enhances the maximum response of the drug (efficacy), but also has the potential to reduce the risk of unwanted effects in other tissues, thereby improving safety.

At present a manual qPCR-based assay is used to quantify the cells ability to take up the ASOs by measuring the effect on gene expression. If the potency of ASO conjugated to GLP1 for silencing target gene expression in cells expressing the GLP1 receptor is better compared to parent ASO (without a peptide), this is interpreted as an increase in productive uptake of ASO. The manual qPCR-based assay is time consuming, expensive and has a low throughput, and there is a need for a high-throughput assay to enable screening and ranking of many GLP1-ASO conjugates based on the concentration required to give a response/effect (potency) and efficacy.

1.1 Aims

The aims of the project were to set up and validate a two-step qPCR-based high-throughput assay to evaluate the productive uptake of available peptide-ASO conjugates in a GLP1 receptor overexpressing HEK293 cell line and mouse pancreatic islet cells.

1.2 Objectives

During the project, questions were raised to guide and drive the investigation forward.

These where the following questions:

- Is it possible to set up a semi-automated high-throughput qPCR assay for screening of ASOs in a GLP1 receptor overexpressing human embryonic kidney 293 cell line (GLP1R-HEK293)?
- Is it possible to modify the high-throughput assay protocol to be used on intact mouse or human islets? If not, is it possible to use dispersed islet cells?
- Is it possible to test ASOs at different concentrations and rank them according to their efficacy and potency?

1.3 Limitations

The uptake of ASOs will only be investigated by quantifying the effect silencing gene expression with the semi-automated high-throughput qPCR assay. How much of the ASOs that the cells have taken up and the mechanism how it inhibits gene expression will not be covered in project due to limitations in time and access to additional technologies.

ASOs can be designed in diverse ways and against different target genes, conjugated to different peptides using different linker chemistry. The only ASOs that

will be used in this project targets an mRNA called *MALAT1*. The ASOs targeting *MALAT1*, a long non-coding mRNA, was selected as it is highly expressed in all mammalian cell types [7, 8], and therefore a good tool for studying effects on gene expression in different cells and tissues [7].

The ideal would be to test the assay on pancreatic islet cells from mouse and human but is difficult as primary pancreatic islet cells from mouse are cumbersome to isolate, and human islets expensive to procure. Therefor using a cell line with stable expression of GLP1R was preferred as it provides uniform and unlimited source of suitable cells for the development of the assay format, for later translation to a primary islet cell type. A cell line also has the added advantage of reducing animal usage.

Time is a limiting factor in this project because setting up and automating the qPCR assay for GLP1R-HEK293 cells and primary pancreatic islet cells from mouse for screening of ASOs have never been done before and with a number of independent experimental parameters having to be optimized, influencing the final protocol.

2

Background

2.1 The pancreas

In adult humans, the pancreas is a 15-20 cm elongated organ that is located in the abdominal cavity laying under the liver and behind the stomach [9], as seen in Figure 2.1.

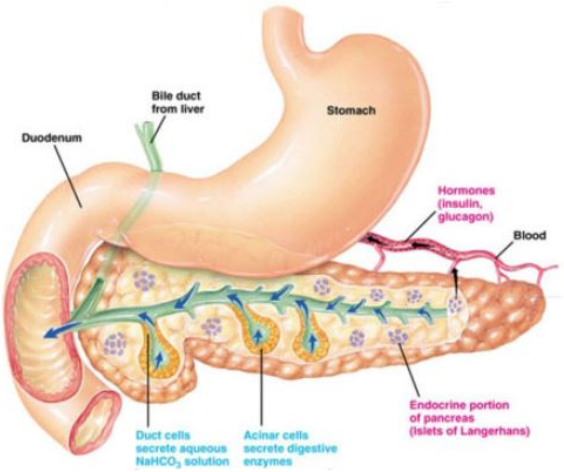

Figure 2.1: The pancreas located behind the stomach. From [10]

The pancreas is divided into three segments (e.g. head, body and a tail) consisting of exocrine and endocrine tissues with two essential functions in the body. The exocrine pancreas regulates the digestion of carbohydrates, proteins and fat from food by secretion of digestive enzymes to the intestine whereas the endocrine portion control the glucose levels by secreting glucoregulatory hormones into the bloodstream [11, 12].

The digestion of nutrients is controlled by the exocrine cells (acinar and pancreatic ductal cells) and regulated by both hormones and neural stimuli [13]. The acini is stimulated to produce pancreatic juices containing diverse enzymes such as amylase, pancreatic lipase and trypsin that are later collected in pancreatic duct and transported to duodenum to assist in degradation [13]. While the function of the

epithelial cells (ductal cells) that are lining the duct tree, is to secrete alkaline fluids containing sodium bicarbonate and water, to dilute and flush out the enzymes from the ducts, to prevent accumulation of the enzymes, and neutralize the acidic chyme coming from the stomach before it ends in the duodenum [13, 14]. The endocrine cells in the pancreas are clustered in small aggregates of hormone secreting cells forming island-like structures called pancreatic islets or Islets of Langerhans, named after the German physician Paul Langerhans who discovered them in 1869 [13].

In humans the pancreas contains approximately 1 million islets, making up about 1-2% of the total pancreatic mass [9] and each islet is made up of anywhere from a few to 10000 of cells or more [15]. There are five different endocrine cell types (α-, δ-, PP-, ϵ- and β-cells) within the islets, each secreting a specific hormone [16, 17] with crucial roles in the regulation of glucose homeostasis in the body [1]. The islets are highly vascularized, (10% of the islet volume is composed of fenestrated capillaries) with 10 times higher blood flow than the exocrine tissues [12] which enables the islet cells to sense and quickly respond to circulating nutrient levels and other hormones to maintain the blood glucose levels in a small and normal range (4-6 mM) [11].

2.1.1 The β-cells

The architecture of the islet of Langerhans and the distribution within the pancreas vary between species. What is common between mammals is that under normal conditions, the β-cells make up the largest fraction of the islet mass. Human islets are composed of about 60% β-cells interspersed with the other endocrine cell types [9, 18], while in other mammals, such as the mouse, 70-80% of an islet is made up of β-cells concentrated in the center and surrounded by a mantle of the other cell types [17]. The function of the β-cell is to secrete insulin in response to elevated blood glucose levels. Insulin is the only hormone in the body able to lower blood glucose, making it critical for glucose homeostasis, under normal conditions keeping glucose levels in a range varying $\sim$4-7.8 mM between the fasting and $\sim$2 hours after food intake in healthy individuals [11, 19, 20]. In humans insulin is encoded by a single gene, *INS*. The *INS* mRNA is translated to a single strand peptide chain, preproinsulin, which is processed in the endoplasmic reticulum where a single peptide is removed and folded and proinsulin formed. Proinsulin is packaged in immature secretary granules in the Golgi apparatus, where the C-peptide is cleaved off and mature insulin formed. Mature insulin is stored in dense core secretory vesicle before release by exocytosis [12, 18]. When blood glucose levels are elevated after a meal, glucose moves into the β-cells through a high capacity low affinity glucose transporter 2 (GLUT2), that is highly expressed on the cell membrane and functions as the glucose sensor. Once inside the cell, glucose is rapidly phosphorylated and broken down by glycolysis and in the Krebs cycle leading to an increase in the cytosolic ATP/ADP ratio, which closes the ATP-sensitive K^+ (K_{ATP} channel). Closure of K_{ATP} channels results in membrane potential depolarization and opening of voltage-gated Ca^{2+}-channels, which increases the cytosolic Ca^{2+} concentration that trigger exocytosis of the secretary granules and insulin is released into the blood [11, 12, 21]. Through circulation, insulin is transported to target tissues such as liver, adipose and

skeletal muscle tissue, where it binds to cell surface receptors and initiate cascades of intracellular signaling events that promote glucose uptake and to lower blood glucose levels [21, 22]. Glucose is then stored as glycogen in the hepatocytes in the liver.

2.2 Diabetes mellitus

Diabetes is a chronic metabolic disease. It is not a single disease but a collection of different syndromes characterized by elevated blood sugar levels due to either absolute or relative insulin insufficiency to appropriately control the blood glucose concentration [19]. The typical symptoms of diabetes are increased urination and thirst. Without treatment the disease can lead to severe conditions such as blindness, cardiovascular diseases, limb amputation or kidney failure. It is important that people get diagnosed early to reduce the risk of complications. In 2015 it was approximated that 1.6 million people died from causes related to diabetes [3]. This debilitating disease does not just effect the patient and the patient's family, it is also a huge burden to the health care system and the economy [9]. The incidence of diabetes is increasing at an alarming rate among the global population and is considered a serious public health issue. According to IDF (International Diabetes Federation), an estimated 629 million people worldwide are likely to be diagnosed with diabetes by 2045. WHO considers diabetes a global epidemic. Multiple factors contribute to the increase in diabetes, such as genetic predisposition, environmental and life style factors and also the fact that the global population is getting older [23, 24].

2.2.1 Type 2 diabetes

The two most common known forms of diabetes are type 1 diabetes (T1D) and type 2 diabetes (T2D). T1D or insulin-dependent diabetes is an auto-immune condition where destruction of β-cells leads to complete insulin deficiency and diabetic ketoacidosis [18]. This type of diabetes can develop at any age but normally develops during childhood, and requires lifelong insulin replacement therapy (injections or pumps) [13]. The majority (95%) of diabetic patients are suffering from T2D or adult-onset diabetes [1]. Although traditionally a disease occurring in adults, hence its common name, diagnosis in both children and younger adults is now increasing, most likely due to the rising rate of childhood obesity. It is believed that unhealthy diet and a sedentary lifestyle increases the risk of developing T2D [23]. Obesity increases insulin resistance in liver, fat and muscle leading to an increased demand for insulin to maintain blood sugar levels in a normal range. The pancreatic β-cells adapt by increasing insulin secretion and expanding β-cell mass, and T2D develops only when the β-cells fail to meet the increasing demand arising from insulin resistance [25, 26]. The cellular mechanisms leading to β-cell dysfunction and insulin resistance are complex and still not fully understood, but are dependent of numerous factors, both genetic and environmental. Obese hyperglycemic subjects have

a metabolic load that is harmful to the β-cells and it has been shown that both elevated fatty acids or glucose contributes to β-cell failure, a process called gluco-lipotoxicity, causing inflammation, oxidative and endoplasmic reticulum stress which impairs insulin secretion [25, 26]. The β-cells are also sensitive to reactive oxygen species (ROS) [26] and therefor susceptible to damage of mitochondria, proteins, lipids, and nucleic acids, also contributing to β-cell dysfunction and later to apoptosis [25, 27] and reduced β-cell mass. People with naturally defective cell proliferation cannot increase the β-cell mass when it is needed for more insulin secreting, and have a greater risk to develop T2D later in life [26].

2.2.2 Treatment for T2D

Most people with T2D are overweight and insulin resistant with a higher risk of developing cardiovascular diseases [28, 29], the main cause of death among T2D patients [30]. When diagnosed with T2D or identified to be at risk of developing the disease patients are first recommended to make lifestyle changes, such as improving diet and increase exercise. Proper diet in combination of regular physical exercise have been shown to prevent or delay onset of T2D and to reduce the risk of complications [28, 29]. Unfortunately, diet and exercise is in most cases only effective short term, and the majority of diabetics will with time require medication to control blood sugar levels [31].

There are diverse groups of oral medications approved for T2D, the major ones are biguanides, sulfonylureas, meglitinide, thiazolidinedione (TZD), dipeptidyl peptidase 4 (DPP-4) inhibitors, sodium-glucose cotransporter (SGLT2) inhibitors, or alpha-glucosidase inhibitors [32–34]. Usually patients across all age groups are prescribed a biguanide called metformin as first line T2D therapy [32]. Metformin is a drug that lower blood glucose by inhibiting gluconeogenesis thereby decreasing the glucose production in the liver. It also reduces insulin resistance in other tissues (e.g. improves the sensitivity of insulin in the skeletal muscles by activating the insulin receptors) leading to an increase in the glucose uptake [32, 35]. Because the disease is complex and progressive, over time patients are usually prescribed additional drugs to maintain glycemic control [33, 36], eventually requiring insulin replacement therapy [36].

G-protein coupled receptors (GPCR) belongs to the largest family of membrane bound proteins, and are involved in a number of cell signaling pathways controlling diverse cell functions. GPCRs is a key therapeutic target class exploited by the pharma industry for a range of treatments [37]. These receptors typically bind ligands outside the cell, such as hormones or neurotransmitters, leading to activation of intracellular G-protein which later gives rise to a cellular response. A promising novel target for the treatment of T2D and recent focus for the pharmaceutical industry have been the glucagon-like peptide 1 receptor (GLP1R) [38, 39]. GLP1R agonists (such as Exenatide) represent a unique class of drugs that have similar and enhanced function of a naturally occurring peptide hormone called Glucagon-like peptide 1 (GLP1) that regulates insulin secretion and synthesis from β-cells [40,

41]. The GLP1R is a GPCR with limited tissue distribution and is mainly found in the pancreas, heart, brain and kidney [41]. The receptor is abundantly expressed in the pancreatic islets, specifically in β-cells and δ-cells [40, 42] making it highly attractive for developing tissue specific drugs, limiting the risk of side effects.

None of the currently available medications cures T2D, and specifically are not able to prevent the progressive decline in normal β-cell function and islet mass occurring over time. With the global increase obesity and the emerging epidemic of T2D new curative treatments for T2D remain a major unmet medical need.

2.3 Antisense oligonucleotides

Antisense oligonucleotides (ASOs) are synthetically modified single-stranded DNA molecules usually consisting of 12-25 nucleotides [7]. The fundamental action of ASOs is to bind complementary with Watson-Crick base pairing to mRNA of specific target genes, thereby silencing or alter the gene expression. How the ASOs degrade, disable, or modify the target RNA is complex and occur by several mechanisms, most commonly through the recruitment of RNase H endonuclease (abundant in all eukaryotic cells) cleaving RNA when bound ASO, forming a duplex in the nucleus. Alternatively, the ASOs can be designed to sterically block ribosomes by capping the 5' end to prevent the translation of RNA without degradation [43]. The majority of the ASOs developed for clinical applications are RNase H-dependent.

One key advantage of ASOs is that they can be designed to be highly specific against selected target genes, making ASOs an attractive therapeutic modality by interfering only with the expression of genes causing or linked to disease, reducing the risk for side effects. Therefore, there is a growing interest within the pharmaceutical industry to develop ASOs as treatments for a range of cardiovascular, and neurodegenerative diseases [44], diabetes [7], HIV, Duchenne muscular dystrophy, asthma and cancer [45]. The idea of using ASOs as therapeutic agents was first proposed in the 1970s, the clinical development of ASOs originated in the early 90s and have been under investigation ever since [46], and today there are more than a thousand of publications on this topic when searching on the literature database Scopus. Currently, there are four clinical ASO-based therapies approved by the FDA with more in late stage development [47].

The main organs in the body taking up ASOs from systemic circulation, with the highest accumulation of ASOs are liver and kidney. ASO are large and charged macromolecules, and how ASOs are transported across the cell membrane, and why certain cell types are better at taking up ASO is not fully understood. The inability of most organs to take up ASOs limits the clinical utility and is a major challenge for the pharmaceutical industry. Different approaches are being explored to improve the stability of the ASOs, enhance specificity for binding to the target mRNA and to increase the cellular delivery to the desired tissue or cell type. Modifications to the ASO molecule includes changes in the backbone or replacement of the hydrogen in

the ribose at the 2' position to an oxygen atom bound to an alkyl group or addition of a completely new ligand to the chain [6, 48]. Chemical modification such as 2'-O-methyl (O-Me) have been shown to increase the stability and binding affinity of the ASOs. Phosphonothioate (PS) backbone modifications give a more hydrophobic structure and an improved passage across the cell membrane and internalization. Conjugation of ASO to ligands of high-capacity cell surface receptors has been shown to enhance cell specificity of productive uptake by using receptor internalization to carry ASOs across cell membrane [49–51].

Parkash et al. [51] have shown that ASOs conjugated to triantennary N-acetyl galactosamine (GalNAc), binds to the asialoglycoprotein receptor (ASGPR) which is abundantly expressed on hepatocytes, dramatically improves the uptake of ASO in hepatocytes and enhances the targeted distribution. There was a 10-60-fold improvement compared to unconjugated ASO silencing gene expression observed *in vivo* in mouse models. Recently a group of scientists from AstraZeneca have shown, in collaboration with Ionis pharmaceuticals, that conjugation of ASOs to a GLP1R peptide agonist increases the uptake in pancreatic islets of Langerhans and delivers ASOs to pancreatic β-cells. This is the first demonstration of targeted delivery of ASO to a tissue other than liver, and shows that it is possible to interfere with gene expression specifically in β-cells, a cell type that is completely refractory to uptake of ASO in mice and primates [7, 8]. This kind of discovery opens opportunities for developing new therapies to treat diabetes by specifically targeting the β-cells in the pancreas [7].

2.4 Quantitiative real-time PCR

Quantitative real-time polymerase chain reaction (qPCR) is a powerful and widely used molecular biology technique, that measures in real time how much of the specific DNA template is present in a biological sample as the reaction progresses [52]. This *in vitro* method is commonly used to analyze the expression of desired genes with high sensitivity and specificity. Ever since the technique has come into commercial use in 1996, the number of publications have increased dramatically [53] and today qPCR is a ubiquitous methodology applied across several areas from medical research to agricultural, environmental and food science.

Scientists are for example using qPCR to understand genetic variations and identify genes linked to different human diseases, monitor new diagnostic biomarkers [54], detect different microbial and plant pathogens [55]. It is also possible to use qPCR in dose-response experiments to screen e.g. evaluate the relationship between ASO concentration and silencing of gene expression in cells and cell lines of interest [7, 56].

The technique is based on the polymerase chain reaction (PCR), and just as PCR, it requires buffer, oligonucleotide primers that hybridize to the opposite ends of the target sequence, a heat stable DNA polymerase that binds near the primers

and deoxynucleotides (dNTPs) [57]. During a PCR reaction, three events occurs, denaturation, annealing and elongation of the DNA template. During the first phase, the temperature rises and makes the double-stranded DNA separate into single strands, in the annealing phase the primers bind to their complementary sequences and during elongation, the DNA polymerase binds and starts to extend the primer into a new strand of DNA complementary to the template. As the reaction continues, the newly synthesized DNA is also used as a template for a new reaction, leading to an exponential increase in number of DNA copies, amplifying the original DNA molecule [52, 58].

The difference between PCR and qPCR is that in qPCR the double-stranded DNA synthesized is labeled with a fluorescent dye that is intercalated that makes it possible to monitor the amplification continuously by measuring the fluorescence during each cycle. The fluorescent signal increases as the DNA amplifies, and the signal is proportional to the amount of PCR product that has been synthesized [52, 59].

qPCR is commonly used to quantify gene expression by measuring the amount of messenger RNA (mRNA). Before using qPCR to quantify mRNA, mRNA needs to be extracted from cells or tissue samples, and reverse transcribed into complementary DNA (cDNA). For proper quantification, one critical step is the isolation of mRNA that determines how good the yield and the quality of the mRNA will be [60].

The first step is to disrupt the cells or tissue samples to make the total RNA available, which includes mRNA, ribosomal RNA (rRNA), small RNA (sRNA) and transfer RNA (tRNA). This can be done by mechanical, physical, enzymatic or chemical methods. The extraction and purification of mRNA can be performed by different methods that are either solution based, precipitation, membrane or magnetic bead based [61].

Nowadays the most common way is to use commercially available kits (e.g. RNeasy Mini kit from Qiagen) where the selective binding properties of silica-membrane spin columns are used to isolate and purify mRNA. The columns from the RNeasy kits bind mainly RNA molecules longer than 200 nucleotides, efficiently removing proteins and the majority of genomic DNA (gDNA). This also excludes the smaller 5.8S rRNA, 5S rRNA, and tRNAs, leading to an enhancement of mRNA [62].

Prior to amplification mRNA the has to be reverse transcribed enzymatically into cDNA to allow the PCR reaction. The reverse transcriptase enzyme uses a single-stranded mRNA as a template in the reverse transcription (RT) reaction to produce double-stranded cDNA. The synthesized cDNA, together with primers, DNA polymerase and fluorescent dyes or probes can then be amplified and the data collected used to quantify gene expression [60].

2.4.1 Primer design

Many factors can influence the outcome of a qPCR experiment. One key factor is the design of the primers used in the RT and qPCR reactions.

When selecting primers for the RT there are several primer strategies; gene specific primers, random sequence primers or oligo(dT) primers. Gene specific primers only amplify a specific mRNA sequence. This gives a better sensitivity but limits amplification to one gene. Random primers are usually short (6 bases long) and can anneal at any point and amplify all RNAs (including rRNA and tRNA) which can lead to dilution of the mRNA fluorescence signal. The last group of the commonly used primers are so called oligo(dT) primers which are made of 12–18 deoxythymidines and binds complementary to the polyadenylated part of the mRNA. The advantage of this type of primers is that full length cDNA can be generated, but the disadvantage is that only genes with a poly(A) tail can be amplified. If the mRNA is long the transcription may be disrupted too early. Often the preference is to use a mix of oligo(dT) and random primers [57, 63].

For the qPCR there are common parameters that good primers pairs should have, such as 40-60% guanine and cytosine content, primer length between 18-24 bases, and should have similar primer melting temperature range at 55-65°C [63, 64]. The ideal amplicon (amplified DNA product) size is ∼70-200 bp, and to avoid amplification of anything other than target sequence (e.g. gDNA) either primers or probe should span an exon-exon junction [65]. The designed primer pairs should be fully complementary to the template DNA sequences. Poorly designed primers decrease specificity and sensitivity of the qPCR if primers bind to the wrong place on the sequence or attach to each other (primer dimer) [66].

The workflow for the primer design is first to find the sequence of the target gene, and then design primers using free primer design software available online. Sequences can be found at the NCBI gene database page (`https://www.ncbi.nlm.nih.gov/gene`). By searching for gene and the right species, the NCBI Reference Sequence (RefSeq) of that gene (e.g. "`NM_000194.2`") will be found. For primer design, e.g. IDT PrimeQuest, RealTimeDesign, and primer-BLAST softwares can be used. Careful design of the primers is important and can save both time and money.

2.4.2 Reporter dyes and hydrolysis probes

Reporter dyes are fluorophores that binds non-specifically with high affinity to double-stranded DNA. One regularly used reporter dye is SYBR Green I, which absorbs blue and emit green light [57]. In the mixture with cDNA the dye binds immediately to the double-stranded DNA, giving rise to intense fluorescence only when bound to DNA [53].

As the denaturation, annealing and extension of the cDNA occurs during the PCR reaction, more dye binds to the newly synthesized double-stranded cDNA during each cycle, which leads to an increase of the fluorescence. The advantage of using SYBR Green in qPCR to track the amplification of DNA is because it is a simple, inexpensive method and can be used with various kinds of primers and templates [67]. A drawback that needs to be considered is that it is non-specific and therefore also bind to unwanted and irrelevant double-stranded PCR products. For

example, primers may hybridize to each other, forming so called primer dimers that is amplified by the DNA polymerase forming a new strand that is used as a template competing for PCR reagents, and SYBR Green will bind the double-stranded DNA by-product produced [57].

An alternative approach is to use so called hydrolysis probes, or 5'-nuclease probes, to detect only specific amplification products. These are short oligonucleotides that are designed to bind specifically to single-stranded DNA sequences between the two primers. The probes have a covalently bound reporter dye at the 5' end of the oligonucleotide strand and a quencher dye at the 3' end. The fluorescent signal transfers from the reporter (donor) to the quencher (acceptor) dye, a mechanism called fluorescence resonance energy transfer (FRET) where the distance between the donor and the acceptor is crucial for the signal to transfer. When the probe is intact, the donor and acceptor are in close proximity and the fluorescence emitted by donor is quenched. During the PCR amplification, the primer is elongated by the DNA polymerase, and eventually reaches the probe bound to the single stranded DNA. As the DNA polymerase have exonuclease activity, it then cleaves the probe at the 5' end, separating donor and acceptor and the fluorescence signal is increased. The probe is thereby removed from the target strand and primer extension continues [66, 68]. In this study the most common and commercially available probe, the so called TaqMan probe was used.

2.4.3 Quantification and normalization

The instrumentation for qPCR reactions contains a thermocycler, an apparatus where the samples are placed and have the function to control the temperature of the environment, a light source that excite the fluorescent dyes that are present in the samples, and a photodetector that measures the emitted fluorescence from either the reporter dye or the hydrolysis probe during each amplification cycle. Fluorescence intensities are collected by a software and presented in graphs that represents amplification curves and melt curves [53, 66, 69]. The amplification curves have typically sigmoidal shape with three distinct phases: lag phase, exponential phase and the plateau phase as seen in Figure 2.2.

The y-axis of the graph shows the ΔRn which is the normalized reporter fluorescence intensity measured during a cycle [70] and the x-axis represents the number of cycles. During the first phase (lag phase) the fluorescence signal is low and the changes are negligible and this phase is called the baseline. Any amplification signal within or below the baseline is considered as background noise. As the DNA product starts to accumulate, the fluorescence signal increases exponentially. Once the fluorescent signal exceeds a defined threshold a quantification cycle (C_q) value is obtained [71]. The C_q value is the cycle number that is used in the analysis and is inversely associated with concentration i.e. how much of the target DNA template is initially present in the sample [52]. A qPCR amplification reaction is typically 40 cycles [72]. The more of DNA template present in the sample, the earlier the fluorescent signal reaches the threshold, giving a lower C_q value. A C_q value of $\sim$37

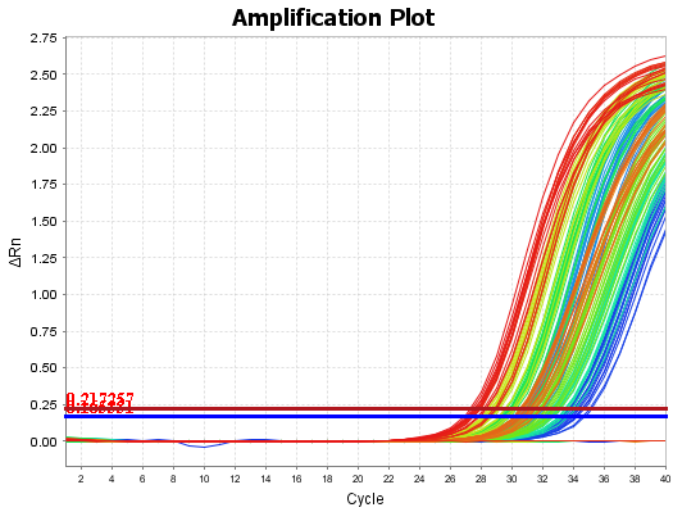

Figure 2.2: Example of amplification plot, showing the generated amplification curves from a qPCR run.

cycles indicates that only one initial DNA template is present in the sample [71]. However, high C_q values could also be a sign of inhibition or degraded RNA in the sample, and different steps in the qPCR process may have to be evaluated.

Most qPCR apparatus also generate melt curves at the completion of a SYBR qPCR reaction, were the fluorescence is measured as a function of temperature [73]. This is when the final PCR products in the samples are exposed to increasing temperature which leads to denaturation of the double-stranded DNA and loss of fluorophores. The melt curve plot visualizes a distinct peak showing the melting point which is unique to the product and depends on the length and composition of the amplicon. A single peak on the melt curve plot suggests that the qPCR product is specific and that there are no other products present [53], see Figure 2.3.

The results that are obtained from the qPCR can be quantified by two different strategies called Absolute quantification or Relative quantification method. The Absolut quantification method determine the amount of molecules in the sample by comparing to a standard curve generated from samples with known concentration [74]. The relative quantification method determines the difference between the target gene and a reference gene, a commonly used method when assessing gene expression [75]. To be able to compare different samples and have reliable results, the mRNA levels of the target gene has to be normalized to the levels of the reference gene in the same sample. A reference gene has to be stably expressed in the cells and tissue types used, and must not change with experimental conditions to serve as a control [74]. Examples of commonly used reference genes for quantifying gene expression are *GAPDH*, *HPRT1*, β-actin and *PPIA* [76].

For accurate normalization it is important to evaluate which reference gene is most stable for a certain cell or tissue type and the experimental conditions used, before performing any qPCR analysis [77]. There are commercially available reference gene panels and different softwares to help select the optimum reference genes [57].

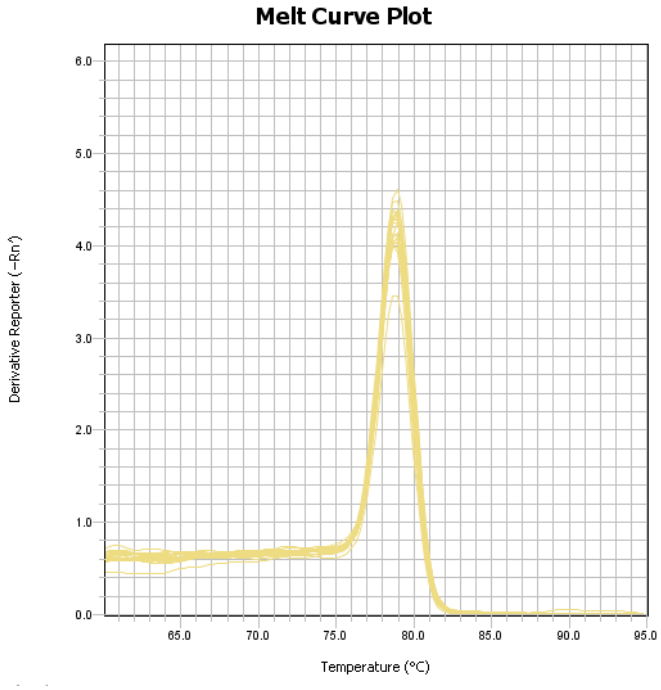

Figure 2.3: Melt curves showing a single peak for a specific product.

The relative expression between samples can be calculated using the Equations 2.1-2.4, were the ΔC_q value between target gene and reference gene is first calculated for each sample and then the difference between e.g. treated and untreated samples are determined by subtracting one from the other. Finally, 2.4 is used to calculate the relative expression ratio. This method is called the $\Delta\Delta C_q$-method or comparative method [78].

$$\Delta C_{q1} = C_q(Target\ gene) - C_q(Reference\ gene) \tag{2.1}$$

$$\Delta C_{q2} = C_q(Target\ gene) - C_q(Reference\ gene) \tag{2.2}$$

$$\Delta\Delta C_q = \Delta C_{q1} - \Delta C_{q2} \tag{2.3}$$

$$Rel.Expr.Ratio = 2^{-\Delta\Delta C_q} \tag{2.4}$$

Another calculation method strategy is the so called ΔC_q-method [79]. This method is used when it is necessary to determine the C_q value for independent samples (and not relate effects to another sample) to establish if a target gene is affected by a treatment or not. The C_q value for the reference gene is subtracted from C_q value for target gene to receive ΔC_q*. The calculated ΔC_q* values from each sample is used in Equation 2.6 to get the relative gene expression.

$$\Delta C_q{}^* = C_q(Target\ gene) - C_q(Reference\ gene) \tag{2.5}$$

$$Rel.Expr.Ratio = 2^{-\Delta C_q{}^*} \tag{2.6}$$

The relative gene expression values can later be used to generate a concentration-response curve by plotting it against the concentration of treatments, in this study the concentration of ASO. For both strategies, the assumption is that the amount of target DNA doubles during each PCR cycle throughout the exponential phase [74, 75].

The amplification efficiency is a measure of the performance of the PCR reaction, and can be determined by measuring how much the DNA increases with each PCR cycle by performing serial dilutions of a sample. For each 2-fold dilution, the difference in C_q values should equal one when the efficiency is 100%, meaning that the DNA doubles with each PCR cycle. Additional content in the samples can interfere with the RT or PCR reaction, leading to an estimated efficiency higher than 100% [74, 80].

2.4.4 Two-step qPCR and one-step qPCR

Reverse Transcription Quantitative PCR (RT-qPCR), i.e. the process of reverse-transcribing RNA into cDNA and then quantitatively amplifing a specific target, can be performed by two different methods; one-step or two-step qPCR. Two-step qPCR is the traditional method, where reverse transcription and qPCR reactions are performed sequentially, in separate tubes. In one-step qPCR, both the reverse transcriptase, DNA polymerase and other reagents are added at the same time, and both reactions are performed in the same tube, leading to less pipetting and lower risk of cross contamination between the samples [81]. Most of the published articles that are using one-step qPCR usually concerns virus detection and development of high-throughput screening assays [82, 83].

As described previously, when quantifying gene expression, the mRNA is usually isolated and purified before continuing with the cDNA synthesis and qPCR reaction. With increasing interest in analyzing the gene expression from single cell or from a small number of cells, other methods are required as purification procedures because there is not enough sample and the purification procedures with multiple washing steps can lead to losses of the already low amounts of transcripts. One way to overcome this, is to do the cDNA synthesis directly on the lyste (solution with lysed cells) without purification step. Lysis buffers disrupt the cell membrane and makes the RNA and all other intracellular components accessible [84].

Commercially available kits have been developed that offer the possibility to perform reactions for reverse transcription and qPCR directly on cell lysates without the isolation and purification steps. However, most cases described in the literature the

focus has been on optimizing and developing assays for analysis of gene expression in single cell [85–87].

Studies have shown that that such assays produce reliable results and can be used in high-throughput (large scale) [86]. For different cell types it is necessary to establish an optimal lysis buffer that does not affect the RNA quality, interfere with cDNA synthesis or qPCR amplification [85]. In this study, using large numbers of cells, all these parameters need to be evaluated.

3

Materials and methods

This section contain information about equipment and materials used and how the different experiments were performed in this project. The general protocol for the two-step qPCR assay used in this study comprises six main steps, seeding cells in a 384-well plate, treating with ASO conjugates, wash and lysis of the cells, performing cDNA synthesis and afterwards running qPCR reaction to generate data and perform data analysis. Systematic trouble-shooting was performed to improve the assay. What was modified or changed will be explained in the following sections.

3.1 Cell culturing

The HEK-293 Flp-In GLP-1R cell line (GLP1R-HEK293) was generated at AstraZeneca, using the Flp-In system (Invitrogen, K6010-01) and the pcDNA5/FRT expression vector (Invitrogen, V6010-20) to stably overexpress the human glucagon-like peptide-1 receptor (GLP1R).

The GLP1R-HEK293 cell line was cultured in DMEM with GlutaMAX (Gibco, 31966) containing 10% FBS and 0.01% Hygromycin B (Invitrogen, 10687010) in a 75 cm^2 T-flask (Thermo Scientific, 156499). Passaging of cells was performed twice a week when the cells had reached 80-90% confluency.

To passage the cells, the cultured cells were washed once with phosphate-buffered saline (PBS) without Ca^{2+} and Mg^{2+} (Gibco, 10010023) and then trypsinized with 0.25% Trypsin-EDTA (Gibco, 25200056) by adding 1.5 mL of the solution to cover the monolayer of cells and incubate at 37°C, 5% CO_2 for 3 minutes. Once the cells started to detach, culture flask was gently tapped on the side. To inactivate trypsin, 10 mL culture medium was added to the flask, followed by gentle pipetting of cell suspension a few times to disrupt any remaining cell clumps. The cell suspension was then transferred to a 15-mL Falcon tube to centrifuge down cells at 270g for 4 min. After the centrifugation, the supernatant was discarded and the cell pellet resuspended in 10 mL of fresh culture medium.

The cell concentration was determined using a NucleoCounter (Chemometec), and a new T75 flask was seeded (13-27.000 cells/cm^2) for continued maintenance culture at 37°C, 5% CO_2.

3.2 Isolation of pancreatic islets from mouse

Islet were isolated from C57BL/B6CrL mice obtained from Charles River. The handling, anesthesia and surgical operations of the mice were performed by AstraZeneca employees educated in these techniques, and in accordance with institutional guidelines for animal experimentation. The protocol used was an AstraZeneca in-house protocol.

Islets were isolated from euthanized mice using collagenase perfusion of the pancreas. Perfused pancreas were then surgically removed and placed in cold Hank's balanced salt solution, HBSS (Gibco, 14025) in 50-mL Falcon tubes, and shaken to dissolve the pancreas. The dissolved tissue was washed four times with HBSS. Between each wash islets were allowed to sediment and the supernatant removed to remove exocrine tissue. The islets were place in a Petri dish (Corning, 430589) and handpicked under a dissecting microscope using a Gilson pipette and transferred to a new Petri dish containing 10 mL RPMI1640 medium (Gibco, 21875-034) with 10% FBS (HyClone, CH30160.03) and 1% Penicillin-Streptomycin (Gibco, 15140-122). Isolated islets are shown in Figure 3.1. The islets were cultured in an incubator at 37 °C, 5% CO_2.

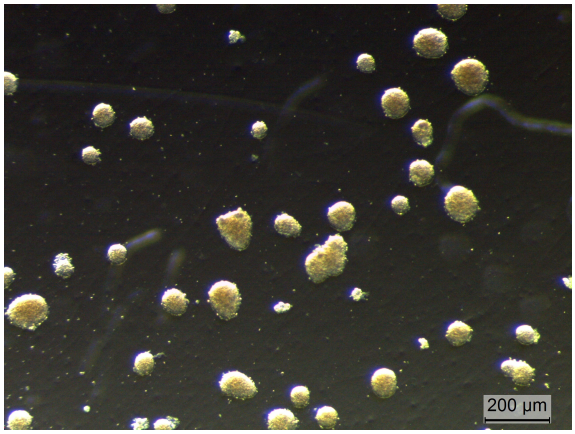

Figure 3.1: Isolated islets from mouse in a Petri dish with culture medium.

3.3 Semi-automated two-step qPCR assay

A research group at AstraZeneca has previously set up a high-throughput two-step qPCR assay for primary differentiated adipocytes to quantify gene expression of a specific target gene in response to compound treatment. Because there is a duty of confidentiality at AstraZeneca, the project mentioned will be referred to as the adipocyte-project throughout this master thesis. The protocol developed was based on the Power SYBR™ Green Cells-to-CT™ Kit from Thermo-Fisher Scientific (4402955) with some modifications made to reduce the costs and allow scaling up the assay.

To mimic the adipocyte cell density at the time of lysis, 7000 GLP1R-HEK293 cells were seeded in a volume of 35 µl medium per well in a 384-well CellBIND®

microplate (Corning, 3770) using a Multidrop Combi Reagent Dispenser (Thermo Scientific). The cells were then cultured for 24 h at 37°C, 5% CO_2. After 24 h, the cells were treated with 14 different ASOs or GLP1-conjugated ASOs (synthesized at Ionis Pharmaceuticals).

Since the purpose of using the assay is to study effects of different concentrations of ASOs, and from the concentration-response curves calculate half-maximal (EC50) and maximal (efficacy) inhibition of gene expression, the ASOs were first serially diluted in a 384-well compound plate (Greiner, 781280). The dilution series were made in 8x higher concentrations than the final concentrations exposing the cells, starting at 80 µM, diluted 1:3 in cell culture medium into 11 points, ending with the lowest concentration, 1.4 nM. Two of the ASOs had to be analysed at lower concentrations, from 24 µM down to 0.4 nM. For each ASO, duplicate dilution series were prepared. The wells of two columns contained only cell culture medium to be added to the cell plate to serve as untreated controls. 5 µl ASO dilutions or medium from the 384-well compound plate were then transferred to the corresponding wells of the 384-well plate seeded with GLP1R-HEK293 cells, using a CyBi-well Multichannel Pipettor (CyBio, Figure 3.2). After the addition of ASOs the cells were cultured for another 24 h at 37°C, 5% CO_2.

Figure 3.2: CyBi-well Multichannel Pipettor was used for transfer of diluted ASO or medium from wells of 384-well compound plate to corresponding wells of cell plate.

The next day, the adipocyte-project lysis buffer was prepared containing 2% TritonX-100 (Sigma, T8787), 2% Nonidet P-40 (synonym IGEPAL® CA-630, Sigma, I8896), RNA Secure (ThermoFisher Scientific, AM 7006), RT buffer (ThermoFisher Scientific, 4391852C) and RNase-free water.

The Bravo Automated Liquid Handling Platform (Agilent, Figure 3.3) was used to remove medium from wells and to wash (twice) with cold Dulbecco's PBS (DPBS, Gibco, 14040). The cells were inspected both before and after the wash using a microscope to see if any cells had detached. After washing the cells, 30 µL lysis buffer was added to each well, using a Multidrop Combi Reagent Dispenser to lyse

the GLP1R-HEK293 cells. Cells were incubated for 5 min and the lysates were then pipetted up and down to mix, using the Bravo Automated Liquid Handling Platform. The cell lysate plate was stored at -20°C prior to cDNA synthesis.

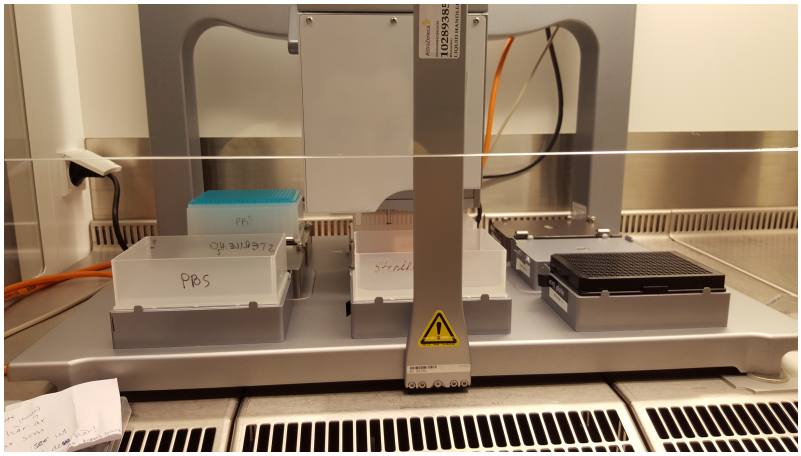

Figure 3.3: Bravo Automated Liquid Handling Platform was used to remove the medium from the 384-well cell plate, wash the cells and mix the lysate.

For the cDNA synthesis, reverse transcription (RT) master mix solution was prepared containing 1x RT Enzyme Mix (ThermoFisher Scientific, 4391852C), 1x RT buffer and RNase-free water. 11 µL of this solution was dispensed to each well of a rigid 384-well PCR plate (Axygen, PCR-384-RGD-C) using a Multidrop Combi Reagent Dispenser. From the plate containing cell lysates, 7 µL was transferred to the rigid 384-well PCR plate using a VPrep Liquid Handling Pipetting Station (Agilent), see Figure 3.4. The rigid PCR plate was then sealed and centrifugated at 216g for 1 min.

Figure 3.4: VPrep Liquid Handling Pipetting Station that was used for transfer of lysate to the rigid 384-well PCR plate containing RT master mix.

The cDNA synthesis was performed in a DNA Engine (MJ Research) with 384-PCR block set on 37°C for 60 min, 95°C for 5 min and 4°C infinity. After the run the plate was removed and stored at -20°C until further processing.

On the day of qPCR analysis, the cDNA plate was thawed and qPCR master mix was prepared by diluting Power SYBR Green PCR Master Mix (Applied Biosystems, 4367659) in RNase-free water. The Multidrop Combi Reagent Dispenser was then used to dispense 6 µL of the qPCR master mix to each well of two MicroAmp Optical 384-well Reaction Plates (Applied Biosystems, 4326270). The VPrep Liquid Handling Pipetting Station was then used to mix and transfer 2 µL cDNA from the cDNA plate to each of the 384-well reaction plates containing the qPCR master mix. One plate was labeled to be used for analysis of expression levels of the target gene, *MALAT1*, and the other for the reference gene *36B4*. The plates were sealed afterwards and centrifuged at 3000g for 1 min to remove any bubbles.

The mixes of forward and reverse primers for *MALAT1* and *36B4* respectively, were added to separate wells of a 384-well polypropylene microplate (Labcyte, PP-0200) and the Echo555 Acoustic Liquid Handler (LabCyte) was then used to transfer 80 nL/well of the primer mixes to the respective 384-well reaction plate containing qPCR master mix and cDNA to get the total concentration of 0.4 µM of the primers. The plates were re-sealed and spun down at 216g for 1 min before the run in a QuantStudio 7 Flex Real-Time PCR System (Applied Biosystems). The expression levels of the target gene of interest (*MALAT1*) were then normalized to the levels of the reference gene *36B4* and data were plotted as ASO concentration-response curves.

3.3.1 Trouble-shooting

The results that were obtained from the first experiment showed unexpectedly large intra-plate variability when comparing C_q-values for *36B4*.

Trouble-shooting was performed to identify which components of the assay causing the variability and need modifications. The trouble-shooting was performed stepwise, and the experiments that will be explained in the following sections involve seeding different cell densities, improving cell attachment, performing smaller manual experiment comparing different lysis buffers, evaluating RNA degradation, modifying programs of the semi-automation equipment used as well as comparing different RT reaction mixes and qPCR assay types.

3.3.1.1 Optimization of cell density and attachment of GLP1R-HEK293 cells

The first step that was investigated was cell seeding density and attachment of the GLP1R-HEK293 cells in the wells. GLP1R-HEK293 cells were seeded in a 384-well CellBIND plate (for comparison), a 384-well BioCoat Collagen 1 plate (Corning, 354667) and a 384-well BioCoat Poly-D-Lysine plate (Corning, 354663) at two different cell densities. The reason for choosing plates coated with collagen 1 and the synthetic polymer Poly-D-Lysine was because these coatings are both commonly known to improve the adhesion of cells to culture vessels.

Half of each plate was seeded with 7000 and the other half with 5000 cells per well in 35 µL culture medium using the MultiDrop Combi Reagent Dispenser to see whether a lower cell density would improve cell attachment. The plates were then cultured for 24h.

The detachment of the cells was investigated by comparing and inspecting the three mentioned 384-well plates, as well as the two cell densities added, before and after the medium was removed and the cells were washed with DPBS using the Bravo Automated Liquid Handling Platform.

To minimize the risk of cells detaching from wells in the 384-well plate when removing medium and washing with DPBS, the program for the Bravo Automated Liquid Handling Platform was modified. The speed of pipetting was further reduced and the distance between tip and well bottom during pipetting was slightly increased. The program for the mixing of the lysis buffer and the cells were kept as it was.

3.3.1.2 Evaluation of adipocyte-project protocol on intact islets

In the interest of time, some initial experiments with primary islets were performed in parallel to the GLP1R-HEK293 cell experiments. Isolation of pancreatic islets from mouse was performed as described in section 3.2. First, the adipocyte-project protocol was tried out on intact mouse and human islets. This was performed manually in a small scale in a 384-well BioCoat Poly-D-Lysine plate.

One, two or seven islets were placed in separate 384-wells and lysed with 30 µL adipocyte-project lysis buffer during incubation at room temperature. A similar setup was used for 3D InSight™ Human Islet Microtissues (from now on called human islets, InSphero, MT-04-002-01). Islets were inspected in a stereo microscope, and the plate was stored at -20°C until the next day.

The following day, the plate was thawed and cDNA synthesis was performed as described before where 11 µL RT master mix were manually pipetted into wells of a 96-well plate and 7 µL of each lysate were transferred to separate wells.

For the qPCR analysis, separate qPCR master mixes were prepared for each species specific gene (mouse *MALAT1* and *36B4* for the cDNA from mouse islets, and human *MALAT1* and *36B4* for the human islets) containing 0.5 µM of each primer, and 1x Power SYBR Green in RNase-free water. 6 µL of the respective mix was then pipetted manually to wells of a 384-well qPCR plate and 2 µL of each cDNA sample was transferred into the corresponding wells of the qPCR plate.

3.3.1.3 Evaluation of adipocyte-project protocol on primary dissociated mouse cells and qPCR analysis of serial dilutions of cDNA

As the results from the lysis of intact mouse islets, similar to GLP1R-HEK293 cells, were quite variable, the protocol was tried out on dispersed islet cells to see

if that would work better. 100 mouse islets were transferred to a well of a Not-Treated Polystyrene 24-well plate (Costar, 3738) containing 1 mL pre-warmed TrypLE (Gibco, 12604013) and incubated at 37°C for 10 minutes to disrupt islets. The islets were then dispersed by using a 1 mL pipette and carefully pipetting up and down while inspecting under a stereo microscope. The dissociated islets were transferred into a 15-mL Falcon tube containing 9 mL of the same RPMI1640 medium used for pre-culture and centrifuged at 180g for 3 min. The majority of the supernatant was then removed and the cell pellet resuspended in ∼0.5 mL remaining culture medium, before counting cells using a Bürker chamber and a microscope. Cells were also control counted using a Countess Cell Counter (Invitrogen).

The islet cells were manually seeded in a 96-well BioCoat Poly-D-Lysine plate; two wells each of 4000, 4500, 5000, 7500, 10000 and 12500 cells/well in 150 µL culture medium. The cells were cultured for 24 h followed by the same procedure for lysis, cDNA synthesis and qPCR analysis of *36B4* and *MALAT1* as described before. Before the qPCR analysis 1:2 dilutions were performed on the cDNA to determine the efficiency of the qPCR. Undiluted or 1:2 or 1:4 diluted samples were used.

The first experiment with dissociated cells resulted in very low C_q-values for both *36B4* and *MALAT1*, meaning that the number of cell per well could be reduced. A similar experiment was therefore performed where only 4000, 2000, 1000, 500 and 250 cells/well were seeded. The cells were cultured for 24 h and lysis and cDNA synthesis was then performed the same day, without freezing of the lysate plate, followed by qPCR analysis. From this experiment and further the cDNA synthesis was always performed directly after the lysis of the cells.

Dilution series were also performed on five cDNA samples from the second experiment with dissociated mouse islets. In these samples, levels of mouse *HPRT1*, *MALAT1*, *GAPDH* and *36B4* were analysed in dilution series from wells containing 4000, 2000, 1000, 500 and 250 cells. All cDNA samples were analysed both undiluted as well as 1:2, 1:4, 1:8 and 1:16 diluted with all 4 qPCR assays.

The results from the qPCR reactions were analysed to evaluate if the amplification were linear and approaching 100% efficiency or whether amplification seemed inhibited.

3.3.1.4 qPCR analysis of serial dilutions of cDNA from GLP1R-HEK293 cells to evaluate the estimated amplification efficiency

To evaluate whether the intra-plate variability was caused by some factor in the lysates inhibiting the qPCR reactions, the estimated amplification efficiencies were determined by diluting cDNA template from GLP1R-HEK293 cells.

Eight cDNA samples from a previous GLP1R-HEK293 two-step cell experiment was used, and diluted 1:4, 1:8, 1:16 and 1:32 in a 96-well non-skirted PCR plate (VWR, 732-2387). For the qPCR analysis, SYBR Green master mixes were prepared for the target gene *MALAT1* and reference genes human *36B4*, *HPRT1* and *GAPDH* and a

separate TaqMan master mix for the reference gene *PPIA* (pre-designed hydrolysis probe qPCR assay, Applied Biosystems, Hs04194521_s1). Some qPCR assays are more sensitive to inhibition than others, therefore some additional reference genes were included in this experiment. SYBR master mixes contained 0.5 µM of each primer and 1x SYBR Green buffer. The TaqMan master mix contained 1xTaqman Gene Expression Master mix and 1x TaqMan assay.

Four cDNA dilution series were analysed with each reference gene, each qPCR reaction consisting of 2 µL cDNA dilution and 6 µL master mix.

Human and murine reference gene panels (TATAA) were later screened by co-supervisor Charlotte Wennberg Huldt to select the optimal, most stably expressed reference gene for GLP1R-HEK293 cells and mouse pancreatic islet cells. The results from the reference gene panels showed that *HPRT1* was the optimal reference gene for normalization both for GLP1R-HEK293 cells and pancreatic islet cells from mouse.

3.3.1.5 Comparison between cell densities, lysis buffers and amount of lysate used for the RT reaction

The results from the experiments described in section 3.3.1.4. indicated major problems with inhibition, possibly both in the RT and qPCR reactions.

A new experiment was set up comparing three different combinations of lysis buffers and activated or non-activated RNA Secure, as well as two different concentrations of lysate in RT reactions. In addition three different cell densities were also used, to see if inhibition of RT or qPCR reactions could be reduced.

The cell densities tested were 7000, 4000 and 1000 cells per well. The lysis buffers used were 0.3% Nonidet P-40/0.1% BSA with activated RNA Secure, and adipocyte-project lysis buffer either with activated or non-activated RNA Secure. Nonidet P-40 will from now on be called NP40 throughout the report. The RT Buffer reagent was excluded from the adipocyte-project lysis buffers, for several reasons. A study performed by Khei Ho, Xu Ting and Phon Too [86] showed that good PCR amplification was achieved using the same lysis buffer without RT Buffer reagent. Also, no arguments as to why this buffer was included in the adipocyte-project protocol was found. Usually, this buffer is used in the RT reaction only.

Three replicates of each combination of conditions were performed. After the addition of lysis buffers to cells, the lysates where RNA Secure should be heat-activated were transferred to wells of a 96 non-skirted PCR plate. The plate was sealed and incubated for 10 min at 60°C, followed by cDNA synthesis in the same way as for the other samples, using either 10% or 4% lysates in the RT reactions. Minus-RT control reactions were also made for each lysis buffer and cell density.

Serial dilutions were then performed of all cDNA samples, resulting in 1:4, 1:8, 1:16 and 1:32 dilutions that were analysed with the recommended reference gene *HPRT1*.

Minus-RT reactions were analysed 1:4 diluted. In addition to this, *36B4* was also included to evaluate the levels of gDNA contamination.

The qPCR master mixes were prepared as described before, and pipetting of 7 µL *HPRT1* master mix and 3 µL cDNA dilution was performed in triplicates using Biomek NX^P liquid handler (Beckman Coulter as seen in Figure 3.5). Pipetting of qPCR reactions for *36B4* was performed manually. The amplification reactions were run in a QuantStudio 7 Flex Real-Time PCR System as for previous experiments.

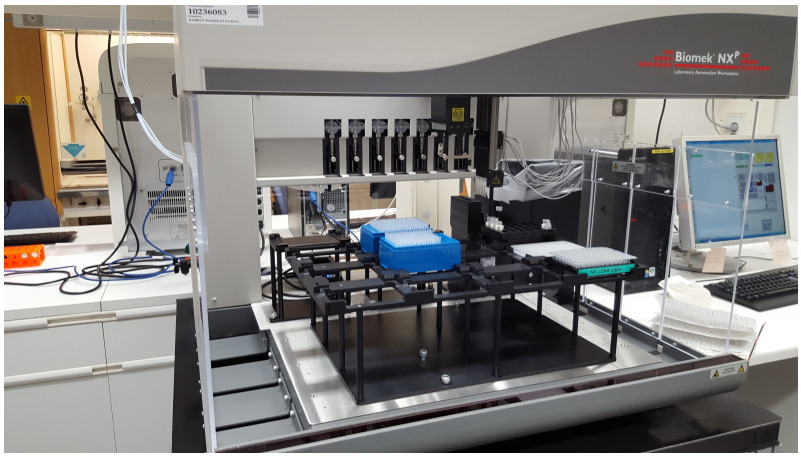

Figure 3.5: Biomek NX^P liquid handler used for pipetting qPCR master mix and transferring cDNA template from a 96-well plate.

3.3.1.6 Comparison of lysis buffers with and without DTT and DNase treatment

In an effort to reduce the gDNA contents of the lysates, 0.3% NP40/0.1% BSA and a second lysis buffer consisting of 0.1% BSA only [84] were tested with and without the addition of 2U DNase/well (Ambion, TURBO DNA-free kit AM1907) and 5 mM Dithiothreitol (DTT) (Thermo Scientific, R0861). DTT was included to reduce the activity of RNases that are present in the lysates and thereby preventing RNA degradation. A comparison was also made to see if spinning down the cell debris in the wells before sampling for cDNA synthesis would reduce the inhibitory effects seen in previous experiments. The RNA Secure solution was not included in this experiment because it seemed not give any noticeable improvement when activated in the previous experiment.

30 µL from the respective lysis buffers were added in three wells each and were left to lyse the cells for 10 min at room temperature. All cDNA syntheses from now on were performed using only 10% lysate in the RT reaction. A RT reaction plate was pre-filled with 18 µL of RT master mix. 2 µL lysates from wells containing only 0.3%NP40/0.1% BSA and 0.1% BSA were transferred to the corresponding wells of the RT reaction plate. 10 µL of the lysates containing DNase and DTT were transferred to separate Eppendorf tubes.

The 384-well lysate plate was then centrifuged at 1000g for 2 min to pellet intact nuclei, and sampling was repeated. From the wells containing only 0.3%NP40/0.1% BSA and 0.1% BSA another 2 µL were transferred to new wells of the RT reaction plate. The remaining lysates in wells containing DTT and DNase were transferred to new Eppendorf tubes. All Eppendorf tubes were then incubated at 37°C for 20 minutes. Afterwards, 0.1 volume resuspended DNA Inactivating Reagent was added to all tubes and incubated 5 minutes at room temperature. The tubes were spun down at 10000g for 2 minutes. 2 µL of each of the DNase-treated lysates were then transferred to the corresponding wells of the RT reaction plate and cDNA synthesis was performed.

All cDNA samples were serially diluted 1:5, 1:10, 1:20 and 1:40 before qPCR analysis. Master mixes containing primers for human *HPRT1*, *MALAT1* and *36B4* were prepared as described before and a Biomek NX^P liquid handler was used to pipette the *HPRT1* and *MALAT1* qPCR reactions in triplicates as in the previous experiment. The qPCR reactions for *36B4* were pipetted manually, consisting of 1:5 diluted cDNA and -RT samples for each lysis buffer.

3.3.1.7 Semi-automation of two-step qPCR assay using 0.3% NP40/0.1% BSA lysis buffer

This experiment was performed to see if automation improved the experiment with 0.3% NP40/0.1% BSA lysis buffer. This experiment was performed in parallel to the one described in section 3.3.1.6.

The program for the VPrep Liquid Handling Pipetting Station was modified to transfer 2 µL lysate instead of 7 µL, to a plate with 18 µL RT-master mix, to get the 10% lysate that was used in the previous manually performed experiment.

A 384-well plate was seeded with 7000 GLP1R-HEK293 cells per well and incubated for 24 h. The following day, a CyBi-well Multichannel Pipettor was used to treat odd columns of cell plate with 0.1 µM of a GLP-1-conjugated *MALAT1* ASO (GLP1-*MALAT1*-ASO), while even columns received the same volume of culture medium. The plate was incubated for another 24 hours.

Cells were washed and lysed in 0.3% NP40/0.1% BSA as described in the previous automation experiment (section 3.3.), and cDNA synthesis set up with 2 µL lysates and 18 µL RT master mix. After cDNA synthesis, a VPrep Liquid Handling Pipetting Station was used to dilute cDNA samples 1:4 before qPCR. The reason for diluting the samples 1:4 prior to qPCR reaction, was because it was seen from previous experiments that the C_q values in the undiluted samples were good and that it was possible to routinely dilute the samples at least 1:4 to try to bring down the concentration of anything that could be inhibiting downstream reactions.

Two qPCR plates were then prepared, one each for human *MALAT1* and *HPRT1*. The master mixes containing qPCR primers were prepared according to previously described protocol. A difference between this experiment and the automated experiment described in section 3.3 was that due to technical problems a Biomek FX^P laboratory automation workstation (Beckman Coulter), seen in Figure 3.6 was used to add 6 µL qPCR master mix and 2 µL diluted cDNA into each plate.

Figure 3.6: The Biomek FX^P laboratory automation workstation was used to pipette qPCR master and transfer diluted cDNA in the 384-well plate.

3.3.1.8 Quality control of the RNA using an agarose gel

To estimate the quality of the mRNA in the lysate, an agarose gel was used. From an agarose gel it is possible to visualize and distinguish degraded and intact RNA by looking at the bands from 18S and 28S ribosomal RNA. If samples contain much gDNA that may sometimes also be seen from the gel.

Fresh lysates were prepared using GLP1R-HEK293 cells that were lysed with four different lysis buffers; 0.3% NP40/0.1% BSA, 0.1% BSA, RLN buffer with 1 mM DTT and Cellulyser Micro lysis buffer (TATAA Biocenter). RLN is a lysis buffer provided in the RNeasy 96 kit (Qiagen, 74181), specifically developed for isolation of cytoplasmic RNA. From the protocol it was recommended to add 1 mM DTT. Cellulyser Micro is a commercially available lysis buffer from TATAA Biocenter.

Five lysates were prepared for each lysis buffer, each lysate representing 7000 GLP1R-HEK293 cells that had been lysed in 30 µL lysis buffer. The five lysates belonging to the same lysis buffer were pooled and loaded in two wells each in a E-gel General Purpose 1.2% agarose (Invitrogen, G501801) containing the nucleic acid stain ethidium bromide (EtBr). Each well contained approximately 20 µL lysate. The gel was run in a E-gel iBase (Invitrogen) to run the electrophoresis.

3.3.1.9 Pre-study to select conditions for a following experiment

To exclude that the variability problems were related to plate format, a comparison was planned between one 96-well plate prepared with the traditional RNeasy 96 kit protocol and one 96-plate manually lysed and analyzed using the two-step qPCR protocol. Before this experiment was performed a pre-study was needed to decide which conditions to use for the two-step qPCR protocol.

The pre-study contained two parts: a visual inspection of cells after lysis with the different lysis buffers, and a qPCR analysis of serial dilutions of cDNA from the selected lysis conditions.

Three lysis buffers were prepared (0.3% NP40/0.1% BSA, 0.1% BSA and the adipocyte-project lysis buffer) including RNA Secure but without 2x RT buffer. RLN lysis buffer from the RNeasy 96 kit was also included, tested both as it is and with the addition of 1 mM DTT mentioned as recommended in the kit protocol. After the addition of lysis buffers to cells, a microscope with a camera was used to follow the lysis process and take pictures. After 5, 10 and 15 minutes, the lysates were mixed carefully to see if it resulted in any visual differences.

Based on the visual inspection 0.1% BSA, RLN buffer and RLN buffer with 1 mM DTT was chosen for the second part of the pre-study. No visual differences were seen between the different time points mentioned.

Two different protocols for the cDNA synthesis were chosen to do a comparison, the adipocyte-project cDNA synthesis protocol and the High-Capacity cDNA Reverse transcription kit (Applied Biosystems, 4368814). One RT plate for each master mix was prepared by pre-dispensing 18 µL RT master mix to the relevant wells. After adding lysis buffers to cells, the lysate plate was incubated for 5 min at room temperature, mixed carefully 3 times and was then placed on ice.

A comparison between samples prepared with and without a centrifugation step to remove nuclei in the lysate (for RLN buffer with and without 1 mM DTT) was done by first transferring 2 µL from all the different lysates to wells of the two RT plates in six replicates each. The lysate plate was then centrifuged at 2000g for 1 minute and 2 µL of each sample transferred to a new RT plates. Minus-RT reactions were only performed for the high-capacity cDNA reverse transcription reactions, on both uncentrifuged and centrifugated lysates. The two RT plates were sealed and spun down at 700g for 1 minute. The adipocyte-project RT reactions were ran as described previously, while the temperature conditions for the High Capacity RT reactions were 10 min at 25°C, 120 min at 37°C, 5 min at 85°C and 4°C ∞.

All cDNA samples were analysed as 1:5 dilutions, and three samples from each RLN buffer condition were also serially diluted 1:10 and 1:20 before the qPCR analysis. Master mixes for human *HPRT1*, *MALAT1* and *36B4* (for the comparison of RT and -RT) were prepared as described previously and a Biomek NX^P liquid handler was used to pipette 7 µL of the master mixes and 3 µL cDNA templates in triplicates to the qPCR plate. The qPCR reactions for *36B4* were pipetted manually, consisting of 1:5 diluted cDNA and -RT samples for each lysis buffer.

3.3.1.10 Comparison between lysate and traditional column-purified RNA

Two replicate 96-well plates of GLP1R-HEK293 cells were treated with ASOs or ASO conjugates. qPCR analyses were then performed either on cDNA from lysates or from traditional RNeasy column-purified RNA.

30000 cells were seeded in 90 µL medium/well in two Poly-D-Lysine coated 96-well plates (Corning, 354461) and were cultured for 24 h.

The cells were then treated with 3 different ASOs or GLP1-conjugated *MALAT1* ASOs, serially diluted in a 96-well compound plate (Greiner, 650201). The dilution

series were made in 10x higher concentrations than the final concentrations to be used on cells, starting at 100 µM, diluted 1:4 in cell culture medium into 9 points, with a final lowest concentration of 1.5 nM. For each ASO, duplicate or triplicate dilution series were prepared. The wells of three columns received cell culture medium only; these wells represented untreated controls. 10 µl from each well of the 96-well compound plate were then manually transferred to corresponding wells of the two 96-well plate with the seeded GLP1R-HEK293 cells, using a multichannel pipette. After the addition of ASOs the cells were cultured for another 24 h.

One 96-well plate was lysed with 150 µL RLT buffer and the RNA purification was performed according to RNeasy 96 spin kit protocol, without DNase-treatment, in an elution volume of 1x45 µL. The RNA concentration was determined using a Nanodrop 1000 (Thermo Scientific) and 14 µL RNA of each sample was used for cDNA synthesis corresponding to ∼770-1350 ng/cDNA synthesis reaction. The cDNA synthesis was performed using the High-Capacity cDNA Reverse Transcription Kit according to previously described temperature program.

The cells in the second 96-well plate was lysed with 120 µL RLN buffer/well and incubated 5 min on ice before centrifugation. The cDNA synthesis was performed directly from the cell lysates as described before using the adipocyte-project RT master mix and 2 µL lysates in a total volume of 20 µL.

Before qPCR analysis the cDNA from the first plate were diluted 1:50 while the second plate were diluted 1:5, estimated to correspond to some 2-4 ng RNA per qPCR reaction. Each template plate was analysed for both human *HPRT1* and *MALAT1* expression, using the Biomek NX^P liquid handler to pipette 3 µL of cDNA and 7 µL Master mix in triplicates for each sample.

To estimate the PCR amplification efficiency, three wells from each cDNA plate were pooled and further diluted 1:2, 1:4 and 1:8. For the qPCR analysis of these dilution series, both SYBR Green and TaqMan (Applied Biosystems, Hs02800695_m1, Hs00273907_s1, Hs00231106_m1) qPCR assays for *HPRT1* and *MALAT1* were used.

3.3.1.11 Comparison of lysis buffers in qPCR analysis using hydrolysis probes

Two 384-well Poly-D-Lysine plates were seeded with 7000 GLP1R-HEK293 cells per well, and cells were cultured for 24 h. After 24 h, the cells were manually treated with serial dilutions of GLP1-*MALAT1*-ASO as described previously. Since five different lysis buffers were evaluated, five replicate blocks of four columns each were treated with the same pattern of ASO serial dilutions in triplicates, or culture medium only as untreated controls. One replicate 4-column block was positioned in cell plate 1 and the remaining four in cell plate 2 to allow for slightly different treatments of the two plates. After the addition of ASOs the cells were cultured for another 24 h.

Cell plates were washed as described previously. In the ASO-treated replicate block of the first cell plate, 30 µL of the adipocyte-project lysis buffer (including RNA

Secure and the RT buffer) was manually added to wells of the four columns and incubated for 5 minutes at room temperature. Cells in the ASO-treated replicate blocks of the second cell plate were lysed with 30µL of either 0.3% NP40/0.1% BSA + RNA Secure, RLN lysis buffer only, RLN + RNA Secure or RLN + 1 mM DTT, and incubated on ice for 5 minutes. Both plates were then mixed as previously described.

Lysate plates were centrifuged at 700g 2 min to pellet cell nuclei and debris before pipetting RT and minus-RT reactions. For the qPCR amplification, TaqMan master mixes (Applied Biosystems, Hs00273907_s1, Hs02800695_m1), for human *MALAT1* and *HPRT1* were prepared as described before and qPCR reactions of 1:4 diluted cDNA and master mix were pipetted using the Biomek FX^P laboratory automation workstation.

3.4 Data analysis

For every experiment mentioned in the materials and methods section, data analysis was performed after the qPCR amplification reaction. The amplification curves from each experiment were inspected to see if they were sigmoidal. The amplification curve for the no template control (NTC) wells were studied to see if there were any contamination and the -RT to see traces of gDNA. The melt curves were studied to see if there were more than one product in the well (several peaks indicating non-specific products).

A data-sheet with listed C_q values from each well was received from each run. The C_q values were compared and the relative gene expression $2^{-\Delta C_q}$ was calculated according to Equation 2.5 - 2.6 found in section 2.7. These values were used to generate the concentration-response curves by plotting against the concentration of ASO.

The estimated efficiency of the qPCR was determined by performing serial 1:2 dilutions of each sample and calculating the difference between C_q values (ΔC_q) sequentially. If the estimated efficiency of the qPCR is 100% there should be a 1 C_q difference between each 1:2 dilution step (log 2 scale).

For all C_q values the standard deviation (SD) was calculated to determine how much the values are spreading from the mean.

4

Results and Discussion

4.1 Semi-automated two-step qPCR

In the adipocyte-project assay, levels of a low expressed target gene was measured and normalized to the expression of the reference gene *36B4*. *36B4* is a single-exon gene, which means that a qPCR assay will also pick up traces of gDNA. Their successful use of *36B4* in the adipocyte-project assay, suggested that the presence of gDNA in the lysates may not be a major problem. With this in mind, the assumption was made that the adipocyte-project protocol would work also in our setting, with some minor changes regarding e.g. cell type, seeding density, compound treatment and target gene qPCR assay. Therefore, the first experiment was performed more or less according to the already available protocol.

A 384-well plate was seeded with similar number of cells as in the adipocyte-project protocol, and after 24 hours treated with 14 different serially diluted GLP1-ASO conjugates. After another 24 hours the cells were lysed with the adipocyte-project buffer and in the cDNA synthesis, 39% of the total volume of the RT reaction solution consisted of lysate. The qPCR analysis was separately performed for *36B4* and *MALAT1* using Power SYBR green PCR Master mix containing primers. From C_q values, relative expression levels of *MALAT1* were calculated and the concentration-response curves were plotted for each ASO. Three of these are exemplified in Figure 4.1.

For this type of assay, concentration-response curve usually has a sigmoidal curve, but none of the curves generated had this feature. As the treatment is expected to inhibit gene expression, there should be dose-dependent reduction of the expression of the target gene. From Figure 4.1 b-c it is possible to see that the relative expression values are variable, with many outliers and large variability between the replicates.

To find out the reason for the strange curves, the C_q values for *36B4* for each well from the qPCR amplification reaction, were presented according to the plate-layout (Figure 4.2) and were studied in more detail. By looking at the plate-layout, a variability of 4 C_q-values difference (15.9-19.9) is seen over the plate. This represents a 16-fold difference in expression levels and the same levels of variability was also seen among untreated control wells around the black lined square; row A and P,

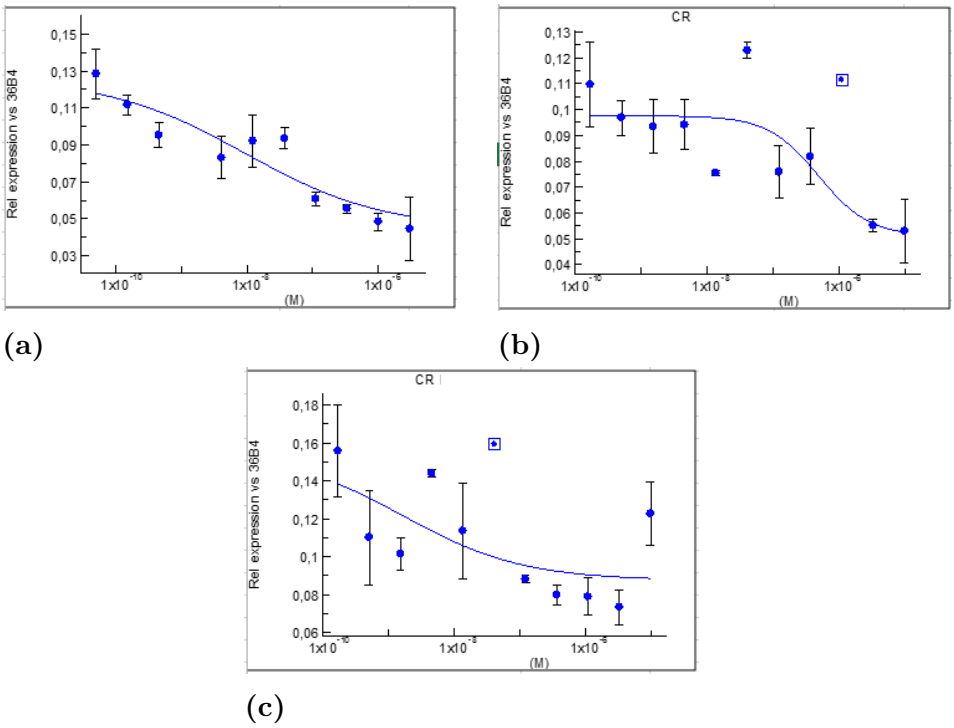

Figure 4.1: Concentration-repose curves, where each data point, the mean±SEM of the relative expression of *MALAT1* normalized to *36B4* was plotted against the concentration of three different GLP1-*MALAT1*-ASO (a-c).

	1	2	3	4	5	6	7	8	9	10	11	12	13	14	15	16	17	18	19	20	21	22	23	24
A	16,7	17,4	17,0	16,7	18,7	17,7	17,5	17,6	16,8	16,9	17,8	18,5	17,6	18,0	17,2	18,2	17,0	17,2	16,7	16,9	16,9	16,6	17,8	16,9
B	16,3	16,8	17,3	16,4	17,1	17,9	19,5	17,1	16,8	17,2	16,6	18,4	17,1	17,2	16,9	17,3	17,4	17,4	17,7	16,9	19,1	17,7	17,3	19,5
C	17,1	17,9	16,8	17,1	18,2	16,4	17,6	18,1	17,9	16,9	17,0	16,8	16,9	16,2	18,3	17,1	17,8	19,1	17,6	16,7	19,6	17,7	17,2	19,1
D	16,9	17,0	17,1	16,9	16,6	16,9	17,1	17,1	18,3	16,5	17,0	17,3	16,6	16,6	16,4	16,4	16,5	16,9	17,2	16,9	17,1	17,8	18,9	17,7
E	17,3	17,3	16,5	16,9	16,8	17,6	16,9	16,4	18,5	17,2	16,4	17,2	16,5	17,9	17,3	16,3	16,5	16,4	17,9	16,8	17,1	17,5	18,2	16,6
F	15,9	16,8	16,2	16,5	17,2	17,4	16,5	16,7	16,4	16,6	17,4	16,3	17,1	16,4	16,6	16,4	16,6	17,4	16,6	17,9	17,2	17,2	19,3	17,6
G	16,5	17,7	16,7	17,0	16,8	16,6	17,3	16,8	17,0	16,5	16,6	17,1	16,8	16,1	16,2	16,5	16,6	17,5	16,9	16,4	16,4	17,4	19,3	16,4
H	16,7	18,0	16,2	16,5	16,7	16,9	17,6	16,7	16,6	16,4	16,6	16,8	17,1	16,2	16,4	17,8	16,3	17,1	16,7	16,7	17,2	17,1	18,0	19,9
I	16,9	17,5	16,5	18,1	17,5	16,5	17,2	16,5	16,9	16,7	16,7	16,8	18,2	16,1	16,7	16,8	16,5	17,4	15,7	16,7	16,6	16,6	17,9	19,4
J	16,6	19,2	16,8	16,4	16,4	16,1	16,7	16,8	16,8	16,9	16,5	18,6	16,7	19,0	15,9	16,7	19,1	17,7	16,7	16,7	16,8	16,8	18,6	19,1
K	16,5	17,7	16,7	17,4	16,6	16,9	16,7	16,7	16,9	16,5	17,4	18,5	17,9	17,1	16,0	17,7	16,8	18,1	17,8	16,4	17,0	17,1	18,2	19,7
L	16,9	19,0	16,5	17,1	16,8	16,9	17,3	17,1	17,5	16,8	18,1	16,8	16,5	16,9	16,7	16,5	17,1	17,3	17,1	17,1	17,1	18,5	17,1	17,8
M	16,9	18,1	17,1	17,8	19,3	16,9	17,2	16,8	17,0	17,1	16,6	17,3	17,8	16,7	16,2	17,1	16,8	16,8	17,0	16,6	16,9	18,5	17,4	17,3
N	16,9	18,8	17,0	17,4	16,8	17,1	16,6	17,3	17,2	16,7	16,5	17,5	17,1	16,0	16,9	16,4	17,0	16,9	17,2	17,6	17,1	19,2	19,9	17,8
O	16,9	17,8	17,2	16,5	17,0	16,9	17,9	17,0	17,5	16,4	17,3	17,8	18,6	16,1	16,3	16,4	16,8	16,8	16,9	17,1	17,4	16,9	17,0	16,6
P	17,6	16,6	16,3	17,1	16,5	17,1	19,7	16,8	16,6	17,1	16,6	18,2	17,4	18,9	17,7	17,4	16,6	16,9	17,1	17,4	17,5	17,8	17,7	18,1

Figure 4.2: Plate-layout with the obtained C_q values for reference gene *36B4* from the first experiment, which was used to normalize the *MALAT1* data.

column 1 and 13. This variability could explain the concentration-response curves in Figure 4.1.

The expression levels of *36B4* should not be affected by ASO-treatments, and should be similar over the plate since the same cell numbers were seeded in all wells. What could be causing this 4 C_q variability? To tackle this unexpected problem in an effective way, possible factors were identified that could be contributing to the variability:

From the visual inspection of the cells before lysis, after removing medium and washing with DPBS, it was noticed that in some wells cells had detached from the plate. Detachment of cells from the wells could be part of explaining the variability in C_q values, but likely not the only reason behind a 16-fold difference in expression. If

variability was caused by detachment alone, the concentration-response curves would look normal since the *MALAT1* expression is normalized to *36B4* (i.e. normalization to a reference gene accounts for any changes in cell number). Another possible factor could be that the cells are lysed unevenly in the wells (incomplete lysis).

During the last step of the experiment (prior to qPCR analysis), the Multidrop Combi Reagent Dispenser was used to dispense the qPCR master mix and the VPrep Liquid Handling Pipetting Station was used to transfer cDNA and mix the solution in each well. Small bubbles were noticed in the wells, that where not possible to remove completely by centrifugation. The Echo555 Acoustic Liquid handler was later used to dispense 80 nL primers in each well. This means that there is a possibility that the primers were dispensed on top of the bubbles and not added to the reaction mixture, leading to an uneven amount of primers in the wells. The assay contains different pipetting steps and small pipetting errors by the different liquid handlers could together add up to a large variability. Another possible factor that was considered was that when the cells are lysed, all intracellular components are accessible, including gDNA, proteins or other components of the lysis buffer that may inhibit the RT or the qPCR reactions. RNA could also be degraded by RNases present in the lysate. To pinpoint the problem, all of these factors were further investigated.

4.2 Optimization of cell density and attachment of GLP1R-HEK293 cells

From the first experiment it was noticed that GLP1R-HEK293 cells were detached after removing of media and the washing steps. Therefore, cell detachment were investigated by seeding 5000 and 7000 cells in three different plates that were visually inspected after media removal and DPBS washes. 384-well plates with different coatings, BioCoat plate with collagen-1 coating, a BioCoat plate with Poly-D-Lysine coating and a CellBIND plate (which was used in the adipocyte-project) were compared to see if there were any improvements. The program for the Bravo Automated Liquid Handling Platform was also modified (adjusting the pipetting speed) to minimize the detachment further. From the inspection it was seen that cells were still detaching from the CellBIND plate. A clear improvement were seen with the BioCoat Collagen-1 plate, but least cell detachment was seen in the Poly-D-Lysine plate which were chosen for all further experiments.

4.3 Evaluation of adipocyte-project protocol on intact islets

One of the aims in this master thesis was to set up the assay for primary mouse islets. Therefore, preliminary experiments with primary islets were performed in

parallel to the GLP1R-HEK293 cell experiments to see if the adipocyte-protocol was applicable.

A small-scale manual experiment was performed following adipocyte-project protocol, where 1, 2 or 7 islets from mouse were lysed and later a qPCR reaction was performed. A similar experiment was also performed with human-derived microislets (InSphero). From the qPCR results (Table 4.1) for the intact islets from mouse it can be seen that also for this cell type, the C_q values varies for *36B4* with no correlation to the number of islets in the wells. Some C_q values in Table 4.1 are very high suggesting that there may have been too little material (mRNA) in these wells. Mouse islets are variable in size, (from 50-200 µm in diameter) [88] and contain as little as 10 cells and up to 10000 cells per islet [89].

No. of islets	C_q **values,** ***MALAT1***	C_q **values,** ***36B4***	**Rel. Gene Expr,** ***MALAT1***
1	31.3	32.2	1.9
1	27.8	31.4	12.4
1	32.4	32.4	1.0
1	24.6	30.8	75.7
1	29.2	34.7	46.7
1	29.7	32.5	6.6
1	31.0	34.7	12.7
2	25.1	31.0	56.5
2	24.6	32.0	168.7
2	24.5	31.4	123.2
2	28.5	31.6	8.4
2	34.6	36.8	4.4
2	26.2	24.2	0.2
7	31.2	32.2	2.1

Table 4.1: C_q values for gene of interest, *MALAT1* and reference gene, *36B4*, and the calculated relative gene expression from 1-7 intact mouse islets.

The human derived micro islets have all a similar size (average size of 150 µm in diameter) and are made up of equal amounts of cells (around 1000 cells) [90]. From Table 4.2 it is seen that the C_q values for *36B4* for the human micro islets were less variable. The relative expression for *MALAT1* differed significantly between the wells for mouse islets, one well with as much as 600 fold higher relative expression than another. The relative expression for the different mouse islets were expected to be more similar, as seen in the human islets. Some natural variation between cells is possible but this large span indicated that something may be wrong with the protocol. The reason for high difference in relative expression values for mouse islets could be because of incomplete lysis. The islets could be lysed differently because the difference in size and cell number (compactness), or the lysis buffer could be too gentle to make the mRNA accessible from the compact islets.

No. of islets	C_q **values,** ***MALAT1***	C_q **values,** ***36B4***	**Rel. Gene Expr,** ***MALAT1***
1	22.7	24.2	2.8
1	22.9	24.5	3.1
1	21.7	24.3	5.9
2	23.7	24.5	1.7
2	21.7	24.0	5.0
2	20.2	23.3	8.5

Table 4.2: C_q values of gene of interest, *MALAT1* and reference gene, *36B4*, and the calculated relative gene expression from 1-2 intact human islets.

4.4 Evaluation of adipocyte-project protocol on primary dissociated mouse cells and qPCR analysis of serial dilutions of cDNA

The C_q values for human islets were shown to be stable, likely due to the uniform islet size. To try to circumvent the potential problem regarding the incomplete lysis of mouse islets, the islets were dissociated into single cells to see if the measured relative gene expression was more stable using the adipocyte-project protocol. The goal was to determine the amount of cells needed for the qPCR assay to generate a signal and to establish the minimum cell density, to reduce the number of animals needed. To assess the estimated amplification efficiency, 1:2 serial dilutions of the cDNA from each well were made.

The islets were disrupted, cells were counted and seeded in a 96-well plate with different cell densities ranging from 4000 to 12500 cells/well. The cells were cultured for 24 h followed by lysis, cDNA synthesis, and qPCR analysis as described before. Table 4.3 shows that the C_q values for *36B4* are low and that with increasing cell number, the lower the C_q values. This gives an indication that cell number could be further reduced, as the C_q values for 4000 cells are still low.

The difference in C_q values between the undiluted and 1:2 diluted samples were used as a simplified estimation of amplification efficiency. As seen in Table 4.4, these ΔC_q values varies and are lower than 1, which shows that estimated amplification efficiency of the PCR is not 100%. Usually this indicates that something is inhibiting the qPCR assay, and the estimated amplification efficiency should improve when samples are diluted as the concentration of the inhibitor decreases. Therefore, it is often possible to find a dilution factor that allows for an estimated ∼100% amplification efficiency of the samples. In this experiment, the ΔC_q values increased with each dilution, therefore further dilution may improve the amplification efficiency.

Since this first experiment with dissociated cells resulted in very low C_q values for both *36B4* and *MALAT1*, a similar experiment was performed with 4000, 2000, 1000, 500 and 250 cells/well seeded, lysed and analyzed.

No. of Cells/well	C_q **values,** ***36B4***	
4000	23.8	23.2
4500	23.8	22.8
5000	24.5	22.3
7500	22.5	22.4
10000	22.0	21.7
12500	21.4	21.9

Table 4.3: C_q values received from qPCR run from wells containing undiluted cDNA from 4000, 4500, 5000, 7500, 10000 and 12500 primary mouse cells from islets.

No. of cells/well	C_q **values,** ***36B4***	ΔC_q
4000 undil	23.8	
1:2 dil	24.2	0.4
1:4 dil	24.8	0.6
4500 undil	23.8	
1:2 dil	24.4	0.6
1:4 dil	25.1	0.7
5000 undil	24.5	
1:2 dil	24.7	0.2
1:4 dil	25.4	0.7
7500 undil	22.5	
1:2 dil	23.0	0.4
1:4 dil	23.4	0.5
10000 undil	22.0	
1:2 dil	22.2	0.2
1:4 dil	22.8	0.7
12500 undil	21.4	
1:2 dil	21.9	0.5
1:4 dil	22.4	0.6

Table 4.4: C_q values and calculated ΔC_q between each dilution from wells containing cDNA from 4000, 4500, 5000, 7500, 10000 and 12500 cells.

The results from this experiment is summarized Table A.2 in Appendix A and reveal that the C_q value for a cell density of 4000 cells/well, was significantly higher than the value found in the first experiment ($\sim$27 vs 23-24, Table 4.4). However, reflecting on the two experiments, a difference was noticed. In the first experiment the lysed cells were placed in a freezer prior to cDNA synthesis which was not done in the second experiment. Freezing the lysates may cause any remaining, un-lysed cells to

burst, which leads to more mRNA and other intracellular components available in the lysate. This can be a reason why the C_q values are lower in the first experiment, also indicating that the islet cells may have been incompletely lysed in the second experiment.

In addition to that, the ΔC_q values (Table A.2) between dilutions differed a lot in these samples. For *HPRT1*, *GAPDH* and *MALAT1*, not even a trend in the right direction was seen in ΔC_q values. The results from this experiment clearly shows that just switching to dissociated cells is not enough to improve the assay and that other changes are required. The results discussed indicates that complete lysis is important, and that 4000 or possibly 2000 cells/well might work. But in interest of time, a decision was made not to continue to optimize the assay conditions for the primary cells from mouse but focus on the GLP1R-HEK293 cell assay.

4.5 qPCR analysis of serial dilutions of cDNA from GLP1R-HEK293 cDNA

The two-step qPCR assay contains different steps (lysis of the cells, RT reaction and qPCR amplification reaction) and it is difficult to determine which step is causing the intra-plate variability in the GLP1R-HEK293 cells. An investigation was performed to find out if something in the cDNA samples was inhibiting the qPCR reaction by estimating the amplification efficiency as described for mouse islets cells. cDNA samples from a previous two-step qPCR experiment was used, which were serially diluted 1:2 in a 96-well plate before qPCR analysis. In this experiment, different reference genes were also tested to see if there are differences between them.

The ΔC_q values (Table A.3) showed a similar variability as the seen in mouse islet samples. No consistent improvement was seen with higher dilutions. The results were less variable than for the islet cells, but there were still signs of inhibition and large variability between the replicates. In conclusion, there are problems with variability between wells and with the estimated amplification efficiency in this assay. The cause of these problems were further investigated.

Since some component in the samples seemed to be interfering with reactions, a decision was also made to dilute all cDNA samples at least 1:4 before qPCR analysis from now on.

4.6 Comparison between cell densities, lysis buffers and amount of lysate used for the RT reaction

From the previous experiment poor amplification efficiency was seen, possibly due to inhibition. Depending on what component of the lysate is causing the inhibition,

different solutions can be considered. Another lysis buffer may interfere less with downstream applications, result in less gDNA or proteins that could affect RT or qPCR reactions. A reduction of the number of cells in the lysate or using less lysate in the RT reaction may also reduce the inhibitory effect.

Le, Huang, Blick, Thompson and Dobrovic [87] have performed direct lysis qPCR studies on small number of breast cancer cells for gene expression analysis. They tested several lysis buffers to determine which one gave the optimal RNA yield. In their experiment, a lysis buffer containing 0.3% NP40/0.1 %BSA gave a better RNA yield compared to the other ones, therefore this lysis buffer was included in this experiment. According to the ThermoFisher website, the RNA Secure reagent needs to be heated to 60°C for 10 min in order to inactivate any RNases present in the lysate. This is not done in the adipocyte-project protocol. Finally, a publication by Khei Ho, Xu Ting and Phon Too [86] stated that inhibition of RT and qPCR reaction was less likely to occur if the volume of lysate made up for less than 10% of the total volume of the RT reaction. Therefore, RT reactions containing only 10% or 4% of lysates were evaluated, instead of the 39% used in the adipocyte-project RT protocol. Also, three different cell densities were compared, 7000, 4000 and 1000 cells/well.

The results from this experiment (Table A.4, A.6 and A.8 in Appendix A) shows that the estimated amplification efficiency was good for all lysis buffers for 7000 and 4000 cells, except when using 4% lysate of adipocyte-project buffer with activated RNA Secure. At 1000 cells/well, only the 0.3% NP40/0.1 %BSA buffer still worked sufficiently. The estimated amplification efficiency for 0.3% NP40/0.1 %BSA samples was good at all three cell densities, and no difference was seen with either 10% or 4% in the RT reactions. The adipocyte-project lysis buffer with non-activated RNA Secure worked well at the highest cell density and at 4000 cells/well if using 10% lysate. Activated RNA Secure did not work as well as non-activated in the adipocyte-project buffer, especially at 4% lysate. Thus, it seems that reducing the amount of lysate in the RT reactions makes a major difference, and 10% was used in all further experiments.

Since a qPCR assay for the single-exon gene *36B4* will also detect gDNA, a comparison of C_q values for RT reactions and minus-reverse transcriptase (-RT) control reactions lacking the reverse transcriptase enzyme, was performed to give an estimate of how much gDNA was present in the sample. The +/-RT C_q values in Table A.5, A.7 and A.9 in appendix A show that gDNA is present in the samples, but that the amount is small and not significantly affecting the qPCR signal. For example, a 5-C_q difference between +RT and –RT, means that the amount of the gDNA is about 32-fold less than the amount of cDNA in the samples [64]. gDNA may still affect cDNA synthesis or qPCR negatively, so it might be good to try to reduce it further.

To sum up, 10% lysate in the RT reaction significantly improved the estimated amplification efficiency and both 0.3%NP40/0.1% BSA and the adipocyte-project lysis buffer with non-activated RNA Secure worked well. No improvement was seen when reducing cell numbers, therefore the cell density will not be changed and 7000 cells/well used.

4.7 Comparison between lysis buffers with and without DTT and DNase

In an attempt to reduce variability, one more lysis buffer (0.1 %BSA) than 0.3% NP40/0.1 %BSA was evaluated. Studies have shown that BSA have enhancing effect on qPCR when included in the lysate as it has protective properties of the RNA [84]. To reduce the gDNA in the lysates, DNase-treatment was also evaluated. DTT was included to reduce the activity of RNases that are present in the lysates and to prevent RNA degradation. A comparison was also made to see if spinning down the cell debris in the wells before the cDNA synthesis would reduce the inhibition. The RNA Secure solution was not included in this experiment as it did not give any noticeable improvement when activated in the previous experiment.

The serial dilutions from this experiment showed that the wells lysed with 0.3% NP40/0.1 %BSA did not amplify *HPRT1* as well as in the previous experiment, (see A.10), and poorly for *MALAT1* (see A.11). The lysis buffer containing 0.1% BSA showed better ΔC_q values (estimated amplification efficiency) for both *HPRT1* and *MALAT1*, but the variability (spread) of C_q values between samples was larger (see standard deviations).

The C_q and ΔC_q values showed that the DTT + DNase treatment did not improve the assay. The C_q values were very high compared to without DTT and DNase, possibly due to degradation of RNA during DNase treatment despite the addition of DTT.

In this setting, the DNase was first activated by incubation at 37°C for 20 min and then inactivated in the lysate before cDNA synthesis. DNases can be heat-inactivated, which can lead to chemical degradation of the RNA by divalent cations present in the DNase buffer. Instead the TURBO DNase was inactivated with a DNase Inactivation Reagent which binds up the DNase and divalent cations and removed by centrifugation.

When testing several factors in one experiment makes it hard to draw conclusions. DTT and DNase treatment should have been tested separately, but due to practical reasons and time it was not possible to handle the large number of different samples. The reason for lower ΔC_q values for 0.3%NP40/0.1% BSA could be due to pipetting errors when performing the dilutions and needs to be investigated further.

Spinning down cell debris in the plate after the lysis was difficult to evaluate. The ΔC_q values deteriorated for *HPRT1* when using 0.3% NP40/0.1 %BSA, while no difference was seen for the other conditions and for *MALAT1*. No improvement of gDNA levels were seen with DNase treatment either, but the difference in C_q values between +RT and –RT was in general larger (see A.12) than in the previous experiment.

In conclusion, 0.3% NP40/0.1 %BSA did not work as well as before but should be tested again with the addition of RNA Secure. The lysis buffer containing 0.1% BSA improved ΔC_q values both for *HPRT1* and *MALAT1*, but might increase the spread of the data. Due to how DNase treatment is performed in general (the nature of traditional DNase treatment) it is not possible to improve that step when using lysates, therefore other ways to reduce the levels of gDNA will be investigated.

4.8 Semi-automation of two-step qPCR assay using 0.3% NP40/0.1 %BSA lysis buffer

To assess if the improvements that had been made so far (since the last semi-automated experiment) were enough, a trial was performed using the 0.3% NP40/0.1 %BSA lysis buffer and adding only 10% lysate for the RT reaction. This experiment was unfortunately performed in parallel with the experiment discussed in section 4.7, otherwise the 0.1% BSA lysis buffer should have been used. Due to the potential problems discussed in section 4.1 regarding the Echo555 Acoustic Liquid handler, this time another pipetting station (Biomek FX^P laboratory automation workstation) was used to transfer qPCR master mix and lysate.

The Figure 4.3 shows that there was still a large variability between the *HPRT1* C_q values from a C_q value of 24.5 to 27.9 (29.0) and the same problem was seen in Figure 4.4 for *MALAT1*, where the C_q values differs between 21.5 to 26.3. The changes that was made regarding using another lysis buffer, using only 10% of the lysate in the RT reaction and using another reference gene, did not give better results compared to the first semi-automation experiment that was performed (see Figure 4.2). The variability between the wells was still an issue.

	1	2	3	4	5	6	7	8	9	10	11	12	13	14	15	16	17	18	19	20	21	22	23	24
A	25,9	25,5	25,5	25,8	25,9	26,3	25,3	27,0	26,5	27,0	26,2	26,0	26,8	26,6	26,3	26,6	26,1	26,8	26,5	26,5	25,7	26,1	25,7	26,7
B	26,0	26,7	26,5	26,5	26,3	26,5	26,6	27,3	27,0	26,6	25,6	26,2	25,9	27,3	26,5	26,4	26,6	26,7	26,1	26,0	26,6	26,9	26,8	27,2
C	25,8	26,2	25,2	25,6	25,7	25,5	25,8	26,5	26,7	27,3	25,9	26,6	25,8	27,2	26,5	26,9	25,8	26,5	26,0	25,9	25,7	26,0	25,5	25,7
D	25,9	26,6	25,3	26,1	26,1	26,1	26,1	26,7	26,6	27,0	26,2	26,8	25,6	27,0	27,0	26,8	26,7	26,7	26,7	26,8	26,6	26,5	26,5	26,8
E	25,2	25,3	25,5	25,4	24,6	26,4	25,6	25,7	26,5	25,9	25,2	26,0	25,9	26,8	26,1	26,5	26,1	26,3	26,0	26,6	25,5	25,7	25,6	25,3
F	25,7	25,8	26,0	26,0	26,2	26,2	26,1	26,9	26,6	26,4	26,1	26,6	26,2	26,8	26,6	26,3	26,5	26,7	26,3	26,5	25,8	26,5	26,6	27,1
G	25,5	25,5	25,7	25,2	25,7	26,0	25,6	26,2	25,4	26,6	25,8	25,8	26,1	26,4	25,9	26,3	26,3	26,2	25,9	26,3	26,0	25,6	26,0	25,7
H	25,5	25,4	26,0	25,7	25,5	25,6	26,3	26,3	26,0	25,9	26,2	26,0	26,0	26,5	26,4	26,5	26,2	26,3	26,0	26,4	26,5	26,5	26,8	27,3
I	25,3	26,2	24,5	25,9	25,8	26,0	25,1	26,2	25,0	26,5	25,9	26,1	25,5	27,1	25,7	27,4	25,5	27,6	24,8	27,9	25,9	27,5	25,3	26,2
J	25,6	25,6	25,8	25,6	29,0	26,4	26,1	26,5	26,3	26,4	26,6	26,0	26,2	26,6	25,9	26,2	27,1	26,4	27,7	26,5	26,5	26,9	27,7	27,4
K	25,5	25,5	25,3	26,3	26,5	26,1	26,1	26,4	26,2	26,1	25,7	26,8	25,8	27,1	25,9	26,0	25,4	26,0	24,8	26,7	24,9	26,4	25,7	26,2
L	26,2	26,6	26,2	26,4	25,9	26,6	26,2	26,1	26,5	26,5	26,2	26,2	26,2	26,6	27,1	26,5	25,6	25,9	27,3	27,0	27,7	26,8	26,9	26,7
M	26,3	26,3	25,7	25,9	25,9	25,9	26,0	26,2	24,6	26,1	26,1	26,1	25,7	26,7	26,4	26,6	25,8	25,7	26,3	26,7	26,0	26,7	25,9	26,7
N	26,9	26,4	26,6	27,0	26,2	25,9	26,2	26,6	26,3	26,9	25,9	26,5	26,4	26,9	26,6	27,0	26,3	26,9	26,2	27,0	27,2	27,2	27,3	27,3
O	26,0	26,2	25,0	25,8	25,6	25,1	26,1	26,4	25,7	25,6	26,4	26,0	26,4	26,7	26,4	26,3	26,1	26,8	26,8	26,3	26,2	26,8	25,8	26,5
P	26,2	25,5	26,7	26,7	26,8	26,2	26,0	26,6	26,4	27,3	26,7	27,0	26,5	26,7	26,2	26,8	26,5	27,3	26,7	27,3	27,0	27,2	26,9	27,5

Figure 4.3: Plate layout with the obtained C_q values for the reference gene *HPRT1*.

	1	2	3	4	5	6	7	8	9	10	11	12	13	14	15	16	17	18	19	20	21	22	23	24
A	22,9	22,7	22,9	23,6	23,1	23,6	22,8	23,7	23,9	24,0	23,2	23,3	24,1	23,3	23,6	23,5	23,0	23,5	22,9	23,7	22,5	23,1	22,4	23,3
B	22,6	22,8	23,2	23,1	23,0	22,9	23,3	24,0	23,5	23,2	22,6	23,1	22,2	23,4	23,2	23,3	23,2	23,4	22,8	23,1	23,2	23,7	23,6	24,3
C	23,4	23,6	22,7	23,2	22,9	23,3	23,5	23,6	24,4	24,2	23,6	23,9	23,2	23,9	24,1	23,9	23,1	23,4	22,4	23,4	22,8	23,5	22,8	23,2
D	22,0	22,8	21,6	22,6	22,2	22,4	22,5	22,9	22,7	23,0	22,1	23,0	22,2	23,3	23,0	23,3	23,1	23,1	22,8	22,8	23,0	22,8	23,1	22,9
E	22,1	23,4	22,8	22,9	22,7	23,6	22,9	23,6	23,8	24,0	22,9	23,5	23,1	24,4	23,2	24,0	23,2	23,8	23,4	23,8	22,9	23,4	23,0	22,9
F	21,9	21,5	22,4	23,1	22,5	23,9	22,7	23,6	22,6	23,3	22,7	23,4	22,9	24,1	22,9	23,9	23,0	23,9	23,0	24,1	22,6	24,3	23,5	24,6
G	23,7	24,3	23,6	23,7	24,2	25,3	23,7	24,2	23,4	24,6	23,7	24,3	24,4	24,8	23,8	24,2	24,0	24,3	24,0	24,0	23,8	23,9	24,5	23,8
H	23,9	23,5	23,1	24,1	22,9	24,7	23,6	24,0	23,0	24,3	23,5	24,4	23,2	24,5	24,2	24,4	24,0	24,2	23,6	24,4	24,3	24,8	24,7	25,7
I	23,4	25,5	22,3	24,8	24,2	25,1	23,0	24,6	23,0	24,9	24,0	24,4	23,5	25,5	23,7	25,8	23,4	26,1	23,4	26,0	24,1	26,1	23,0	24,1
J	23,9	23,2	23,7	24,0	26,3	24,8	23,7	24,2	23,8	23,7	24,3	24,6	24,0	24,5	23,8	23,9	24,5	23,7	25,0	24,1	24,5	24,7	24,9	25,8
K	23,4	24,4	22,9	24,5	24,2	24,9	23,9	24,8	22,9	24,8	23,1	25,3	22,1	25,2	22,8	24,5	22,9	24,2	22,8	25,1	22,7	24,1	22,8	24,6
L	23,6	23,8	23,3	23,7	23,2	23,7	23,1	23,5	23,3	24,4	23,1	23,5	23,4	23,8	23,7	23,5	22,9	23,5	24,5	24,3	24,6	24,3	24,4	24,3
M	25,2	25,8	23,7	24,3	24,2	24,3	24,5	25,3	22,6	24,6	24,1	24,3	24,0	24,7	24,6	24,9	24,1	24,6	24,7	25,0	24,1	24,8	23,9	25,2
N	24,3	24,6	24,0	24,6	23,6	23,8	24,2	24,0	23,6	23,9	23,6	23,7	24,2	24,4	24,5	24,2	24,0	24,4	23,9	24,7	25,2	25,0	25,3	25,3
O	24,3	24,4	22,8	24,3	23,9	23,3	24,1	25,2	23,6	23,8	24,9	24,9	24,9	24,6	24,8	25,2	24,3	24,8	25,2	24,5	24,1	24,8	23,6	25,0
P	23,3	23,3	24,1	24,0	24,3	23,6	23,9	24,1	23,7	24,4	24,0	24,1	23,8	23,8	23,8	24,4	24,0	24,7	24,4	24,9	24,3	24,9	24,4	25,3

Figure 4.4: Plate layout with the obtained C_q values for the target gene *MALAT1*.

4.9 Quality control of the RNA using an agarose gel

Right concentration and high quality of RNA are important when quantifying gene expression using qPCR [91], as degraded RNA can cause variability in the qPCR results [92]. The quality of the RNA can usually be determined by using gel electrophoresis. If a purified RNA sample containing intact RNA is loaded and separated on a gel, two distinct bands representing the 28S and 18S ribosomal RNA should appear, against a faint background of mRNA of different sizes and a faint band at the lower part of the gel consisting of 5S ribosomal RNA, tRNAs and other small RNA molecules. Since only 1-3% of total RNA is mRNA, it should barely be seen. If the RNA is degraded the 28S and 18S bands are fainter or disappear completely, and are replaced by a strong smear of degraded RNA in the lower part of the gel [93]. The different lysates were loaded on a 1.2% agarose gel and the results from the agarose gel electrophoresis can be seen in Figure 4.5. No RNA ladder was available, so the first well was loaded with a DNA ladder, to visualize how far samples could be allowed to migrate onto the gel before stopping electrophoresis. The second well was loaded with purified RNA from a previous experiment that was extracted using Qiagen RNeasy kit, wells 3 and 4 were loaded with 0.3% NP40/0.1 %BSA lysates, wells 5, 6 and 11 with 0.1% BSA lysates, wells 7, 8 and 12 were loaded with RLN buffer with 1 mM DTT, and wells 9 and 10 with Cellulyser Micro lysates. RLN is a lysis buffer provided in the RNeasy 96 kit for isolation of cytoplasmic RNA. From the protocol it was recommended to add 1 mM DTT. Cellulyser Micro is a commercially available lysis buffer from TATAA Biocenter.
Figure 4.5 shows that for the column-extracted RNA, three bands are visualized, 28S rRNA, 18S rRNA and a band above them with contaminating gDNA. The staining pattern in the lanes with lysates, was very unexpected, with no ribosomal bands and no smear of degraded RNA seen. The only staining seen was about the same size as 5S rRNA, tRNA and other small RNA molecules, and a diffuse band or area above the position of a 28S band. There is a possibility that there were too little material in the lysates and that more need to be loaded on the gel to see the ribosomal bands and/or degraded RNA, but this does not explain the presence of the large band. A mammalian cell contains around 10 pg RNA [94], which means that there are around 70 ng RNA in 7000 cells. At the TermoFisher website there was found that when using a denaturing agarose gel the recommendation is 200 ng of RNA to load the gel with at least to be able to see the bands with EtBr (ethidium bromide) [93]. According to that information, there was too little material loaded in the gel. But if all RNA was degraded, the qPCR would not detect high levels of *36B4* and *MALAT1*, as seen in results from the qPCR assay.
To find out purity and how much RNA there is in a sample, a spectrophotometer can be used by measuring the absorbance at 260 nm. Another strategy that can be used to determine the RNA quality, is to use a microfluidics instrument such as the Agilent 2100 Bioanalyzer. But what is common for these instruments is that it cannot be used on lysates since they will detect both salts, polysaccharides, RNA, DNA and proteins [92]. Studies that are using a Bioanalyzer usually determines the quality of extracted RNA [95].

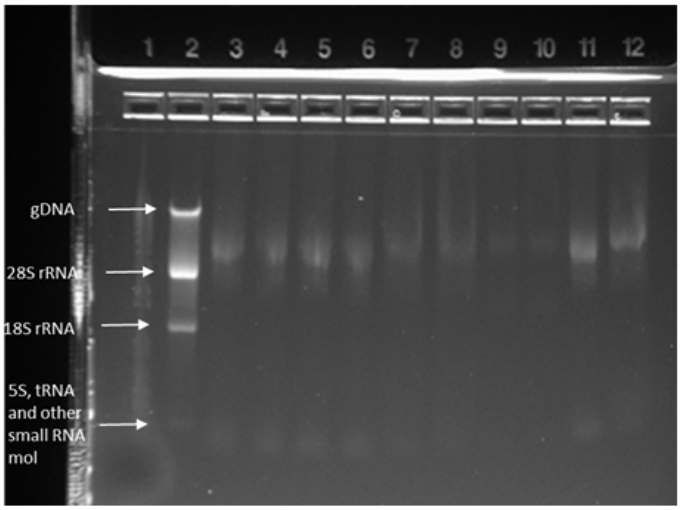

Figure 4.5: E-gel General Purpose 1.2% agarose. Lane 1: DNA ladder, 2: purified RNA isolated using Qiagen RNeasy kit, 3 and 4: 0.3% NP40/0.1 %BSA lysate, 5, 6 and 11: 0.1% BSA lysate, 7, 8 and 12: RLN+1mM DTT lysate, 9 and 10 Cellulyser Micro lysate

4.10 Pre-study to select conditions for a following experiment

An experiment was planned to compare a 96-well plate prepared with the traditional RNeasy 96 kit protocol and one 96-well plate manually lysed and analyzed using the two-step qPCR protocol. A pre-study was performed to decide what conditions to use for the two-step qPCR protocol. In this study two different cDNA master mix solutions and the effect of centrifugation of the lysates to pellet nuclei were compared to determine the optimal condition for the following experiment.

The pre-study was divided into two parts where the first part was to visually inspect the lysis of the cells using 5 different lysis buffers and based on the degree of lysis, select a couple of lysis buffers for the second part where cDNA synthesis and qPCR analysis was performed. Besides the already tested adipocyte-project lysis buffer, 0.3% NP40/0.1 %BSA and 0.1 %BSA, RLN was also included. This buffer was tested both with and without the optional 1 mM DTT mentioned in the manufacturer's protocol.

The photos taken from the visual inspection can be seen in Figure 4.6. The visual inspection showed that the cells were completely lysed in the adipocyte-project lysis buffer and 0.3% NP40/0.1 %BSA. The wells with RLN and RLN+DTT left the nuclei intact and in 0.1 %BSA the cells were swelling, forming round structures, likely opening pores. RLN, RLN+DTT and 0.1% BSA was chosen for the second part of the study because they appeared to leave the nuclei intact or components of the nuclei enclosed, and therefore should reduce the levels of contaminating gDNA.

The reason for not selecting 0.3% NP40/0.1% BSA was that although it showed good ΔC_q values (estimated amplification efficiency was close to 100%) in the experiment described in section 4.6, it did not replicate in 4.7 and in 4.8, the C_q

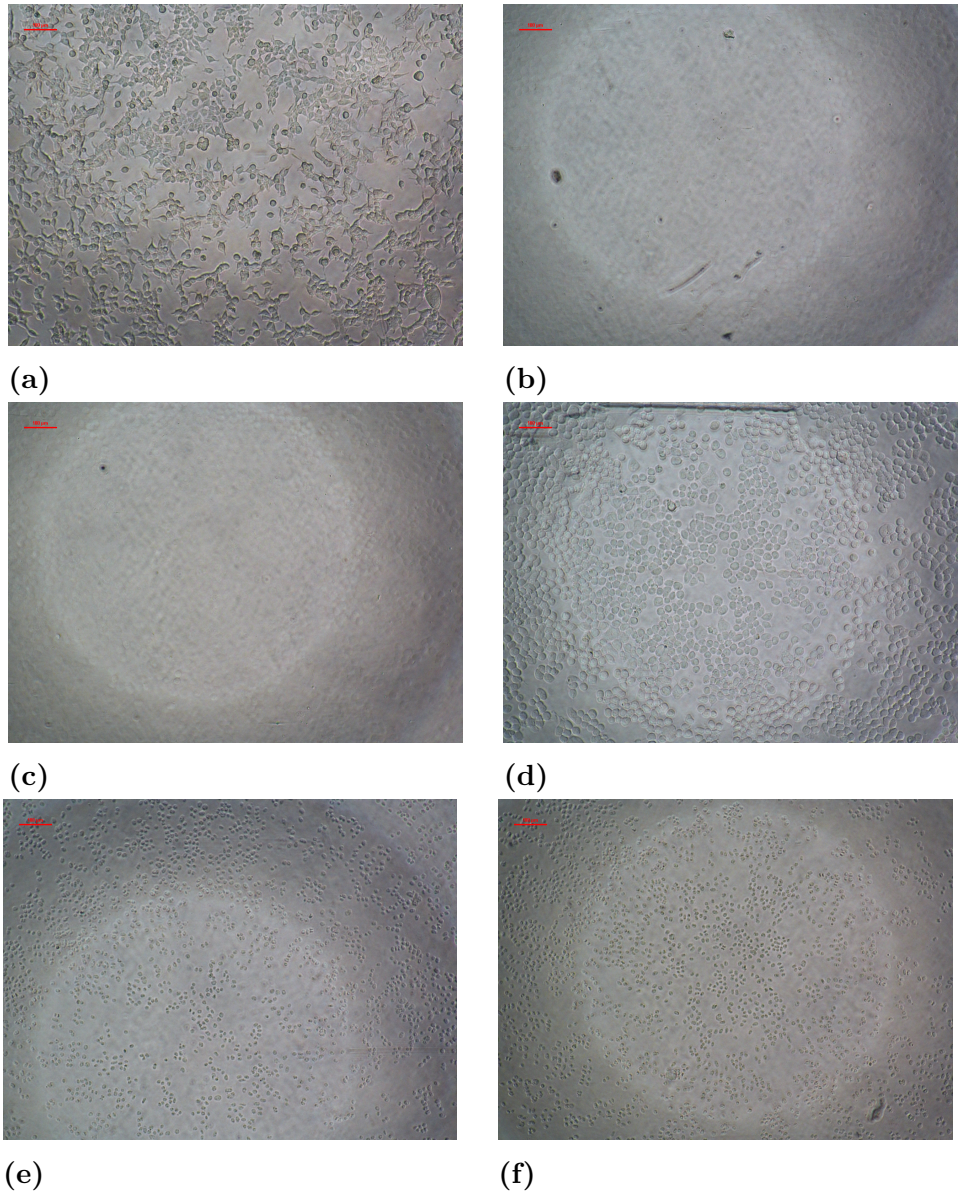

Figure 4.6: a) Cells without lysis buffer, b) Cells lysed with adipocyte-project lysis buffer, c) Cells lysed with 0.3% NP40/0.1% BSA, d) 0.1% BSA, e) RLN, f) RLN with 1 mM DTT.

variability between samples was very large. The adipocyte-project lysis buffer improved significantly when using only 10% lysate in the RT reaction in 4.6, but since both the adipocyte-project and 0.3% NP40/0.1% BSA buffers were similar visually, a decision was made to evaluate the ones that differed and select the lysis buffer that have never had been tested in a full-plate experiment before.

Table A.13 in Appendix shows that the variability of 0.1% BSA samples was very large, 3 C_q-values with adipocyte-project RT mix and more than 5 C_q values with High Capacity RT mix. This confirmed the trend seen in experiment 4.7. The High Capacity RT samples were 1 C_q-value higher than the same adipocyte-project RT samples. One reason why adipocyte-project cDNA RT mix was better might be

because it contains a mixture of both random and oligo(dT) primers, allowing for optimal reverse transcription, while the High Capacity mix only contains random primers.

The two RLN buffers looked promising since they only varied ∼1 C_q-value between samples where the lysate had been centrifuged before pipetting RT reactions. For some unknown reason, the RLN only samples showed poor ΔC_q values after spin. The estimated amplification efficiency was good for *HPRT1* in the RLN-based lysis buffers, but very poor for *MALAT1* (see Table A.14).

Neither 0.1% BSA nor the RLN buffers were perfect; for the first a large variability between wells that might indicate incomplete lysis not releasing all mRNA from cells, and the for the latter, like for 0.3% NP40/0.1% BSA, the poor ΔC_q values for *MALAT1* due to some unknown inhibition. The RLN buffer was chosen for the next experiment.

4.11 Comparison between lysate and traditional column-purified RNA

To exclude that the variability and issues with estimated amplification efficiency were related to the 384-plate format, a comparison was made between one 96-well plate prepared with the traditional RNeasy 96 kit protocol and one 96-plate manually lysed and analyzed using the two-step qPCR protocol. From the pre-study, the RLN lysis buffer and the RT master mix from the adipocyte-project were selected for the two-step qPCR protocol. The cells in the plates were treated with three different ASOs (two GLP1-conjugated *MALAT1* ASOs and one *MALAT1*-ASO without GLP1).

When comparing the plate-layouts seen in Figure 4.7 and 4.8 a much larger variability in *HPRT1* than in the previous experiment was seen across wells in the lysate-based plate. Surprisingly, a similar variability was also seen in the plate based on purified RNA. This means that even if the same number of cells were seeded in all wells, there were differences also in the amounts of RNA isolated from different wells of the latter plate. This experiment shows that the C_q variability is not specific neither for the 384-well plate format nor the lysis-based two-step qPCR protocol.

From the graphs in Figure 4.9 and 4.10 it is seen that the concentration-response curve using the two-step protocol is not perfect but decent and the relative expression is varying compared to the curve in Figure 4.10, where the concentration-response curve shows a nice dose-dependent reduction. The variability in the relative expression indicates that the lysates must be disturbing the RT and qPCR reactions and that the assay needs further improvements.

When comparing the ΔC_q (to find out the estimated amplification efficiency) for the assays using hydrolysis probes or reporter dyes in Figure 4.11, samples from purified

	1	2	3	4	5	6	7	8	9	10	11	12
A	25,8	26,1	26,2	26,4	26,4	26,9	26,0	26,4	26,3	26,7	26,8	25,9
B	25,8	26,2	25,9	26,2	26,5	26,4	26,1	26,5	26,7	26,6	26,7	27,0
C	25,9	26,0	25,9	26,3	26,4	26,1	26,3	26,6	26,7	26,6	27,1	27,0
D	26,0	25,9	26,0	26,2	26,4	26,4	26,1	26,4	26,4	26,9	26,9	27,1
E	26,0	26,1	26,0	26,3	26,2	26,4	25,9	26,5	26,7	26,8	26,7	27,1
F	25,8	25,7	25,7	25,9	25,9	26,1	26,1	26,1	26,5	26,9	26,8	27,2
G	26,0	25,5	25,5	26,0	25,8	26,2	25,9	26,5	26,7	26,7	26,8	25,1
H	25,9	25,5	25,6	26,2	26,1	26,4	26,0	26,5	26,2	26,5	26,8	24,3

Figure 4.7: Plate-layout showing the received C_q values for *HPRT1* using the two-step qPCR protocol

	1	2	3	4	5	6	7	8	9	10	11	12
A	24,4	24,4	25,3	25,6	25,4	26,4	24,8	26,0	23,9	24,4	24,0	25,0
B	24,4	25,2	25,8	25,0	24,6	27,5	25,9	24,6	24,7	24,9	23,0	23,5
C	23,6	24,1	25,0	25,5	25,6	27,7	27,6	25,9	24,3	23,6	23,3	23,1
D	23,8	24,3	24,8	24,5	25,3	26,0	26,2	26,2	25,8	24,2	23,8	23,1
E	24,9	25,5	25,0	24,8	25,1	26,2	27,3	25,9	25,5	24,8	23,7	23,2
F	25,0	25,9	25,8	24,6		27,0	26,5	26,3	25,7	24,4	24,0	23,2
G	24,4	26,0	24,7	25,9	24,5	27,2	26,5	25,9	24,8	23,9	23,6	23,1
H	24,0	24,9	24,2	24,1	26,0	24,8	25,8	24,9	23,5	23,1	23,8	23,7

Figure 4.8: Plate-layout showing the received C_q values for *HPRT1* using the traditional protocol with column purification of RNA

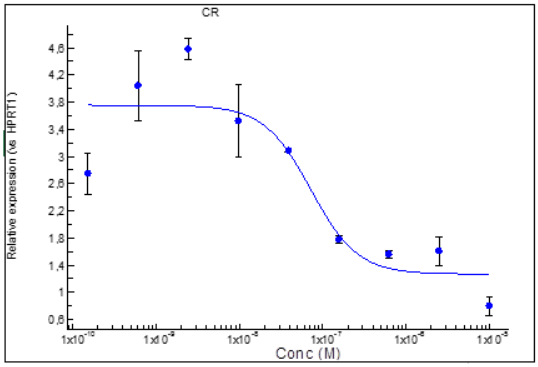

Figure 4.9: Concentration-response curve generated from lysate using two-step protocol, where each data point, the mean±SEM of the relative expression of *MALAT1* normalized to *HPRT1* was plotted against the concentration of GLP1-*MALAT1*-ASO

RNA (blue lines) were linearly amplified both when using TaqMan and SYBR Green qPCR assays, while the amplification of most lysate samples were linear only when using TaqMan assays. Some of the samples from the lysate improved when using the SYBR Green assay for *HPRT1* as seen in Figure 4.11 a. It is not surprising that the samples from column-purified RNA showed one C_q value between the dilutions, because the RNA used were purified and probably did not contain any cellular components that could interfere with the SYBR or TaqMan assays. The TaqMan assays used were also commercial, and validated and tested by experts to determine the optimal conditions. An advantage of using TaqMan assay is that the probes increase the specificity. Another difference between TaqMan and SYBR assays is

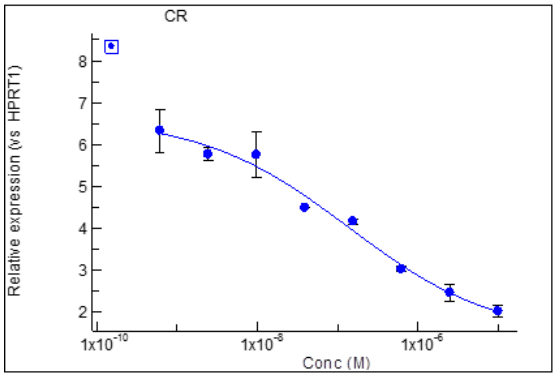

Figure 4.10: Concentration-response curve generated from RNA purified from Qiagen spin columns, where each data point, the mean±SEM of the relative expression of *MALAT1* normalized to *HPRT1* was plotted against the concentration of GLP1-*MALAT1*-ASO

that different master mix buffers are used and the combination of all these factors could be the reason why TaqMan assays were less sensitive to inhibition. Based on the results it is less likely that the inhibition in the qPCR reactions are less severe and that the lines were more linear (ΔC_q values were improved) because hydrolysis probes were used.

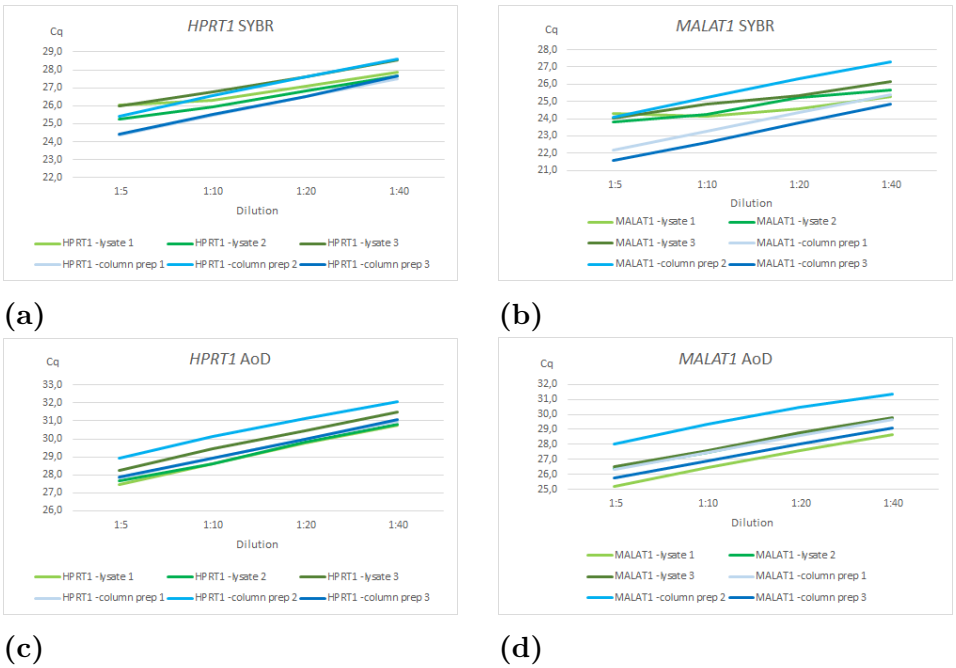

Figure 4.11: The graphs shows the difference in linearity when using hydrolysis probes (AoD) (c and d) and reporter dyes (SYBR) (a and b) for traditional and two-step qPCR assays for *MALAT1* and *HPRT1*. The x-axis of the graphs shows the dilution and the y-axis the C_q values.

This experiment showed that using hydrolysis probes improved the amplification efficiency for the samples containing lysate. It is possibly that this discovery together with the other findings (using Poly-D-Lysine plate which improved the attachment of the cells after the washing step prior to lysis, using only 10% lysate in the cDNA synthesis) could reduce variability also for other lysates using other lysis buffers.

4.12 Comparison of lysis buffers and qPCR analysis using hydrolysis probes

The goal of this experiment was to see if there were any improvements when using different lysis buffer when running the qPCR reaction with hydrolysis probes. Cells were seeded in a 384-well plate with Poly-D-lysine coating, and manually treated with a GLP1-*MALAT1*-ASO. The washing step of the cells was performed using the BRAVO Automated Liquid Handling Platform and five different lysis buffers were evaluated. The later steps were performed as described before, where 10% lysate was used in the RT reaction.

The improvement in the estimated amplification efficiency (by observing the ΔC_q values) that was made when using the hydrolysis probes, made it worth comparing the adipocyte-project, 0.3% NP40/0.1% BSA and RLN lysis buffer one last time to see if it could improve the variability of C_q values. For this experiment the original protocol for the adipocyte-project buffer was used and 0.3% NP40/0.1% BSA with RNA Secure to see if it had an effect without activation. The RLN buffer was tested both with and without RNA Secure, and 1 mM DTT (as recommended in Rneasy Mini Handbook). According to different descriptions of DTT and RNA Secure, both should inactivate RNases.

The results in Figure 4.12 shows that depending on which lysis buffer used, different variability in the C_q value is seen, where RLN with RNA Secure had the lowest C_q value (29.4-27.1=2.3), representing a ∼5-fold difference. The difference in C_q values in adipocyte-project lysis is 30.1-26.2=3.9, 0.3% NP40/0.1% BSA+RNA Secure 31.0-27.2=3.8, RLN 29.9-27.5=2.4 and RLN with DTT 30.6-27.3=3.3. These values seem to be fairly constant and have also been seen in previous experiments.

When comparing the C_q-values for *MALAT1* and *HPRT1* in the control wells (untreated wells) similar patterns was seen. A low C_q value in a well on the *HPRT1* plate corresponded to a low C_q value on the *MALAT1* plate. This means that even if the amount of *HPRT1* differs between wells, the *MALAT1* levels differ with the same pattern. Therefore, the variability does not affect the relative expression of *MALAT1* as it is normalized to *HPRT1*. There was only a 2-fold difference in relative expression of *MALAT1* in controls wells using the adipocyte-project lysis buffer, RLN or RLN+RNA Secure lysis buffers. When normalizing the data the variability gets reduced (data gets tighter), compared to the relative expression values for *HPRT1* and *MALAT1* separately.

The remaining variability in C_q values may be caused by DPBS solution remaining in the wells after washing cells. When pipetting liquid from wells by hand, almost all solution can be removed without losing cells, by tilting plate and pipetting in the side of the well. Whereas when using automation, the pipette tips are vertical and it is not possible to remove all solution completely without also removing cells. To avoid cell detachment (section 3.3.1.1) the program for the liquid handler was changed to increase the distance between the bottom of the plate and the tips, which

HPRT1 Cq	3	4	5	6	7	8	9	10	11	12	13	14	15	16	17	18	19	20	21	22
A	26,6	26,9	27,4	27,1	27,2	28,6	31,0	29,1	27,6	28,9	28,8	28,0	27,1	28,7	28,2	28,5	27,7	29,1	29,4	28,0
B	28,6	27,4	28,6	29,3	28,0	29,0	29,8	28,7	27,9	28,2	28,5	28,7	27,9	28,2	29,0	28,1	28,7	29,5	29,0	28,5
C	27,5	26,8	28,6	28,0	29,4	28,5	28,9	27,9	28,1	27,6	27,8	27,8	27,6	28,2	27,8	27,7	27,6	28,9	28,5	27,7
D	27,7	27,6	28,6	27,3	28,0	28,1	28,4	27,7	28,5	27,6	27,8	27,5	27,3	28,2	28,2	28,6	28,9	29,2	29,2	29,5
E	27,0	28,2	28,7	29,9	28,8	28,7	29,6	30,7	28,5	28,6	28,2	27,8	27,1	28,2	27,6	28,3	29,2	29,0	28,5	28,5
F	28,6	28,0	28,9	27,8	29,3	30,1	29,5	28,7	27,8	28,0	28,2	28,6	28,0	28,3	28,2	28,3	28,7	29,5	28,2	28,5
G	27,1	28,6	28,4	28,9	28,6	28,2	29,1	29,4	28,0	28,1	28,0	28,8	28,4	28,0	27,3	27,6	28,1	28,2	28,1	27,4
H	26,5	28,2	29,9	28,9	28,5	28,0	29,2	28,9	29,1	28,8	29,0	29,1	28,7	28,6	28,3	29,1	29,0	29,5	29,8	29,0
I	29,1	28,3	28,9	28,5	29,5	29,5	30,1	29,4	28,4	28,7	28,7	29,5	28,6	29,0	29,0	29,3	28,2	29,9	29,0	28,8
J	28,0	28,6	28,6	28,1	29,5	29,5	30,0	29,3	27,8	29,1	29,6	29,1	28,3	27,8	28,5	27,9	27,9	28,8	28,8	28,0
K	26,2	27,4	29,0	29,0	29,0	29,3	28,8	29,3	29,6	29,9	27,9	27,9	28,2	28,0	28,2	28,2	27,3	28,7	27,6	28,2
L	28,4	28,8	29,1	29,4	29,4	29,8	29,1	28,9	28,9	29,1	28,3	28,1	28,4	28,4	28,9	28,2	29,8	30,6	28,8	29,6
M	27,9	27,7	28,7	29,7	28,8	29,6	29,2	29,9	28,5	28,3	27,7	27,9	28,2	27,7	28,9	27,7	28,3	28,1	28,5	29,0
N	27,9	28,9	28,9	28,7	28,6	29,1	29,7	29,8	28,5	28,6	29,0	28,6	28,7	28,4	28,6	28,2	28,3	28,5	28,7	28,6
O	27,9	29,0	29,2	28,5	27,7	28,6	29,0	29,0	28,7	28,8	28,9	29,0	28,7	29,4	28,5	29,1	29,0	28,7	29,7	28,7
P	29,5	29,2	30,1	29,5	28,2	28,5	29,3	29,0	27,7	28,6	27,6	28,2	28,6	29,3	29,4	28,2	29,1	28,9	29,3	29,0

Malat1 Cq	3	4	5	6	7	8	9	10	11	12	13	14	15	16	17	18	19	20	21	22
A	26,1	26,8	27,1	26,9	24,8	26,4	28,9	27,0	25,8	26,8	26,7	26,1	25,2	27,0	26,0	26,6	26,3	28,6	28,4	27,2
B	27,9	27,2	27,9	28,7	26,4	27,4	27,7	26,8	26,6	27,2	26,6	26,8	25,9	26,5	27,1	26,7	28,3	28,9	28,3	27,6
C	27,0	28,5	29,9	29,3	26,8	28,5	28,9	27,5	26,3	27,8	27,9	27,8	25,4	28,7	27,8	28,3	26,9	30,4	29,4	29,5
D	27,4	28,9	29,8	28,5	25,6	27,5	28,1	27,1	26,3	28,0	28,0	27,2	25,6	27,3	28,0	28,5	28,3	30,4	30,7	29,9
E	26,8	28,6	29,0	29,9	26,7	27,9	28,9	30,1	26,5	27,8	27,4	27,4	25,0	27,4	26,6	27,9	28,3	29,3	28,9	29,6
F	28,0	28,1	29,1	27,9	27,4	29,4	28,8	27,8	25,9	27,5	27,6	27,7	25,7	27,3	27,1	27,3	28,4	29,8	29,3	29,1
G	26,8	28,6	28,4	28,9	26,7	27,4	27,9	27,8	26,5	26,9	26,5	27,9	26,2	26,9	25,8	26,1	26,6	28,5	27,7	27,6
H	26,3	27,7	29,7	28,6	26,6	26,5	28,0	27,5	27,8	27,6	27,8	28,5	26,9	27,1	26,3	27,6	27,9	29,1	29,3	29,0
I	28,2	28,4	28,1	28,0	28,0	28,0	28,7	27,8	26,8	27,1	27,4	28,3	26,6	27,2	26,8	27,6	27,1	29,0	27,9	29,0
J	27,0	27,9	27,9	27,9	28,7	27,9	28,8	27,1	26,4	27,6	28,4	27,6	26,6	25,7	26,2	26,0	27,6	27,8	29,0	27,0
K	26,1	26,9	27,8	28,4	27,3	27,9	26,9	27,0	28,2	28,4	26,1	26,5	26,2	26,2	26,0	26,1	26,2	27,9	26,5	27,8
L	27,7	28,2	28,3	28,6	27,7	28,0	27,8	27,0	27,9	27,5	26,4	26,4	26,6	26,6	27,1	26,5	29,6	29,2	27,7	28,8
M	27,5	27,0	27,8	28,9	26,5	27,9	27,6	27,7	26,8	26,6	25,6	26,2	25,9	25,9	26,6	25,9	27,3	27,9	27,4	27,7
N	27,5	27,0	28,2	28,1	27,2	27,1	28,0	27,9	26,8	26,8	27,4	27,2	26,1	25,9	26,8	26,3	28,4	27,3	28,2	27,7
O	27,0	28,1	28,0	28,0	25,8	26,9	27,0	26,9	26,9	27,8	27,3	27,4	26,7	27,4	26,3	27,3	27,7	27,6	28,5	28,3
P	28,3	28,5	29,2	28,9	26,0	26,7	27,2	26,6	26,1	26,8	26,5	26,6	26,2	27,2	27,4	26,3	28,8	28,5	28,3	27,6

Rel expr Malat1	3	4	5	6	7	8	9	10	11	12	13	14	15	16	17	18	19	20	21	22
A	1,4	1,1	1,2	1,1	5,0	4,5	4,2	4,2	3,5	4,5	4,2	3,6	3,8	3,2	4,7	3,7	2,6	1,5	2,0	1,7
B	1,7	1,2	1,6	1,5	3,1	3,0	4,3	3,9	2,5	2,1	3,6	3,9	4,1	3,3	3,9	2,7	1,3	1,5	1,6	1,9
C	1,4	0,3	0,4	0,4	6,1	1,0	1,0	1,3	3,5	0,9	0,9	1,0	4,5	0,7	1,0	0,7	1,7	0,4	0,5	0,3
D	1,2	0,4	0,5	0,4	5,1	1,5	1,3	1,5	4,5	0,8	0,9	1,3	3,1	1,8	1,1	1,1	1,5	0,4	0,3	0,8
E	1,2	0,7	0,8	1,0	4,4	1,7	1,7	1,5	4,1	1,7	1,8	1,3	4,3	1,7	2,1	1,3	1,8	0,8	0,8	0,5
F	1,5	0,9	0,9	0,9	3,8	1,7	1,6	1,9	3,9	1,4	1,5	1,9	4,8	2,0	2,2	2,0	1,2	0,8	0,5	0,7
G	1,2	1,0	1,0	1,1	3,8	1,8	2,2	3,0	2,8	2,3	2,9	1,9	4,8	2,1	2,9	2,8	2,8	0,8	1,3	0,9
H	1,2	1,3	1,2	1,3	3,6	2,7	2,3	2,6	2,4	2,4	2,4	1,6	3,4	2,9	4,0	2,9	2,1	1,3	1,4	1,0
I	1,9	0,9	1,8	1,4	3,0	2,8	2,5	3,0	3,1	3,0	2,5	2,3	4,1	3,5	4,6	3,3	2,1	1,8	2,2	0,9
J	2,0	1,6	1,6	1,2	1,7	3,0	2,3	4,7	2,7	3,0	2,3	2,9	3,3	4,1	5,1	3,7	1,2	2,0	0,9	1,9
K	1,0	1,4	2,3	1,6	3,1	2,6	3,9	4,9	2,8	2,7	3,5	2,7	4,2	3,3	4,6	4,1	2,1	1,7	2,0	1,3
L	1,6	1,5	1,8	1,8	3,3	3,4	2,4	3,9	2,0	3,0	3,7	3,4	3,4	3,6	3,5	3,2	1,1	2,6	2,2	1,8
M	1,3	1,6	1,9	1,7	3,7	3,1	3,0	4,7	3,3	3,3	4,4	3,3	4,7	3,5	5,2	3,5	2,0	1,2	2,1	2,4
N	1,3	3,9	1,6	1,5	2,6	4,0	3,3	3,8	3,1	3,5	3,1	2,7	6,0	5,6	3,6	3,9	0,9	2,3	1,4	1,8
O	1,8	1,9	2,3	1,4	3,7	3,2	4,0	4,5	3,5	2,0	3,1	3,0	4,0	3,8	4,4	3,7	2,3	2,1	2,3	1,3
P	2,3	1,6	1,8	1,5	4,8	3,7	4,4	5,2	3,1	3,5	2,2	2,9	5,3	4,3	4,1	3,8	1,3	1,3	1,9	2,7

Figure 4.12: Plat-layout with the received C_q values from qPCR assay for *HPRT1* (upper layout) and *MALAT1* (middle layout), and the relative *MALAT1* expression (lower layout). Columns 3-6 represent wells with cells lysed with adipocyte-project lysis buffer+RNA Secure, columns 7-10 cells lysed with 0.3% NP40/0.1 %BSA+RNA Secure, columns 11-14 cells lysed with RLN, columns 15-19 cells lysed with RLN + RNA Secure, and columns 19-22 cells lysed with RLN with DTT.

could result in solution remaining in the wells. If DPBS is left in some of wells it would dilute the lysis buffer and possibly causing incomplete lysis of cells i.e. the cells are differently lysed in each well. This needs further investigation.

The concentration-response curves seen in Figure 4.13, shows that all lysis buffers gives decent curves with less outliers compared to the experiment in section 4.1,

Figure 4.1. A difference in variability between the replicates can mostly be seen with 0.3% NP40/0.1 %BSA+RNA Secure and RLN with DTT. RLN with RNA Secure gives a slightly larger assay window (the difference in relative expression between untreated and maximum suppressed samples) and lower variability between replicates which facilitates when comparing and ranking different ASOs.

To sum up, the results from the experiment showed that the TaqMan assay did not improve the variability in C_q values. But the concentration-dose response curves were significantly improved for all assays tested. A potential explanation for the variability could be dilution of lysis buffers leading to less efficient lysis in some wells. From Figure 4.12 is seen that the variability over the plate, does not effect the data for the relative expression of *MALAT1*.

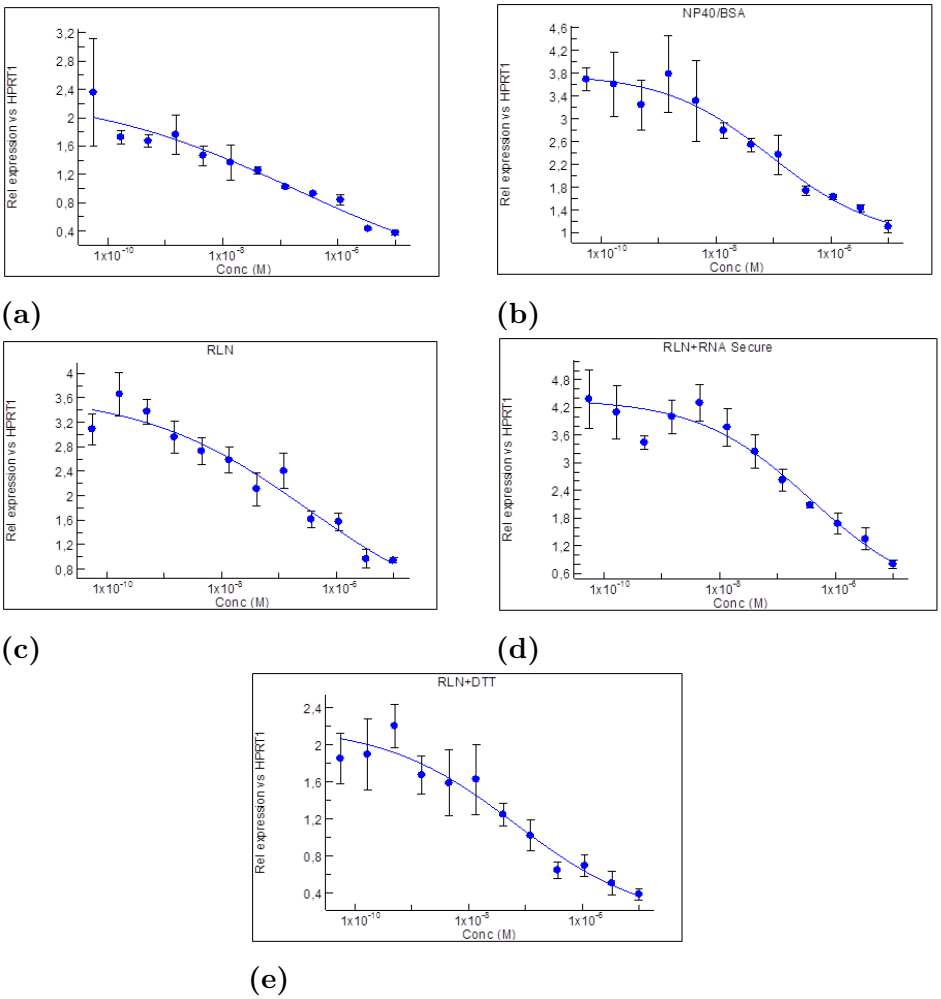

Figure 4.13: Concentration-response curves for the different lysis buffers (a. adipocyte-project lysis buffer + RNA secure, b. 0.3% NP40/0.1 %BSA + RNA Secure, c. RLN, d. RLN + RNA Secure and e. RLN + DTT, where each data point, the mean±SEM of the relative expression of *MALAT1* normalized to *HPRT1* was plotted against the concentration of GLP1-*MALAT1*-ASO.

5

Conclusion

Applying an assay to a new cell model can be time consuming, and unexpected problems can show up. What was assumed to be a simple adaptation of the adipocyte-project qPCR protocol to GLP1R-HEK293 cells proved to be really complicated as the cells unexpectedly behaved very different. The problems faced regarding the assay (poor concentration-response curves, variability in C_q values and varying ΔC_q values) were not easy to solve.

However, this study have shown that it is possible to set up a semi-automated high-throughput two-step qPCR based assay for whole cell lysates of GLP1R-HEK293 cells. This assay will now be used to quantify the productive uptake of GLP1-*MALAT1*-ASO by measuring a concentration-dependent reduction of the relative gene expression of the target gene, *MALAT1* after treatment with different ASO conjugates. In this study, a tool ASO was used to establish the assay but will from now on be used to screen and rank different GLP1 peptide conjugated to *MALAT1*-ASO, for optimizing and selecting of peptides with different length and linkers based on potency and efficacy.

The knowledge gained during the project about optimization of a direct lysis assay and what can affect the qPCR reaction have shown that a new assay needs to be optimized separately depending on which cell type is used. This includes finding the optimal reference gene for specific cells, finding the right lysis buffer and evaluate different qPCR assays. Cells differ depending on origin, and can be more or less sensitive to the different conditions. In this study, the HEK293-GLP1R cells behaved very different from the primary adipocytes when using the lysis buffer used in the adipocyte-project. Another learning is that it is important to ensure that the amplification of the cDNA samples in the PCR reaction is efficient and that the ΔC_q values are linear for an optimized assay. The variability in the C_q values seen over the plate can be due to incomplete lysis, because of remaining DPBS in the wells after the washing step and needs further evaluation.

Major improvements that were made during the trouble-shooting of the two-step qPCR assay, were using a Poly-D-Lysine coated plate, RLN+RNA Secure lysis buffer, reducing the lysate amount in the RT master mix from 39% to 10% improved the amplification in the PCR for *HPRT1*, that the switching from using SYBR Green dyes to TaqMan probes, whether it was due to the master mix composition or the quality of the assay design, made the estimated amplification efficiency of *MALAT1* close to 100%.

6

Future work

When setting up a new assay it is important to determine the reproducibility which is the measure of how precise the assay is (i.e if the assay give the same result when an experiment is repeated, and to make sure that the data are accurate) [96]. The next step would be to repeat the last experiment semi-automated, with RLN and RNA Secure, 10% lysate in the RT reaction and hydrolysis probes in the qPCR, using the final protocol found in A.6.

The reproducibility can be determined by repeating an experiment with the same plate layout on (e.g. three) different occasions, treated with different GLP1 conjugated ASOs, with multiple replicates for each condition. In such set up, the variation within a plate, between plates and between different runs can be compared for each condition to determine the reproducibility statistically (usually expressed as CV, coefficient of variation) [96, 97]. Statistical tools can also be used to determine how many replicates are needed to get an acceptable variability between the wells. When conditions with acceptable variability and reproducibility have been decided, the assay is ready for screening and ranking of different GLP1-ASO conjugates targeting *MALAT1*.

The knowledge gained in this project will be used to find the right lysis buffer and to customize the protocol and apply to dispersed primary mouse islet cells. The high-throughput assay will be set up according what was found in this study, using 10% lysate in the RT reaction and hydrolysis probes in the qPCR reaction.

Bibliography

[1] C. K. Mathews, K. E. Van Holde, D. R. Appling, and S. J. Anthony-Cahill, *Biochemistry*, Fourth edition. Toronto, CA: Pearson, 2013.

[2] S. I. Ahmad, *Diabetes: An Old Disease, a New Insight*. Springer Science & Business Media, 2013.

[3] World Health Organization, *Diabetes*, 2018-02-21, Jul. 2017. [Online]. Available: `http://www.who.int/mediacentre/factsheets/fs312/en/`.

[4] F. Leti and J. K. DiStefano, "Long noncoding rnas as diagnostic and therapeutic targets in type 2 diabetes and related complications", *Genes*, vol. 8, no. 8, pp. 1–19, 2017.

[5] S. J. Persaud, "Islet g-protein coupled receptors: Therapeutic potential for diabetes", *Current opinion in pharmacology*, vol. 37, pp. 24–28, 2017.

[6] A. Khvorova and J. K. Watts, "The chemical evolution of oligonucleotide therapies of clinical utility", *Nature biotechnology*, vol. 35, no. 3, pp. 238–248, 2017.

[7] C. Ämmälä, W. Druny III, L. Knerr, I. Ahlstedt, P. Stillemark-Billton, C. Wennberg-Huldt, E.-M. Andersson, E. Valeur, R. Jansson-Löfmark, L. Sundström, J. Meuller, J. Claesson, P. Andersson, C. Johansson, R. Lee, T. Pakresh, B. Monia, S. Andersson, and P. Seth, "Targeted delivery of antisense oligonucleotides to pancreatic beta-cells", *Submitted*, 2018, Unpublished.

[8] G. Hung, X. Xiao, R. Peralta, G. Bhattacharjee, S. Murray, D. Norris, S. Guo, and B. P. Monia, "Characterization of target mrna reduction through in situ rna hybridization in multiple organ systems following systemic antisense treatment in animals", *nucleic acid therapeutics*, vol. 23, no. 6, pp. 369–378, 2013.

[9] A. A. Hardikar, *Pancreatic Islet Biology*. Springer, 2016.

[10] Medical Pictures Info, *Islands of langerhans*, 2018-01-21, [Online]. Available: `http://medicalpicturesinfo.com/islands-of-langerhans/`.

[11] P. V. Röder, B. Wu, Y. Liu, and W. Han, "Pancreatic regulation of glucose homeostasis", *Experimental & molecular medicine*, vol. 48, no. 3, e219, 2016.

[12] J. E. Cade and J. Hanisen, "The pancreas", *Anaesthesia & Intensive Care Medicine*, vol. 18, pp. 527–531, 2017.

[13] K. N. Frayn, *Metabolic regulation: a human perspective*. Wiley-blackwell, 2010.

[14] P. Hegyi, J. Maléth, V. Venglovecz, and Z. Rakonczay, "Pancreatic ductal bicarbonate secretion: Challenge of the acinar acid load", *Frontiers in physiology*, vol. 2, p. 36, 2011.

[15] E. Joslin and C. Kahn, *Joslin's Diabetes Mellitus: Edited by C. Ronald Kahn ... [et Al.]*. Ser. Diabetes Mellitus. Lippincott Williams & Willkins, 2005, ISBN:

9780781727969. [Online]. Available: `https://books.google.dk/books?id=ohgjG0qAvfgC`.

[16] L. Jansson, A. Barbu, B. Bodin, C. J. Drott, D. Espes, X. Gao, L. Grapensparr, Ö. Källskog, J. Lau, H. Liljebäck, *et al.*, "Pancreatic islet blood flow and its measurement", *Upsala journal of medical sciences*, vol. 121, no. 2, pp. 81–95, 2016.

[17] D. J. Steiner, A. Kim, K. Miller, and M. Hara, "Pancreatic islet plasticity: Interspecies comparison of islet architecture and composition", *Islets*, vol. 2, no. 3, pp. 135–145, 2010.

[18] S. Seino and G. I. Bell, *Pancreatic beta cell in health and disease*. Springer, 2008.

[19] A. D. Association, "Diagnosis and classification of diabetes mellitus", *Diabetes care*, vol. 31, no. Suppl 1, S62–S67, 2008.

[20] J. Grasman, H. L. Callender, and M. Mensink, "Proportional insulin infusion in closed-loop control of blood glucose", *PloS one*, vol. 12, no. 1, e0169135, 2017.

[21] M. G. Bonini and R. M. Sargis, "Environmental toxicant exposures and type 2 diabetes mellitus: Two interrelated public health problems on the rise", *Current Opinion in Toxicology*, 2017.

[22] T. Satoh, "Molecular mechanisms for the regulation of insulin-stimulated glucose uptake by small guanosine triphosphatases in skeletal muscle and adipocytes", *International journal of molecular sciences*, vol. 15, no. 10, pp. 18 677–18 692, 2014.

[23] I. D. Federation, *IDF Diabetes Atlas 8th Edition*. International Diabetes Federation, 2017.

[24] S. Chatterjee, K. Khunti, and M. J. Davies, "Type 2 diabetes", *The Lancet*, vol. 389, no. 10085, pp. 2239–2251, 2017.

[25] M. E. Cerf, "Beta cell dysfunction and insulin resistance", *Frontiers in endocrinology*, vol. 4, p. 37, 2013.

[26] A. Swisa, B. Glaser, and Y. Dor, "Metabolic stress and compromised identity of pancreatic beta cells", *Frontiers in genetics*, vol. 8, p. 21, 2017.

[27] P. A. Halban, K. S. Polonsky, D. W. Bowden, M. A. Hawkins, C. Ling, K. J. Mather, A. C. Powers, C. J. Rhodes, L. Sussel, and G. C. Weir, "Beta-cell failure in type 2 diabetes: Postulated mechanisms and prospects for prevention and treatment", *Diabetes Care*, vol. 37, pp. 1751–1758, 2014.

[28] M. Asif, "The prevention and control the type-2 diabetes by changing lifestyle and dietary pattern", *Journal of education and health promotion*, vol. 3, 2014.

[29] R. Holt, C. Cockram, A. Flyvbjerg, and B. Goldstein, *Textbook of Diabetes*. Wiley, 2016, ISBN: 9781118924860. [Online]. Available: `https://books.google.dk/books?id=fvyzDQAAQBAJ`.

[30] B. M. Leon and T. M. Maddox, "Diabetes and cardiovascular disease: Epidemiology, biological mechanisms, treatment recommendations and future research", *World journal of diabetes*, vol. 6, no. 13, pp. 1246–1258, 2015.

[31] A. B. Ganiyu, L. H. Mabuza, N. H. Malete, I. Govender, and G. A. Ogunbanjo, "Non-adherence to diet and exercise recommendations amongst patients with type 2 diabetes mellitus attending extension ii clinic in botswana", *African*

Journal of Primary Health Care and Family Medicine, vol. 5, no. 1, pp. 1–6, 2013.

[32] A. Chaudhury, C. Duvoor, R. Dendi, V. Sena, S. Kraleti, A. Chada, R. Ravilla, A. Marco, N. S. Shekhawat, M. T. Montales, *et al.*, "Clinical review of antidiabetic drugs: Implications for type 2 diabetes mellitus management", *Frontiers in endocrinology*, vol. 8, p. 6, 2017.

[33] H. Nguyen, R. Dufour, and A. Caldwell-Tarr, "Glucagon-like peptide-1 receptor agonist (glp-1ra) therapy adherence for patients with type 2 diabetes in a medicare population", *Advances in therapy*, vol. 34, no. 3, pp. 658–673, 2017.

[34] M. Jahangir, S. Imam, I. Kazmi, *et al.*, "Type 2 diabetes current and future medications: A short review", *Int J Pharm Pharmacol 2017; 1*, vol. 101, 2017.

[35] J. Upadhyay, S. A. Polyzos, N. Perakakis, B. Thakkar, S. A. Paschou, N. Katsiki, P. Underwood, K.-H. Park, J. Seufert, E. S. Kang, *et al.*, "Pharmacotherapy of type 2 diabetes: An update", *Metabolism-Clinical and Experimental*, vol. 78, pp. 13–42, 2018.

[36] J. J. Chamberlain, W. H. Herman, S. Leal, A. S. Rhinehart, J. H. Shubrook, N. Skolnik, and R. R. Kalyani, "Pharmacologic therapy for type 2 diabetes: Synopsis of the 2017 american diabetes association standards of medical care in diabetes", *Annals of internal medicine*, vol. 166, no. 8, pp. 572–578, 2017.

[37] M. Jo and S. T. Jung, "Engineering therapeutic antibodies targeting g-protein–coupled receptors", *Experimental & molecular medicine*, vol. 48, no. 2, e207, 2016.

[38] S. Kalra, M. P. Baruah, R. K. Sahay, A. G. Unnikrishnan, S. Uppal, and O. Adetunji, "Glucagon-like peptide-1 receptor agonists in the treatment of type 2 diabetes: Past, present, and future", *Indian journal of endocrinology and metabolism*, vol. 20, no. 2, p. 254, 2016.

[39] J. R. Unger and C. G. Parkin, "Glucagon-like peptide-1 (glp-1) receptor agonists: Differentiating the new medications", *Diabetes Therapy*, vol. 2, no. 1, pp. 29–39, 2011.

[40] B. Finan, C. Clemmensen, and T. D. Müller, "Emerging opportunities for the treatment of metabolic diseases: Glucagon-like peptide-1 based multiagonists", *Molecular and cellular endocrinology*, vol. 418, pp. 42–54, 2015.

[41] J.-I. Hwang, S. Yun, M. J. Moon, C. R. Park, and J. Y. Seong, "Molecular evolution of gpcrs: Glp1/glp1 receptors", *Journal of molecular endocrinology*, vol. 52, no. 3, T15–T27, 2014.

[42] Å. Segerstolpe, A. Palasantza, P. Eliasson, E.-M. Andersson, A.-C. Andréasson, X. Sun, S. Picelli, A. Sabirsh, M. Clausen, M. K. Bjursell, *et al.*, "Single-cell transcriptome profiling of human pancreatic islets in health and type 2 diabetes", *Cell metabolism*, vol. 24, no. 4, pp. 593–607, 2016.

[43] T. Golden, N. M. Dean, and R. E. Honkanen, "Use of antisense oligonucleotides: Advantages, controls, and cardiovascular tissue", *Microcirculation*, vol. 9, no. 1, pp. 51–64, 2002.

[44] O. Khorkova and C. Wahlestedt, "Oligonucleotide therapies for disorders of the nervous system", *Nature biotechnology*, vol. 35, no. 3, p. 249, 2017.

[45] B. Gurav and G. Srinivasan, "Antisense oligonucleotides as therapeutics and their delivery", *Current Science*, vol. 112, no. 3, p. 490, 2017.

[46] K. E. Lundin, O. Gissberg, and C. E. Smith, "Oligonucleotide therapies: The past and the present", *Human gene therapy*, vol. 26, no. 8, pp. 475–485, 2015.

[47] C. Godfrey, L. R. Desviat, B. Smedsrød, F. Piétri-Rouxel, M. A. Denti, P. Disterer, S. Lorain, G. Nogales-Gadea, V. Sardone, R. Anwar, *et al.*, "Delivery is key: Lessons learnt from developing splice-switching antisense therapies", *EMBO molecular medicine*, e201607199, 2017.

[48] R. L. Juliano, "The delivery of therapeutic oligonucleotides", *Nucleic acids research*, vol. 44, no. 14, pp. 6518–6548, 2016.

[49] S. F. Dowdy, "Overcoming cellular barriers for rna therapeutics", *Nature biotechnology*, vol. 35, no. 3, pp. 222–229, 2017.

[50] S. T. Crooke, S. Wang, T. A. Vickers, W. Shen, and X.-h. Liang, "Cellular uptake and trafficking of antisense oligonucleotides", *Nature biotechnology*, vol. 35, no. 3, pp. 230–237, 2017.

[51] T. P. Prakash, M. J. Graham, J. Yu, R. Carty, A. Low, A. Chappell, K. Schmidt, C. Zhao, M. Aghajan, H. F. Murray, *et al.*, "Targeted delivery of antisense oligonucleotides to hepatocytes using triantennary n-acetyl galactosamine improves potency 10-fold in mice", *Nucleic acids research*, vol. 42, no. 13, pp. 8796–8807, 2014.

[52] B. R. Glick, J. J. Pasternak, and C. L. Patten, *Molecular Biotechnology Principles and Applications of Recombinant DNA*, Fourth edition. Washington, DC: ASM PRESS, 2010.

[53] M. A. Valasek and J. J. Repa, "The power of real-time pcr", *Advances in physiology education*, vol. 29, no. 3, pp. 151–159, 2005.

[54] S. Lohmann, A. Herold, T. Bergauer, A. Belousov, G. Betzl, M. Demario, M. Dietrich, L. Luistro, M. Poignée-Heger, K. Schostack, *et al.*, "Gene expression analysis in biomarker research and early drug development using function tested reverse transcription quantitative real-time pcr assays", *Methods*, vol. 59, no. 1, pp. 10–19, 2013.

[55] S. Deepak, K. Kottapalli, R. Rakwal, G. Oros, K. Rangappa, H. Iwahashi, Y. Masuo, and G. Agrawal, "Real-time pcr: Revolutionizing detection and expression analysis of genes", *Current genomics*, vol. 8, no. 4, pp. 234–251, 2007.

[56] L. Li, X. Shen, Z. Liu, M. Norrbom, T. P. Prakash, D. O'Reilly, V. K. Sharma, M. J. Damha, J. K. Watts, F. Rigo, *et al.*, "Activation of frataxin protein expression by antisense oligonucleotides targeting the mutant expanded repeat", *nucleic acid therapeutics*, 2018.

[57] M. Kubista, J. M. Andrade, M. Bengtsson, A. Forootan, J. Jonák, K. Lind, R. Sindelka, R. Sjöback, B. Sjögreen, L. Strömbom, *et al.*, "The real-time polymerase chain reaction", *Molecular aspects of medicine*, vol. 27, no. 2-3, pp. 95–125, 2006.

[58] A. Evrard, N. Boulle, and G. Lutfalla, "Real-time pcr", in *Nanoscience*, Springer, 2009, pp. 841–869.

[59] ThermoFisher, *Introduction to gene expression: Getting started guide*, 2018-01-21, 2018. [Online]. Available: `https://www.thermofisher.com/se/en/home/life-science/pcr/real-time-pcr/real-time-pcr-learning-`

center/gene-expression-analysis-real-time-pcr-information/introduction-gene-expression.html.

[60] S. Bustin, *A-z of quantitative pcr*, La Jolla, CA, 2004.

[61] R. E. Farrell Jr, *RNA Methodologies A Laboratory Guide for Isolation and Characterization*, Fourth edition. San Diego, CA: Elsevier Inc, 2010.

[62] QIAGEN, *RNeasy Mini Handbook*, Fourth edition. QIAGEN, 2012.

[63] ThermoFisher, *Reverse transcription reaction setup—seven important considerations*, 2018-01-21, 2018. [Online]. Available: https://www.thermofisher.com/se/en/home/life-science/cloning/cloning-learning-center/invitrogen-school-of-molecular-biology/rt-education/reverse-transcription-setup.html.

[64] T. Biocenter, *Hands-on qpcr, tataa biocenter*, Lecture slides, 2017.

[65] Integrated DNA Technologies, Inc, *Steps for a successful qpcr experiment*, 2018-01-21, 2018. [Online]. Available: https://eu.idtdna.com/pages/education/decoded/article/successful-qpcr.

[66] J. T. Keer, "Quantitative real-time pcr analysis", in *Essentials of Nucleic Acid Analysis*, 2008, pp. 132–166.

[67] editor@gene-quantification.info, *Dyes & fluorescence detection chemistry in qpcr*, 2018-01-21, 2018. [Online]. Available: http://dyes.gene-quantification.info/.

[68] ThermoFisher, *Taqman vs. sybr chemistry for real-time pcr*, 2018-01-21, 2018. [Online]. Available: https://www.thermofisher.com/se/en/home/life-science/pcr/real-time-pcr/real-time-pcr-learning-center/real-time-pcr-basics/taqman-vs-sybr-chemistry-real-time-pcr.html.

[69] M. Arya, I. S. Shergill, M. Williamson, L. Gommersall, N. Arya, and H. R. Patel, "Basic principles of real-time quantitative pcr", *Expert review of molecular diagnostics*, vol. 5, no. 2, pp. 209–219, 2005.

[70] M. T. Dorak, *Real-time PCR*. Taylor & Francis, 2007.

[71] E. Van Pelt-Verkuil and M. Tevfik, *Principles and Technical Aspects of PCR Amplification*. Springer, 2008.

[72] L. T. Corporation, *Real-time PCR handbook*. lifetechnologies.com, 2012.

[73] M. Seifi, A. Ghasemi, S. Heidarzadeh, M. Khosravi, A. Namipashaki, V. M. Soofiany, A. A. Khosroshahi, and N. Danaei, "Overview of real-time pcr principles", in *Polymerase Chain Reaction*, InTech, 2012.

[74] M. L. Wong and J. F. Medrano, "Real-time pcr for mrna quantitation", *Biotechniques*, vol. 39, no. 1, pp. 75–88, 2005.

[75] M. W. Pfaffl, "Relative quantification", *Real-time PCR*, vol. 63, pp. 63–82, 2006.

[76] A. B. Riemer, D. B. Keskin, and E. L. Reinherz, "Identification and validation of reference genes for expression studies in human keratinocyte cell lines treated with and without interferon-gamma-a method for qrt-pcr reference gene determination", *Experimental dermatology*, vol. 21, no. 8, pp. 625–629, 2012.

[77] T.-M. Dai, Z.-C. Lü, W.-X. Liu, and F.-H. Wan, "Selection and validation of reference genes for qrt-pcr analysis during biological invasions: The thermal adaptability of bemisia tabaci med", *PloS one*, vol. 12, no. 3, e0173821, 2017.

[78] J. Winer, C. K. S. Jung, I. Shackel, and P. M. Williams, "Development and validation of real-time quantitative reverse transcriptase–polymerase chain reaction for monitoring gene expression in cardiac myocytesin vitro", *Analytical biochemistry*, vol. 270, no. 1, pp. 41–49, 1999.

[79] K. J. Livak and T. D. Schmittgen, "Analysis of relative gene expression data using real-time quantitative pcr and the 2-deltadeltact method", *methods*, vol. 25, no. 4, pp. 402–408, 2001.

[80] D. Svec, A. Tichopad, V. Novosadova, M. W. Pfaffl, and M. Kubista, "How good is a pcr efficiency estimate: Recommendations for precise and robust qpcr efficiency assessments", *Biomolecular detection and quantification*, vol. 3, pp. 9–16, 2015.

[81] ThermoFisher, *Basic principles of rt-qpcr*, 2018-01-21, 2018. [Online]. Available: `https://www.thermofisher.com/se/en/home/brands/thermo-scientific/molecular-biology/molecular-biology-learning-center/molecular-biology-resource-library/basic-principles-rt-qpcr.html`.

[82] H. Tian, J. Wu, Y. Shang, Y. Cheng, and X. Liu, "The development of a rapid sybr one step real-time rt-pcr for detection of porcine reproductive and respiratory syndrome virus", *Virology journal*, vol. 7, no. 1, p. 90, 2010.

[83] C. Bardelle, L. McWilliams, S. Mounfield, M. Wigglesworth, and K. Rich, "Validation of miniaturized one-step reverse transcription qpcr assays for high-throughput screening and comparison to a reporter gene methodology", *Assay and drug development technologies*, vol. 13, no. 2, pp. 94–101, 2015.

[84] D. Svec, D. Andersson, M. Pekny, R. Sjöback, M. Kubista, and A. Ståhlberg, "Direct cell lysis for single-cell gene expression profiling", *Frontiers in oncology*, vol. 3, p. 274, 2013.

[85] A. Ståhlberg, M. Kubista, and P. Åman, "Single-cell gene-expression profiling and its potential diagnostic applications", *Expert review of molecular diagnostics*, vol. 11, no. 7, pp. 735–740, 2011.

[86] Y. K. Ho, W. T. Xu, and H. P. Too, "Direct quantification of mrna and mirna from cell lysates using reverse transcription real time pcr: A multidimensional analysis of the performance of reagents and workflows", *PloS one*, vol. 8, no. 9, e72463, 2013.

[87] A. V.-P. Le, D. Huang, T. Blick, E. W. Thompson, and A. Dobrovic, "An optimised direct lysis method for gene expression studies on low cell numbers", *Scientific reports*, vol. 5, p. 12 859, 2015.

[88] A. Kim, K. Miller, J. Jo, G. Kilimnik, P. Wojcik, and M. Hara, "Islet architecture: A comparative study", *Islets*, vol. 1, no. 2, pp. 129–136, 2009.

[89] J. Jo, M. Y. Choi, and D.-S. Koh, "Size distribution of mouse langerhans islets", *Biophysical journal*, vol. 93, no. 8, pp. 2655–2666, 2007.

[90] insphero, *Characterization data*, 2018-01-21, 2018. [Online]. Available: `https://insphero.com/products/islet/human/`.

[91] V. Carvalhais, M. Delgado-Rastrollo, L. D. Melo, and N. Cerca, "Controlled rna contamination and degradation and its impact on qpcr gene expression in s. epidermidis biofilms", *Journal of microbiological methods*, vol. 95, no. 2, pp. 195–200, 2013.

[92] S. Fleige and M. W. Pfaffl, "Rna integrity and the effect on the real-time qrt-pcr performance", *Molecular aspects of medicine*, vol. 27, no. 2-3, pp. 126–139, 2006.

[93] ThermoFisher, *Agarose gel electrophoresis of rna*, 2018-01-21, 2018. [Online]. Available: `https://www.thermofisher.com/se/en/home/references/protocols/nucleic-acid-purification-and-analysis/rna-protocol/agarose-gel-electrophoresis-of-rna.html`.

[94] K. Huang, F. Doyle, Z. E. Wurz, S. A. Tenenbaum, R. K. Hammond, J. L. Caplan, and B. C. Meyers, "Fastmir: An rna-based sensor for in vitro quantification and live-cell localization of small rnas", *Nucleic acids research*, vol. 45, no. 14, e130–e130, 2017.

[95] G. Wang, G. Wang, X. Zhang, F. Wang, and R. Song, "Isolation of high quality rna from cereal seeds containing high levels of starch", *Phytochemical Analysis*, vol. 23, no. 2, pp. 159–163, 2012.

[96] S. A. Bustin, V. Benes, J. A. Garson, J. Hellemans, J. Huggett, M. Kubista, R. Mueller, T. Nolan, M. W. Pfaffl, G. L. Shipley, *et al.*, "The miqe guidelines: Minimum information for publication of quantitative real-time pcr experiments", *Clinical chemistry*, vol. 55, no. 4, pp. 611–622, 2009.

[97] C. A. Allen, S. L. Payne, M. Harville, N. Cohen, and K. E. Russell, "Validation of quantitative polymerase chain reaction assays for measuring cytokine expression in equine macrophages", *Journal of immunological methods*, vol. 328, no. 1-2, pp. 59–69, 2007.

A

Appendix

A.1 Primary islet cells from mouse

No. of cells/well	Cq values		ΔCq between dilutions	
4000 undil	23,8	23,2		
1:2 dil	24,2	23,5	0,4	0,3
1:4 dil	24,8		0,6	
4500, undil	23,8	22,8		
1:2 dil	24,4	23,0	0,6	0,2
1:4 dil	25,1		0,7	
5000	24,5	22,3		
1:2 dil	24,7	22,7	0,2	0,4
1:4 dil	25,4		0,7	
7500 undil	22,5	22,4		
1:2 dil	23,0	23,0	0,4	0,5
1:4 dil	23,4		0,5	
10000 undil	22,0	21,7		
1:2 dil	22,2	22,1	0,2	0,4
1:4 dil	22,8		0,7	
12500 undil	21,4	21,9		
1:2 dil	21,9	22,3	0,5	0,4
1:4 dil	22,4		0,6	

Table A.1: C_q values received from the qPCR run for *36B4* and was used to calculate the ΔC_q values between each dilution for 4000, 4500, 5000, 7500, 10000 and 12500 primary islet cells from mouse to find out the estimated amplification efficiency.

Mouse dissociated islets								
	36B4		HPRT1		GAPDH		MALAT1	
Dilution	Cq values	ΔCq	Cq values	ΔCq	Cq values	ΔCq	Cq values	ΔCq
4000, undil	26,9		32,7					
1:2	27,2	0,3	31,5	-1,2	33.8		25,7	
1:4	27,8	0,6	31,3	-0,2	32,7	-1,1	25,7	0,0
1:8	28,7	0,9	30,5	-0,8	31,6	-1,1	25,4	-0,3
1:16	29,4	0,7	Undeterminated		29,0	-2,6	26,0	0,6
2000, undil	27,5		35,4					
1:2	27,8	0,3	33,6	-1,8	Undeterminated		29,9	
1:4	28,2	0,4	32,8	-0,8	33,7		27,8	-2,1
1:8	28,9	0,7	32,2	-0,6	33,7	0	26,7	-1,1
1:16	30,1	1,2	32,6	0,4	33,7	0	26,8	0,1
1000, undil	29,8		35,0					
1:2	30,3	0,5	34,0	-1,0	38,8		29,8	
1:4	30,9	0,6	35,0	1,0	35,4	-3,4	29,2	-0,6
1:8	31,0	0,1	Undeterminated		29,7	-5,7	28,2	-1,0
1:16	31,3	0,3	Undeterminated		30,1	0,4	27,8	-0,4
500, undil	32,8		Undeterminated		Undeterminated		32,4	
1:2	32,5	-0,3	Undeterminated		Undeterminated		35,5	3,1
1:4	32,6	0,1	36,4		Undeterminated		33,2	-2,3
1:8	33,6	1	Undeterminated		37,9		30,4	-2,8
1:16	34,2	0,6	37,7		25,8	-12,1	30,8	0,4
250, undil	34,4		Undeterminated		Undeterminated		Undeterminated	
1:2	34,2	-0,2	34,5		Undeterminated		Undeterminated	
1:4	35,6	1,4	Undeterminated		Undeterminated		37,0	
1:8	35,5	-0,1	Undeterminated		Undeterminated		33,8	-3,2
1:16	35,1	-0,4	Undeterminated		Undeterminated		31,7	-2,1

Table A.2: C_q values and calculated ΔC_q values that were received from the wells containing 4000, 2000, 1000, 500 and 250 primary islet cells from mouse for different reference genes.

A.2 GLP1R-HEK293 cells

HEK293 GLP-1R cells								
	HPRT1		PPIA (AoD)		MALAT1		36B4		GAPDH	
Dilution	Cq-values	ΔCq	Cq-values	ΔCq	Cq-values	ΔCq	Cq-values	ΔCq	Cq-values	ΔCq
Sample 1, 1:4 dil	23,0		26,2		25,7		19,1		18,7	
1:8 dil	24,2	1,1	26,2	0,0	26,3	0,6	19,9	0,8	27,1	8,4
1:16 dil	24,8	0,6	27,8	1,6	26,8	0,5	20,5	0,6	20,9	-6,2
1:32 dil	25,4	0,7	28,4	0,6	27,0	0,2	21,0	0,5	21,5	0,5
Sample 2, 1:4 dil	25,0		26,6		27,9		20,0		19,3	
1:8 dil	25,1	0,1	27,7	1,1	27,5	-0,4	20,8	0,8	27,8	8,5
1:16 dil	25,6	0,5	27,9	0,2	27,9	0,4	21,4	0,6	21,5	-6,3
1:32 dil	26,5	0,8	28,9	0,9	28,2	0,4	22,0	0,6	22,2	0,7
Sample 3, 1:4 dil	25,4		26,0		25,0		21,2		20,2	
1:8 dil	25,7	0,4	26,7	0,8	25,7	0,7	21,5	0,3	30,1	9,8
1:16 dil	26,4	0,7	28,0	1,3	26,2	0,4	22,0	0,5	22,1	-7,9
1:32 dil	27,1	0,7	28,3	0,3	26,8	0,6	22,4	0,4	23,0	0,8
Sample 4, 1:4 dil	23,3		26,7		25,6		20,2		19,0	
1:8 dil	24,6	1,3	27,6	0,8	26,3	0,7	20,5	0,3	27,8	8,8
1:16 dil	25,0	0,4	28,3	0,7	27,5	1,2	21,2	0,6	21,1	-6,8
1:32 dil	25,8	0,8	28,8	0,5	27,9	0,4	21,4	0,2	21,9	0,8

Table A.3: C_q values and calculated ΔC_q that was recived from the qPCR run for 7000 GLP1R-HEK293 cells using different reference genes.

A.3 Comparison between different cell numbers and lysis buffers

HPRT1

Lysis buffer	Cq values			Ave. Cq	SD	ΔCq		
A-project, non-act 10% 1:4	22,2	22,1	22,3	22,2	0,09			
A-project non-act 10% 1:8	23,1	23,1	23,4	23,2	0,16	0,9	1,0	1,0
A-project non-act 10% 1:16	24,2	24,1	24,3	24,2	0,11	1,1	1,0	0,9
A-project non-act 10% 1:32	25,2	25,0	25,2	25,1	0,13	1,0	0,9	0,9
A-project non-act 4% 1:4	Undetermined	24,2	24,0	24,1	0,18			
A-project non-act 4% 1:8	Undetermined	25,1	24,9	25,0	0,12		0,9	0,9
A-project non-act 4% 1:16	Undetermined	26,0	25,8	25,9	0,13		0,9	0,9
A-project non-act 4% 1:32	Undetermined	26,9	26,5	26,7	0,26		0,9	0,7
NP40/BSA act 10% 1:4	21,9	21,5	21,6	21,6	0,21			
NP40/BSA act 10% 1:8	22,9	22,9	22,8	22,9	0,05	1,0	1,4	1,2
NP40/BSA act 10% 1:16	24,1	23,7	23,9	23,9	0,18	1,2	0,8	1,1
NP40/BSA act 10% 1:32	24,9	24,7	25,1	24,9	0,19	0,9	1,0	1,2
NP40/BSA act 4% 1:4	22,7	22,5	22,5	22,6	0,12			
NP40/BSA act 4% 1:8	23,8	23,6	23,6	23,7	0,12	1,1	1,1	1,1
NP40/BSA act 4% 1:16	24,8	24,7	24,7	24,7	0,05	0,9	1,1	1,0
NP40/BSA act 4% 1:32	25,8	25,7	25,7	25,7	0,09	1,1	1,0	1,0
A-project act 10% 1:4	22,1	22,4	22,3	22,3	0,17			
A-project act 10% 1:8	23,3	23,5	23,4	23,4	0,07	1,2	1,1	1,1
A-project act 10% 1:16	24,1	24,3	24,1	24,2	0,12	0,7	0,8	0,7
A-project act 10% 1:32	24,9	24,9	24,8	24,9	0,01	0,8	0,6	0,7
A-project act 4% 1:4	25,0	24,8	25,4	25,1	0,28			
A-project act 4% 1:8	25,0	25,7	25,9	25,5	0,47	0,0	0,9	0,5
A-project act 4% 1:16	26,3	26,3	26,5	26,3	0,11	1,2	0,6	0,5
A-project act 4% 1:32	26,8	27,0	27,1	27,0	0,12	0,6	0,8	0,6
-RT A-project non-act 10% 1:4 1	36,7	36,7	35,4	36,3	0,71			
-RT A-project act 10% 1:4 1	35,4	35,0	35,3	35,2	0,20			
-RT NP40/BSA act 10% 1:4 1	36,1	34,9	35,2	35,4	0,62			

Table A.4: C_q values and calculated ΔC_q for 7000 GLP1R-HEK293 cells lysed with different lysis buffers, adipocyte lysis buffer and 0.3% NP40/0.1% BSA containing activated or non-activated RNA Secure.

36B4

Lysis buffer	Cq	Cq	Cq	ΔRT	ΔRT	ΔRT
A-project non-act 10% 1:4	20,9	20,0	20,0	7,3	8,6	7,7
A-project act 10% 1:4	22,0	21,4	20,8	6,2	7,8	8,8
NP40/BSA act 10% 1:4	21,2	20,6	20,6	**8,7**	**11,5**	**9,9**
-RT A-project non-act 10% 1:4	28,2	28,6	27,7			
-RT A-project act 10% 1:4	28,2	29,2	29,7			
-RT NP40/BSA act 10% 1:4	29,9	32,1	30,6			

Table A.5: C_q values from 7000 GLP1R-HEK293 cells/well used for comparison between RT reaction with and without reverse transcriptase, to give indication of gDNA contamination

HPRT1

Lysis buffer	Cq values			Ave. Cq	SD	ΔCq		
A-project, non-act 10% 1:4	24,7	23,9	24,6	24,4	0,42			
A-project non-act 10% 1:8	25,6	25,0	25,7	25,4	0,38	0,9	1,1	1,1
A-project non-act 10% 1:16	26,6	25,9	26,7	26,4	0,40	0,9	0,9	1,0
A-project non-act 10% 1:32	28,1	26,9	27,5	27,5	0,61	1,5	0,9	0,8
A-project non-act 4% 1:4	26,4	26,4	27,3	26,7	0,53			
A-project non-act 4% 1:8	27,4	27,4	28,0	27,6	0,36	1,0	1,0	0,7
A-project non-act 4% 1:16	28,3	28,0	28,7	28,3	0,35	0,9	0,6	0,7
A-project non-act 4% 1:32	28,8	28,8	29,6	29,1	0,47	0,5	0,8	0,9
NP40/BSA act 10% 1:4	23,3	23,5	23,4	23,4	0,11			
NP40/BSA act 10% 1:8	24,6	24,8	24,6	24,7	0,11	1,4	1,3	1,2
NP40/BSA act 10% 1:16	25,6	25,8	25,8	25,7	0,09	1,0	1,0	1,2
NP40/BSA act 10% 1:32	26,7	27,2	26,8	26,9	0,28	1,0	1,4	1,0
NP40/BSA act 4% 1:4	24,5	24,9	24,5	24,6	0,23			
NP40/BSA act 4% 1:8	25,5	25,9	25,8	25,7	0,23	1,0	1,0	1,3
NP40/BSA act 4% 1:16	26,5	27,1	26,7	26,8	0,31	1,0	1,2	0,9
NP40/BSA act 4% 1:32	27,5	27,9	27,7	27,7	0,20	1,0	0,8	1,0
A-project act 10% 1:4	24,3	24,7	24,3	24,4	0,23			
A-project act 10% 1:8	25,2	25,6	25,3	25,4	0,21	0,9	0,9	1,0
A-project act 10% 1:16	26,0	26,3	26,1	26,1	0,15	0,8	0,7	0,8
A-project act 10% 1:32	27,0	27,1	26,9	27,0	0,10	1,0	0,8	0,8
A-project act 4% 1:4	27,4	28,0	27,8	27,7	0,31			
A-project act 4% 1:8	28,0	28,6	28,5	28,4	0,32	0,6	0,6	0,7
A-project act 4% 1:16	28,4	29,1	29,0	28,8	0,38	0,4	0,5	0,5
A-project act 4% 1:32	29,1	29,6	29,4	29,4	0,25	0,7	0,5	0,4
-RT A-project non-act 10% 1:4	39,0	37,5	29,8	35,4	4,94			
-RT A-project act 10% 1:4	37,5	39,1	36,8	37,8	1,18			
-RT NP40/BSA act 10% 1:4	40,0	39,0	37,7	38,9	1,15			

Table A.6: C_q values and calculated ΔC_q for 4000 GLP1R-HEK293 cells lysed with different lysis buffers, adipocyte lysis buffer and 0.3% NP40/0.1% BSA containing activated or non-activated RNA Secure.

36B4

Lysis buffer	Cq	Cq	Cq	ΔRT	ΔRT	ΔRT
A-project non-act 10% 1:4	21,544	20,816	20,185	6,7	4,0	8,6
A-project act 10% 1:4	21,629	21,648	22,474	6,8	6,4	5,7
NP40/BSA act 10% 1:4	22,037	20,986	21,380	**7,0**	**6,8**	**5,9**
-RT A-project non-act 10% 1:4	28,212	24,822	28,799			
-RT A-project act 10% 1:4	28,434	28,045	28,190			
-RT NP40/BSA act 10% 1:4	29,018	27,741	27,328			

Table A.7: C_q values for *36B4* for 4000 GLP1R-HEK293 cells used for comparison between RT reaction with and without reverse transcriptase, to give indication of gDNA contamination.

HPRT1

Lysis buffer	Cq values			Ave. Cq	SD	ΔCq		
A-project, non-act 10% 1:4	28,6	28,1	28,6	28,4	0,30			
A-project non-act 10% 1:8	28,7	28,6	28,9	28,7	0,19	0,1	0,5	0,3
A-project non-act 10% 1:16	28,9	28,8	29,5	29,1	0,38	0,3	0,3	0,6
A-project non-act 10% 1:32	29,5	29,3	29,9	29,5	0,28	0,5	0,5	0,3
A-project non-act 4% 1:4	32,4	33,0	30,2	31,9	1,47			
A-project non-act 4% 1:8	31,7	32,1	29,9	31,2	1,20	-0,7	-0,9	-0,3
A-project non-act 4% 1:16	31,6	31,8	30,2	31,2	0,90	-0,1	-0,3	0,3
A-project non-act 4% 1:32	31,8	32,3	30,7	31,6	0,83	0,1	0,5	0,5
NP40/BSA act 10% 1:4	24,2	24,4	24,1	24,2	0,15			
NP40/BSA act 10% 1:8	25,3	25,7	25,2	25,4	0,26	1,1	1,3	1,1
NP40/BSA act 10% 1:16	26,3	26,4	26,2	26,3	0,11	1,0	0,8	1,1
NP40/BSA act 10% 1:32	27,3	27,6	27,3	27,4	0,15	1,0	1,1	1,1
NP40/BSA act 4% 1:4	25,7	25,7	25,7	25,7	0,00			
NP40/BSA act 4% 1:8	26,7	26,6	26,5	26,6	0,11	1,0	0,9	0,8
NP40/BSA act 4% 1:16	27,9	27,6	27,5	27,6	0,19	1,1	1,0	1,0
NP40/BSA act 4% 1:32	28,7	28,6	28,6	28,6	0,06	0,8	1,0	1,1
A-project act 10% 1:4	28,0	28,2	29,8	28,7	0,98			
A-project act 10% 1:8	28,1	28,7	29,3	28,7	0,62	0,1	0,5	-0,5
A-project act 10% 1:16	28,5	28,8	29,3	28,9	0,44	0,4	0,1	0,0
A-project act 10% 1:32	28,8	29,3	29,7	29,3	0,43	0,4	0,5	0,4
A-project act 4% 1:4	32,0	32,4	34,2	32,9	1,14			
A-project act 4% 1:8	31,6	31,7	32,7	32,0	0,60	-0,4	-0,7	-1,5
A-project act 4% 1:16	31,7	31,1	31,7	31,5	0,36	0,0	-0,6	-1,0
A-project act 4% 1:32	31,9	32,0	33,0	32,3	0,59	0,2	0,9	1,3
-RT A-project non-act 10% 1:4	Undetermined	Undetermined	Undetermined					
-RT A-project act 10% 1:4	33,0	Undetermined	Undetermined					
-RT NP40/BSA act 10% 1:4	Undetermined	33,6	Undetermined					

Table A.8: C_q values and calculated ΔC_q for 1000 GLP1R-HEK293 cells lysed with different lysis buffers, adipocyte lysis buffer and 0.3% NP40/0.1% BSA containing activated or non-activated RNA Secure

36B4

Lysis buffer	Cq	Cq	Cq	ΔRT	ΔRT	ΔRT
A-project non-act 10% 1:4	24,9	24,8	25,2	7,9	7,9	8,2
A-project act 10% 1:4	25,1	25,1	25,4	1,9	4,1	5,8
NP40/BSA act 10% 1:4	23,0	22,8	23,1	6,8	5,2	5,8
-RT A-project non-act 10% 1:4	32,8	32,7	33,4			
-RT A-project act 10% 1:4	27,0	29,2	31,2			
-RT NP40/BSA act 10% 1:4	29,8	28,0	28,9			

Table A.9: C_q values for *36B4* used for comparison between RT reaction with and without reverse transcriptase, to give indication of gDNA contamination in wells containing 1000 GLP1R-HEK293 cells.

A.4 Comparison between cells lysed with different lysis buffers with and without DTT and DNase treatment

Lysis buffer, No/After spin, dilution	Cq values			Ave. Cq	SD	ΔCq		
NP40BSA No spin 1:5	23,946	24,084	23,873	23,968	0,10703			
NP40BSA No spin 1:10	24,773	24,900	24,844	24,839	0,06344	0,8	0,8	1,0
NP40BSA No spin 1:20	25,714	25,588	25,443	25,582	0,13576	0,9	0,7	0,6
NP40BSA No spin 1:40	26,140	26,184	26,148	26,157	0,02339	0,4	0,6	0,7
NP40BSA After spin 1:5	24,702	24,288	24,296	24,429	0,23669			
NP40BSA After spin 1:10	25,188	24,876	24,889	24,984	0,17688	0,5	0,6	0,6
NP40BSA After spin 1:20	25,757	25,433	25,319	25,503	0,22716	0,6	0,6	0,4
NP40BSA After spin 1:40	26,554	26,126	26,142	26,274	0,2427	0,8	0,7	0,8
NP40BSA DTT DNase No spin 1:5	35,346	34,728	34,237	34,771	0,55589			
NP40BSA DTT DNase No spin 1:10	Undetermined	33,765	32,386	33,076	0,97522		-1,0	-1,9
NP40BSA DTT DNase No spin 1:20	33,138	35,119	31,808	33,355	1,66595		1,4	-0,6
NP40BSA DTT DNase No spin 1:40	34,963	33,191	33,359	33,837	0,97817	1,8	-1,9	1,6
NP40BSA DTT DNase After spin 1:5	35,576	36,606	35,514	35,899	0,61324			
NP40BSA DTT DNase After spin 1:10	37,556	Undetermined	35,339	36,448	1,56713	2,0		-0,2
NP40BSA DTT DNase After spin 1:20	34,555	36,212	38,425	36,397	1,94168	-3,0		3,1
NP40BSA DTT DNase After spin 1:40	34,823	34,188	Undetermined	34,505	0,44891	0,3	-2,0	
BSA No spin 1:5	26,155	23,624	23,007	24,262	1,66807			
BSA No spin 1:10	26,788	24,637	24,234	25,220	1,37277	0,6	1,0	1,2
BSA No spin 1:20	27,891	25,891	25,322	26,368	1,34896	1,1	1,3	1,1
BSA No spin 1:40	29,079	26,739	26,148	27,322	1,54973	1,2	0,8	0,8
BSA After spin 1:5	24,981	23,774	22,597	23,784	1,19164			
BSA After spin 1:10	25,691	24,537	23,553	24,594	1,06988	0,7	0,8	1,0
BSA After spin 1:20	26,325	25,313	24,465	25,368	0,93093	0,6	0,8	0,9
BSA After spin 1:40	27,540	26,833	25,473	26,615	1,05058	1,2	1,5	1,0
BSA DTT DNase No spin 1:5	32,724	31,445	30,383	31,517	1,17265			
BSA DTT DNase No spin 1:10	32,458	33,043	31,602	32,368	0,72476	-0,3	1,6	1,2
BSA DTT DNase No spin 1:20	35,158	33,411	31,533	33,367	1,81318	2,7	0,4	-0,1
BSA DTT DNase No spin 1:40	33,963	33,790	32,265	33,339	0,9342	-1,2	0,4	0,7
BSA DTT DNase After spin 1:5	35,312	Undetermined	30,597	32,954	3,33466			
BSA DTT DNase After spin 1:10	33,770	Undetermined	30,500	32,135	2,31208	-1,5		-0,1
BSA DTT DNase After spin 1:20	34,513	Undetermined	33,412	33,962	0,77869	0,7		2,9
BSA DTT DNase After spin 1:40	35,238	Undetermined	34,857	35,047	0,26993	0,7		1,4

Table A.10: C_q values received from qPCR reaction for *HPRT1* and calculated ΔC_q for different lysis buffers (0.3% NP40/0.1% BSA, 0.3% NP40/0.1% BSA with DTT and DNase and 0.1%BSA with and without DTT and DNase) for each dilution.

Lysis buffer, No/after spin, dilution	Cq values			Ave. Cq	SD	ΔCq		
NP40BSA, No spin, 1:5	21,6	21,5	20,9	21,3	0,4			
NP40BSA No spin 1:10	22,1	21,9	22,2	22,0	0,2	0,5	0,3	1,3
NP40BSA No spin 1:20	22,3	22,5	22,4	22,4	0,1	0,2	0,6	0,2
NP40BSA No spin 1:40	22,8	22,8	22,9	22,8	0,0	0,5	0,3	0,4
NP40BSA After spin 1:5	22,2	21,7	21,2	21,7	0,5			
NP40BSA After spin 1:10	22,7	22,3	21,8	22,3	0,5	0,5	0,6	0,6
NP40BSA After spin 1:20	22,8	22,5	22,1	22,5	0,3	0,0	0,2	0,3
NP40BSA After spin 1:40	23,3	22,8	22,7	22,9	0,3	0,5	0,3	0,6
NP40BSA DTT DNase No spin 1:5	34,6	38,8	36,8	36,8	2,1			
NP40BSA DTT DNase No spin 1:10	34,5	33,7	32,4	33,5	1,0	-0,2	-5,1	-4,4
NP40BSA DTT DNase No spin 1:20	32,3	32,7	30,9	32,0	0,9	-2,1	-1,0	-1,5
NP40BSA DTT DNase No spin 1:40	32,7	30,8	31,3	31,6	1,0	0,4	-1,9	0,4
NP40BSA DTT DNase After spin 1:5	35,2	38,1	33,5	35,6	2,3			
NP40BSA DTT DNase After spin 1:10	32,8	34,1	Undetermined	33,5	0,9	-2,4	-4,0	
NP40BSA DTT DNase After spin 1:20	31,6	30,4	Undetermined	31,0	0,8	-1,3	-3,7	
NP40BSA DTT DNase After spin 1:40	32,0	34,3	Undetermined	33,2	1,7	0,4	3,9	
BSA No spin 1:5	23,7	20,3	19,8	21,3	2,1			
BSA No spin 1:10	24,5	21,3	20,9	22,3	1,9	0,8	1,1	1,1
BSA No spin 1:20	25,5	22,5	22,2	23,4	1,8	1,0	1,2	1,2
BSA No spin 1:40	26,4	23,3	22,8	24,1	1,9	0,9	0,8	0,6
BSA After spin 1:5	22,8	21,0	19,8	21,2	1,5			
BSA After spin 1:10	23,4	21,8	20,7	21,9	1,4	0,6	0,8	0,9
BSA After spin 1:20	24,4	22,8	21,6	22,9	1,4	1,0	1,0	1,0
BSA After spin 1:40	25,6	23,7	22,7	24,0	1,5	1,2	1,0	1,1
BSA DTT DNase No spin 1:5	31,4	29,8	29,0	30,1	1,2			
BSA DTT DNase No spin 1:10	31,6	30,7	29,7	30,7	0,9	0,2	1,0	0,7
BSA DTT DNase No spin 1:20	32,9	31,4	30,2	31,5	1,3	1,3	0,7	0,5
BSA DTT DNase No spin 1:40	33,6	32,2	30,4	32,0	1,6	0,7	0,8	0,1
BSA DTT DNase After spin 1:5	34,9	39,4	29,1	34,5	5,1			
BSA DTT DNase After spin 1:10	35,8	33,7	29,2	32,9	3,4	1,0	-5,6	0,1
BSA DTT DNase After spin 1:20	33,8	Undetermined	30,6	32,2	2,3	-2,0		1,4
BSA DTT DNase After spin 1:40	32,7	Undetermined	32,7	32,7	0,0	-1,2		2,0

Table A.11: C_q values received from qPCR run for *MALAT1* and calculated ΔC_q for different lysis buffers (0.3% NP40/0.1% BSA, 0.3% NP40/0.1% BSA with DTT and DNase, 0.1% BSA with and without DTT and DNase) for each dilution.

Lysis buffer, No/After spin, Dilution	Ave. Cq, +RT	Ave. Cq, -RT	ΔRT
NP40BSA No spin 1:5	20,3	36,7	16,4
BSA No spin 1:5	20,1	33,1	13,1
NP40BSA DTT DNase No spin 1:5	28,5	39,5	11,0
BSA DTT DNase No spin 1:5	27,3	38,9	11,6
NP40BSA After spin 1:5	20,6	37,5	16,9
BSA After spin 1:5	19,5	36,4	16,8
NP40BSA DTT DNase After spin 1:5	29,6	38,9	9,3
BSA DTT DNase After spin 1:5	31,7	40,0	8,3

Table A.12: Average of the C_q values received from the qPCR run for *36B4* used for comparison between RT reaction with and without reverse transcriptase, (as control) to give indication of gDNA contamination.

A.5 Pre-study

HPRT1

	Cq values, No spin						Ave. Cq	SD	ΔCq	Cq values, After spin						Ave. Cq	SD	ΔCq
A-project RT, RLN buffer, 1:5 dil	25,2	**24,9**	24,9	26,0	26,1	25,2	25,5	0,5		26,6	26,7	26,2	**26,7**	25,8	**25,7**	26,3	0,5	
	25,3	25,0	25,1	**26,2**	26,2	25,2	25,1											
	25,4	25,0	25,1	25,9	26,2	25,3												
1:10 dil	26,2	25,8	25,7				25,9	0,3	0,81	26,6	27,0	26,7	26,6	27,1	26,7	26,8	0,2	0,51
	26,1	25,8	25,9															
	26,3	25,8	26,0															
1:20 dil	26,6	26,4	26,5				26,7	0,2	0,75	27,2	27,8	27,3	27,4	27,3	27,1	27,3	0,2	0,54
	26,8	26,5	26,7															
	26,9	26,6	26,9															
A-project RT, RLN buffer + DTT, 1:5 dil	26,2	25,3	27,4	**24,6**	24,9	25,7	25,8	1,0		25,7	25,8	**25,3**	**26,4**	25,9	25,4	25,9	0,3	
	26,2	25,5	**27,8**	24,8	25,0	25,9	26,3			25,9	25,9	25,4	26,2	26,2	25,6	25,7		
	26,3	25,6	27,7	24,8	24,8	25,7				26,0	26,1	25,6	26,2	26,2	25,6			
1:10 dil	26,8	26,1	28,2				27,1	0,9	0,69	26,5	26,5	26,1				26,5	0,2	0,79
	27,0	26,2	28,4							26,6	26,6	26,3						
	27,0	26,3	28,3							26,7	26,9	26,4						
1:20 dil	27,4	26,8	29,0				27,8	0,9	0,69	27,2	27,2	26,8				27,2	0,2	0,70
	27,5	27,0	29,0							27,2	27,5	27,1						
	27,4	27,2	29,2							27,4	27,6	27,1						
High Cap RT, RLN buffer, 1:5 dil	26,8	26,6	26,9	26,9	27,2	**26,1**	26,8	0,4		27,2	27,1	27,1	**27,6**	26,7	26,6	27,1	0,3	
	26,9	26,7	27,0	26,9	27,3	26,1	26,8			27,2	27,2	27,1	27,6	26,8	**26,4**	27,2		
	26,3	26,7	27,2	26,8	**27,3**	26,3				27,2	27,3	27,1	27,5	26,7	26,6			
1:10 dil	27,6	27,3	27,6				27,6	0,2	0,80	27,7	27,7	27,5				27,7	0,2	0,59
	27,5	27,5	27,8							27,8	27,8	27,6						
	27,8	27,7	27,8							27,9	28,0	27,7						
1:20 dil	28,3	27,9	28,4				28,3	0,2	0,70	28,2	28,4	27,9				28,3	0,2	0,56
	28,3	28,1	28,5							28,5	28,3	28,3						
	28,6	28,3	28,5							28,5	28,3	28,3						
High Cap RT, RLN buffer + DTT, 1:5 dil	27,6	26,2	27,7	26,9	27,4	**26,0**	27,0	0,7		26,8	26,8	26,2	26,6	26,5	**26,2**	26,6	0,3	
	27,9	26,5	27,7	26,9	27,2	26,1	27,3			27,0	26,9	26,2	26,7	26,6	26,3	26,7		
	27,9	26,4	**28,0**	26,9	27,1	26,1				26,9	**27,0**	26,2	26,7	26,7	26,3			
1:10 dil	28,3	27,0	28,3				28,0	0,6	0,70	27,5	27,4	27,0				27,4	0,3	0,76
	28,5	27,4	28,4							27,6	27,7	27,1						
	28,5	27,2	28,6							27,7	27,7	27,2						
1:20 dil	28,9	27,8	28,8				28,7	0,6	0,70	28,2	28,3	27,8				28,1	0,2	0,70
	29,1	27,9	29,4							28,1	28,3	27,9						
	29,3	28,2	29,1							28,3	28,3	28,1						
A-project RT, BSA buffer, 1:5 dil	25,0	25,6	26,8	25,0	25,4	28,0	26,1	1,1										
	24,9	25,6	26,9	25,1	25,7	28,2												
	25,2	25,8	27,0	25,4	25,9	**28,3**												
High Cap RT, BSA buffer, 1:5 dil	**24,7**	25,4	28,4	25,3	27,5	29,8	26,9	1,9										
	24,8	25,3	28,2	25,2	27,7	29,8												
	25,0	25,6	28,5	25,4	27,9	**30,2**												

Table A.13: C_q and ΔC_q for *HPRT1* from the wells that contained GLP1R-HEK293 cells lysed with RLN lysis buffer, RLN + DTT lysis buffer or 0.1% BSA, where two different cDNA kit (A-project and High-Capacity cDNA Reverse transcription kit) was used for the cDNA synthesis.

MALAT1 (Cq-values)

	No spin						Average	SD	ΔCq	After spin						Average	SD	ΔCq
A-project RT, RLN buffer, 1:5 dil	22,077	21,816	21,561	22,882	22,781	21,709	22,2	0,5		23,192	24,065	23,818	23,745	24,000	23,449	23,7	0,3	
	22,107	22,188	21,607	22,932	22,781	21,840	22,4											
	22,271	22,315	21,810	23,013	22,802	21,780												
1:10 dil	22,654	22,350	22,355				22,6	0,2	0,64	23,209	23,551	23,924	25,023	24,115	23,760	23,9	0,6	0,22
	22,733	22,470	22,526															
	22,878	22,711	22,820															
1:20 dil	23,166	22,822	22,742				23,1	0,2	0,47	23,870	24,065	24,066	24,100	24,334	23,887	24,1	0,2	0,12
	23,308	22,954	22,991															
	23,330	23,135	23,280															
A-project RT, RLN buffer + DTT, 1:5 dil	22,815	22,219	24,557	21,292	21,001	22,208	22,4	1,2		22,632	22,500	22,220	22,601	22,649	22,197	22,5	0,2	
	22,880	22,389	24,533	21,292	21,197	21,901	23,3			22,726	22,648	22,402	22,540	22,723	22,304	22,7		
	22,874	22,435	24,615	21,176	21,203	21,907				22,754	22,741	22,437	22,616	22,757	22,234			
1:10 dil	23,242	22,684	24,786				23,6	0,9	0,37	23,006	23,140	22,843				23,1	0,1	0,52
	23,339	22,790	24,834							23,099	23,238	22,973						
	23,383	22,836	24,766							23,134	23,239	22,987						
1:20 dil	23,778	23,300	24,929				24,1	0,7	0,47	23,590	23,611	23,349				23,6	0,2	0,55
	23,761	23,406	24,971							23,567	23,777	23,585						
	23,937	23,624	25,145							23,608	23,885	23,743						
High Cap RT, RLN buffer, 1:5 dil	23,679	23,227	24,247	23,932	24,285	22,940	23,8	0,5		24,362	24,625	24,207	24,357	23,807	23,206	24,1	0,5	
	24,049	23,694	24,219	23,793	24,322	23,131	23,9			24,373	24,568	24,226	24,368	23,924	23,197	24,1		
	24,116	23,727	24,186	23,715	24,072	22,980				24,403	24,516	24,117	24,148	23,800	23,229			
1:10 dil	24,208	24,124	24,302				24,3	0,1	0,35	24,473	24,428	24,125				24,4	0,2	0,02
	24,275	24,119	24,318							24,530	24,506	24,231						
	24,370	24,166	24,408							24,535	24,534	24,184						
1:20 dil	24,353	24,233	24,472				24,5	0,1	0,20	24,441	24,612	24,337				24,5	0,2	0,14
	24,433	24,372	24,619							24,502	24,787	24,326						
	24,649	24,408	24,588							24,603	24,696	24,459						
High Cap RT, RLN buffer + DTT, 1:5 dil	24,541	22,584	24,388	23,350	23,314	21,951	23,4	0,9		23,370	22,904	22,631	22,779	21,292	22,601	22,7	0,7	
	24,531	22,851	24,287	23,487	23,338	22,080	23,9			23,510	23,550	22,815	22,841	21,292	22,540	22,7		
	24,577	22,780	24,427	23,509	23,336	22,193				23,386	23,413	22,541	22,986	21,176	22,616			
1:10 dil	24,806	23,263	24,487				24,3	0,6	0,37	23,746	23,588	23,169				23,6	0,3	0,47
	24,786	23,557	24,605							23,928	23,724	23,260						
	24,763	23,498	24,571							23,923	23,763	23,266						
1:20 dil	24,850	23,908	25,000				24,7	0,5	0,47	24,007	23,924	23,541				24,0	0,3	0,39
	25,000	24,214	24,998							24,136	24,121	23,693						
	25,188	24,230	25,190							24,305	24,323	23,831						
A-project RT, BSA buffer, 1:5 dil	21,885	21,384	23,924	21,247	22,523	24,337	22,6	1,2										
	21,643	21,466	24,083	21,456	22,590	24,233												
	21,936	21,702	24,178	21,615	22,730	24,381												
High Cap RT, BSA buffer, 1:5 dil	21,095	21,625	24,945	21,349	24,504	27,003	23,5	2,3										
	21,279	21,675	25,241	21,427	24,577	26,993												
	21,566	21,814	25,296	21,628	24,734	27,125												

Table A.14: C_q and ΔC_q for *MALAT1* from each well that contained GLP1R-HEK293 cells lysed with RLN + DTT lysis buffer or 0.1% BSA, where two different cDNA kit (A-project and High-Capacity cDNA Reverse transcription kit) was used for the cDNA synthesis.

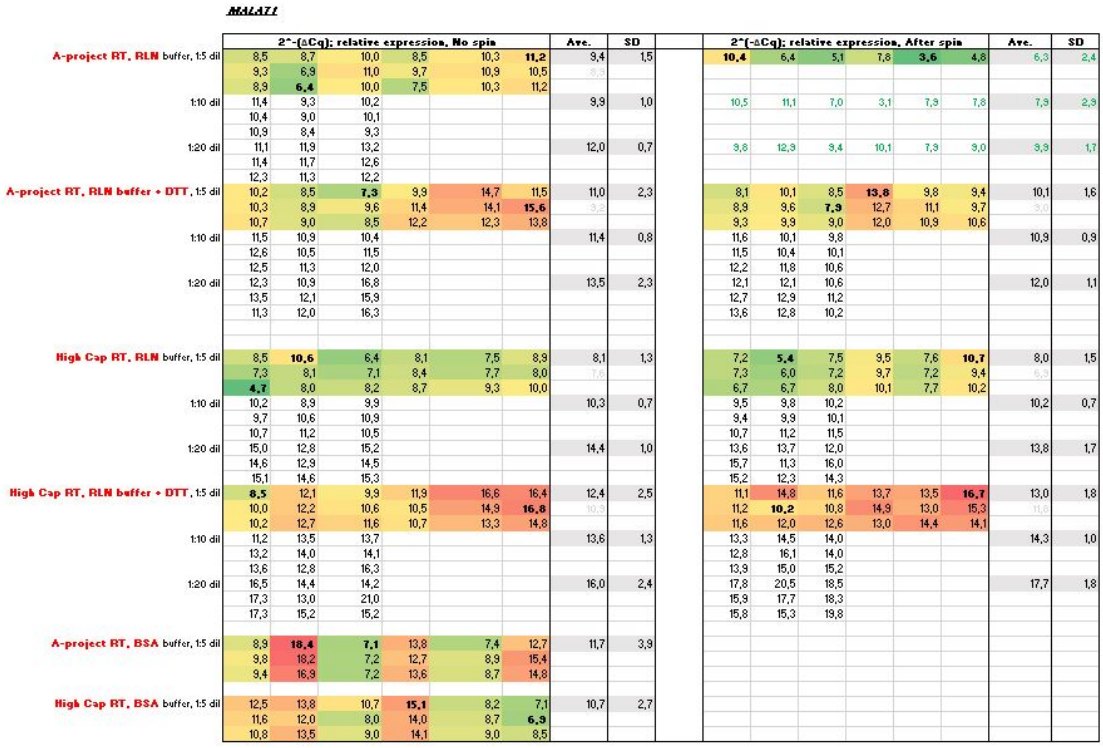

MALAT1

	2^-(ΔCq); relative expression, No spin						Ave.	SD		2^(-ΔCq); relative expression, After spin						Ave.	SD
A-project RT, RLN buffer, 1:5 dil	8,5	8,7	10,0	8,5	10,3	**11,2**	9,4	1,5		**10,4**	6,4	5,1	7,8	**3,6**	4,8	6,3	2,4
	9,3	6,9	11,0	9,7	10,9	10,5											
	8,9	**6,4**	10,0	7,5	10,3	11,2											
1:10 dil	11,4	9,3	10,2				9,9	1,0		10,5	11,1	7,0	3,1	7,9	7,8	7,9	2,9
	10,4	9,0	10,1														
	10,9	8,4	9,3														
1:20 dil	11,1	11,9	13,2				12,0	0,7		9,8	12,9	9,4	10,1	7,9	9,0	9,9	1,7
	11,4	11,7	12,6														
	12,3	11,3	12,2														
A-project RT, RLN buffer + DTT, 1:5 dil	10,2	8,5	**7,3**	9,9	14,7	11,5	11,0	2,3		8,1	10,1	8,5	**13,8**	9,8	9,4	10,1	1,6
	10,3	8,9	9,6	11,4	14,1	**15,6**				8,9	9,6	**7,9**	12,7	11,1	9,7		
	10,7	9,0	8,5	12,2	12,3	13,8				9,3	9,9	9,0	12,0	10,9	10,6		
1:10 dil	11,5	10,9	10,4				11,4	0,8		11,6	10,1	9,8				10,9	0,9
	12,6	10,5	11,5							11,5	10,4	10,1					
	12,5	11,3	12,0							12,2	11,8	10,6					
1:20 dil	12,3	10,9	16,8				13,5	2,3		12,1	12,1	10,6				12,0	1,1
	13,5	12,1	15,9							12,7	12,9	11,2					
	11,3	12,0	16,3							13,6	12,8	10,2					
High Cap RT, RLN buffer, 1:5 dil	8,5	**10,6**	6,4	8,1	7,5	8,9	8,1	1,3		7,2	**5,4**	7,5	9,5	7,6	**10,7**	8,0	1,5
	7,3	8,1	7,1	8,4	7,7	8,0				7,3	6,0	7,2	9,7	7,2	9,4		
	4,7	8,0	8,2	8,7	9,3	10,0				6,7	6,7	8,0	10,1	7,7	10,2		
1:10 dil	10,2	8,9	9,9				10,3	0,7		9,5	9,8	10,2				10,2	0,7
	9,7	10,6	10,9							9,4	9,9	10,1					
	10,7	11,2	10,5							10,7	11,2	11,5					
1:20 dil	15,0	12,8	15,2				14,4	1,0		13,6	13,7	12,0				13,8	1,7
	14,6	12,9	14,5							15,7	11,3	16,0					
	15,1	14,6	15,3							15,2	12,3	14,3					
High Cap RT, RLN buffer + DTT, 1:5 dil	**8,5**	12,1	9,9	11,9	16,6	16,4	12,4	2,5		11,1	14,8	11,6	13,7	13,5	**16,7**	13,0	1,8
	10,0	12,2	10,6	10,5	14,9	**16,8**				11,2	**10,2**	10,8	14,9	13,0	15,3		
	10,2	12,7	11,6	10,7	13,3	14,8				11,6	12,0	12,6	13,0	14,4	14,1		
1:10 dil	11,2	13,5	13,7				13,6	1,3		13,3	14,5	14,0				14,3	1,0
	13,2	14,0	14,1							12,8	16,1	14,0					
	13,6	12,8	16,3							13,9	15,0	15,2					
1:20 dil	16,5	14,4	14,2				16,0	2,4		17,8	20,5	18,5				17,7	1,8
	17,3	13,0	21,0							15,9	17,7	18,3					
	17,3	15,2	15,2							15,8	15,3	19,8					
A-project RT, BSA buffer, 1:5 dil	8,9	**18,4**	**7,1**	13,8	7,4	12,7	11,7	3,9									
	9,8	18,2	7,2	12,7	8,9	15,4											
	9,4	16,9	7,2	13,6	8,7	14,8											
High Cap RT, BSA buffer, 1:5 dil	12,5	13,8	10,7	**15,1**	8,2	7,1	10,7	2,7									
	11,6	12,0	8,0	14,0	8,7	**6,9**											
	10,8	13,5	9,0	14,1	9,0	8,5											

Table A.15: Calculated relative gene expression for each well containing RLN lysis buffer, RLN + DTT lysis buffer or 0.1% BSA, where two different cDNA kit (A-project and High-Capacity cDNA Reverse transcription kit) was used for cDNA synthesis.

36B4

+/-RT, cDNA synthesis kit, lysis buffer, dil.	Cq, No spin	Ave. Cq	Cq, After spin	Ave. Cq
+RT, High Cap RT, RLN buffer, 1:5 dil	23,1	23,0	23,4	23,4
	23,0		23,6	
	23,0		23,0	
-RT, High Cap RT, RLN buffer, 1:5 dil	32,7	33,3	26,2	27,1
	32,8		26,7	
	34,4		28,3	
+RT, High Cap RT, RLN buffer + DTT, 1:5 dil	23,6	23,1	22,9	22,8
	22,2		23,0	
	23,5		22,5	
-RT, High Cap RT, RLN buffer + DTT, 1:5 dil	32,8	32,3	Undetermined	39,9
	31,6		39,9	
	32,4		Undetermined	

Table A.16: C_q values (for *36B4*) used for comparison between well containing containing RLN buffer and RLN buffer + DTT where the cDNA synthesis was performed using High Capacity kit with and without reverse transcriptase to see if there are any contamination of gDNA.

A.6 Protocol

The section described here contains the final protocol of the semi-automated two-qPCR assay for GLP1-HEK293 cells.

B.1 Final protocol

Seeding of GLP1R- HEK293 cells in 384-well plate

1. Calculate the desired cell concentration that each well should contain and how much of the cell suspension and medium that needs to be added in a 50 mL Falcon tube if the total volume of cell culture in each well in the 384-well plate should be 35 µL.
2. Use a MultiDrop to seed the cells in a Poly-D-Lysine coated 384-well plate (Corning, 354663 384).
3. Incubate the cells at 37°C, 5% CO_2 overnight.

ASO treatment of GLP1- HEK293 cells in 384-well plate

4. Determine the concentration (content of the oligonucleotides) of the ASOs dissolved in PBS by measuring the OD at 260 nm and using the Lambert-Beers law.
5. Prepare vials with 8X higher concentration for each ASO by using the values gained from previous step to get the right amount for each well, so that it is enough to have duplicates or triplicates of each ASO.
6. Serial dilute 1:3 the ASOs in culture medium in a 384-well compound plate (Greiner, 781280) to get 11-12 points (starting from the highest to the lowest concentration).
7. Add 30 µL cell medium to all other well that will serve as negative (untreated) control.
8. Use the CyBi-well Multichannel Pipettor (CyBio) to transfer 5 µL from the 384-well compound plate to the 384-well plate containing cells.
9. Perform extra washing step of tips if several plates are used.
10. Incubate the cell plate at 37°C, 5% CO_2 for another 24 hours.

Cell lysis

11. Prepare RLN (Qiagen, 74181) with RNA Secure (ThermoFisher Scientific, AM 7006) lysis buffer according to Equation (B1-B2) to add 30 µL in each well in a 50-mL Falcon tube.

$$(\text{No. of wells} \cdot 30\ \mu\text{L} \cdot 1.1) \cdot \frac{1}{25} = \text{RNA Secure (mL)} \quad \text{(B1)}$$

$$(\text{No. of wells} \cdot 30\ \mu\text{L} \cdot 1.1) - \text{RNA Secure (mL)} = \text{RLN (mL)} + \text{RNA Secure (mL)} \quad \text{(B2)}$$

12. Place the tube on ice.
13. Prepare RT-master by adding 20X RT Enzyme Mix (20x), 2x RT Buffer (2x) and RNase-free water in a Falcon tube to have enough for 18 µL per well. Place the tube on ice.
14. Inspect the cells under a microscope, before and after wash.
15. Use the Bravo pipetting station to remove medium and wash the cells with DPBS (Gibco, 14040).
16. Dispense 30µL of the prepared lysis buffer in each well of the 384-well plate using a Multidrop.
17. Seal the plates with LightCycler 480 Sealing Foil.
18. Keep the plates on ice until transferring and pipetting RT master mix.

RT reaction

19. Spin down the cell lysate plate at 700g for 2 min to centrifuge down the cell debris.
20. Add 18 µL of the master mix to all wells of the PCR plate (Axygen, PCR-384-RGD-C) using the MultiDrop.

21. Use the Vprep/Velocity 11 pipetting station to transfer 2 µL of the lysate to the wells of the PCR plates (Axygen, PCR-384-RGD-C).
22. Seal the plate with (LightCycler 480 Sealing Foil) and spin down plate at 1000 rpm, 216g for 1 min.
23. Use the DNA Engine with 384-PCR blocks for RT reaction.
24. Set the program to 37°C 60min, 95°C 5min, 4°C infinity.
25. Run the RT reaction.

qPCR amplification reaction

26. Use the Multidrop to dispense 6 µL RNase-free water to a qPCR plate (Applied Biosystems 4326270).
27. Transfer 2 µL cDNA template to a qPCR plate containing water by using the Vprep/Velocity 11 pipetting station.
28. Prepare separate qPCR master mixes (3 mL for one 384-well plate) for *HPRT1* and *MALAT1* in 15-mL falcon tubes by adding 4x TaqMan Gene expression master mix (Applied Biosystems 4369016), 1.6x Rnase free water and 0.4x Assay-on-Demand primers for the target gene and reference gene (applied Biosystems). Vortex all reagents.
29. Pour out the master mix in one plastic tray.
30. Use the Biomek FX^{P} laboratory automation workstation (Beckman Coulter), to add 6 µL qPCR master mix, transfer 2 µL diluted cDNA from qPCR plate (Applied Biosystems 4326270) the into MicroAmp Optical 384-well Reaction Plate (Applied Biosystems 4326270) and mix.
31. Seal the plate with MicroAmp Optical Adhesive Film (Applied Biosystems 4311971) and centrifuge the plate at 700g for 1 min to remove bubbles.
32. Run the qPCR amplification reaction using the QuantStudio 7 Flex Real-Time PCR System (Applied Biosystems).